IVW - Schriftenreihe Band 84
Institut für Verbundwerkstoffe GmbH - Kaiserslautern

Rosa María Medina Barrón

Rubber Toughened and Nanoparticle Reinforced Epoxy Composites

Rubber Toughened and Nanoparticle Reinforced Epoxy Composites

Vom Fachbereich für Maschinenbau und Verfahrenstechnik
der Technischen Universität Kaiserslautern
vorgelegte Dissertation
zur Verleihung des akademischen Grades

Doktor-Ingenieur (Dr.-Ing.)

genehmigte Dissertation

von

M. Sc. Rosa María Medina Barrón

aus Mexiko Stadt, Mexiko

Tag der mündliche Prüfung:	12 Dezember 2008
Prüfungsvorsitzender:	Prof. Dr.-Ing. Dr. h. c. Klaus Friedrich
1. Berichterstatter:	Prof. Dr.-Ing. Alois K. Schlarb
2. Berichterstatter:	Prof. Dr.-Ing. Volker Altstädt

Bibliografische Information Der Deutschen Bibliothek

Die Deutsche Bibliothek verzeichnet diese Publikation in der Deutschen Nationalbibliografie; detaillierte bibliografische Daten sind im Internet über <http://dnb.ddb.de> abrufbar.

Bibliographic information published by Die Deutsche Bibliothek

Die Deutsche Bibliothek lists this publication in the Deutsche Nationalbibliografie; detailed bibliographic data is available in the Internet at <http://dnb.ddb.de>.

Herausgeber: Institut für Verbundwerkstoffe GmbH
Prof. Dr.-Ing. Peter Mitschang
Erwin-Schrödinger-Straße
TU Kaiserslautern, Gebäude 58
67663 Kaiserslautern
http://www.ivw.uni-kl.de

Verlag: Institut für Verbundwerkstoffe GmbH

Druck: Technische Universität Kaiserslautern
ZBT – Abteilung Foto-Repro-Druck

D 386

„Gedruckt mit Unterstützung des Deutschen Akademischen Austauschdienstes“

Als Manuskript gedruckt. Printed in Germany.
ISSN 1615-021X
ISBN 978-3-934930-80-3
ISBN 3-934930-80-8

A Sebastian y Santiago,
lo más grande en mi vida.

Acknowledgements

The present work was completed between April 2005 and December 2008 at the Institute for Composite Materials (IVW, GmbH) of the Technical University of Kaiserslautern, Germany.

I would like to express my gratitude to Prof. Dr.-Ing. Alois K. Schlarb and Prof. Dr.-Ing. Dr. h. c. Klaus Friedrich for their scientific support and constant interest on my work. I thank also Prof. Dr.-Ing. Volker Altstädt for accepting to be co-referent of this thesis.

I am thankful to the IVW for providing me the opportunity of working in an outstanding environment from scientific and technical point of view. I express my great appreciation to the IVW staff, especially to my colleges of Division II- Material Science, for their friendly attitude and helpful advices.

This work was carried out thanks to the financial support of the German Service of Academicals Exchange (DAAD). Thanks are also extended to Nanoresins GmbH (Germany) and Cetepox GmbH (Germany) for the donation of materials.

Table of Contents

Abstract

Epoxy resins have achieved acceptance as adhesives, coatings, and potting compounds, but their main application is as matrix to produce reinforced composites. However, their usefulness in this field still limited due to their brittle nature. Some studies have been done to increase the toughness of epoxy composites, of which the most successful one is the modification of the polymer matrix with a second toughening phase.

Resin Transfer Molding (RTM) is one of the most important technologies to manufacture fiber reinforced composites. In the last decade it has experimented new impulse, due to its favorable application to produce large surface composites with good technical properties and at relative low cost.

This research work focuses on the development of novel modified epoxy matrices, with enhanced mechanical and thermal properties, suitable to be processed by resin transfer molding technology, to manufacture Glass Fiber Reinforced Composites (GFRC's) with improved performance in comparison to the commercially available ones.

In the first stage of the project, a neat epoxy resin (EP) was modified using two different nano-sized ceramics: silicium dioxide (SiO_2) and zirconium dioxide (ZrO_2); and micro-sized particles of silicone rubber (SR) as second filler. Series of nanocomposites and hybrid modified epoxy resins were obtained by systematic variation of filler contents. The rheology and curing process of the modified epoxy resins were determined in order to define their aptness to be processed by RTM. The resulting matrices were extensively characterized qualitatively and quantitatively to precise the effect of each filler on the polymer properties.

It was shown that the nanoparticles confer better mechanical properties to the epoxy resin, including modulus and toughness. It was possible to improve simultaneously the tensile modulus and toughness of the epoxy matrix in more than 30 % and 50 % respectively, only by using 8 vol.-% nano-SiO_2 as filler. A similar performance was obtained by nanocomposites containing zirconia. The epoxy matrix modified with 8

vol.-% ZrO_2 recorded tensile modulus and toughness improved up to 36% and 45% respectively regarding EP.

On the other hand, the addition of silicone rubber to EP and nanocomposites results in a superior toughness but has a slightly negative effect on modulus and strength. The addition of 3 vol.-% SR to the neat epoxy and nanocomposites increases their toughness between 1.5 and 2.5 fold; but implies also a reduction in their tensile modulus and strength in range 5-10%. Therefore, when the right proportion of nanoceramic and rubber were added to the epoxy resin, hybrid epoxy matrices with fracture toughness 3 fold higher than EP but also with up to 20% improved modulus were obtained.

Widespread investigations were carried out to define the structural mechanisms responsible for these improvements. It was stated, that each type of filler induces specific energy dissipating mechanisms during the mechanical loading and fracture processes, which are closely related to their nature, morphology and of course to their bonding with the epoxy matrix. When both nanoceramic and silicone rubber are involved in the epoxy formulation, a superposition of their corresponding energy release mechanisms is generated, which provides the matrix with an unusual properties balance.

From the modified matrices glass fiber reinforced RTM-plates were produced. The structure of the obtained composites was microscopically analyzed to determine their impregnation quality. In all cases composites with no structural defects (i.e. voids, delaminations) and good superficial finish were reached. The composites were also properly characterized. As expected the final performance of the GFRCs is strongly determined by the matrix properties. Thus, the enhancement reached by epoxy matrices is translated into better GFRC´s macroscopical properties. Composites with up to 15% enhanced strength and toughness improved up to 50%, were obtained from the modified epoxy matrices.

Kurzfassung

Epoxidharze werden als Kleber, Beschichtungen und Einbettmassen verwendet. Ihre Hauptanwendung finden sie jedoch als Matrixharz zur Herstellung von Faser-Kunststoff-Verbunden. Allerdings ist ihr Einsatz in vielen Anwendungen aufgrund der grundsätzlich limitierten Zähigkeit von duroplastischen Systemen begrenzt. Daher wurden in der Vergangenheit eine Fülle von Arbeiten mit dem Ziel der Zähigkeitsverbesserung von epoxidharzenbasierten Faserverbundwerkstoffen durchgeführt. Am erfolgreichsten war dabei die Modifikation des Epoxidharzes mit einer zweiten, zähigkeitsverbessernden Phase.

Das Harzinjektionsverfahren (RTM) ist eines der wichtigsten Technologien zur Herstellung von Bauteilen aus faserverstärkten Hochleistungsverbundwerkstoffen. In der vergangenen Dekade hat dieses Verfahren wegen seiner besonderen Vorteile bei der Herstellung großflächiger Verbundwerkstoff-Bauteile mit guten technischen Eigenschaften bei relativ niedrigen Kosten erhöhte Beachtung gefunden.

Diese Forschungsarbeit konzentriert sich auf die Entwicklung von modifizierten Epoxidharzen mit erhöhten mechanischen und thermischen Eigenschaften. Die Harze sollen sich durch das Harzinjektionsverfahren verarbeiten lassen, sodass daraus glasfaserverstärkte Verbundwerkstoffe (GFRC's) mit, gegenüber heute üblichen Verbundwerkstoffen, verbesserten mechanischen Eigenschaften herstellbar sind.

In der ersten Projektphase wurde ein reines Epoxidharz (EP) durch Zugabe keramischer Nanopartikel (Siliciumdioxid (SiO_2) oder Zirkoniumdioxid (ZrO_2)) oder in Kombination mit Mikro-Silikonkautschuk (SR) modifiziert. In einer weiteren Phase wurden in-situ hergestellte Nanocomposite durch zusätzliche Additiveren mit Füllstoffen gezielt variiert. Die Rheologie und das Härtungsverhalten der modifizierten Harze wurden charakterisiert, um ihre Eignung für die RTM- Verarbeitung zu überprüfen. Die Harze wurden außerdem ausführlich mechanisch charakterisiert, um quantitativ und qualitativ den jeweiligen Verstärkungseffekt der verschiedenen Füllstoffarten auf die Epoxidharz-Eigenschaften zu ermitteln.

Es wurde gezeigt, dass die verwendeten keramischen Nanopartikel die mechanischen Eigenschaften der Epoxidharze deutlich verbessern, insbesondere deren Elastizitätsmodul und Bruchzähigkeit. So wurden z.B. mit nur 8 Vol.-% an Nano-SiO_2 -

Füllstoff der Zugmodul um ca. 30 % und die Bruchzähigkeit des Epoxidharzes um 50 % gesteigert. Eine ähnliche Leistungsverbesserung ergab sich für die Nanocomposite, die Zirkonium enthielten. Das Epoxidharz, welches mit 8 Vol.-% Nano- ZrO_2 verändert wurde, zeigte einen um 36% höheren Zugmodul und eine um 45% verbesserte Bruchzähigkeit im Vergleich zum reinen Epoxidharz.

Das Einmischen von Mikro-Silikonkautschuk-Partikeln führte zu einer deutlichen Steigerung in der Bruchzähigkeit. Gleichzeitig nahmen der Elastizitätsmodul und die Festigkeit jedoch geringfügig ab. So führte z.B. die Zugabe von 3 Vol.-% SR zu einer Erhöhung der Bruchzähigkeit um den Faktor 1,5 bis 2,5. Gleichzeitig fiel der Zugelastzitätsmodul und die Zugfestigkeit jedoch um 5 % - 10% ab.

Erst in der richtigen Kombination an Nano-Keramik und Mikro-Kautschuk konnte ein hybrid-modifizierter Epoxidharz-Werkstoff mit einer gegenüber einem handelsüblichen Epoxidharz dreifach höheren Bruchzähigkeit und einem um 20% höheren Elastizitätsodul hergestellt werden. Es wurden auch vielfältige Untersuchungen durchgeführt, um die strukturellen Mechanismen, die für die Zähigkeits- und Modulverbesserung verantwortlich sind, zu erforschen. Dabei ergab sich, dass jeder der Füllstoffe spezifische strukturelle Mechanismen auslöst, die mit ihrer Natur, Morphologie und ihrer Kopplung an das Epoxidharz zusammenhängen. Der simultane Effekt von Nano-Keramik und Mikro-Kautschuk als Füllstoff mündete in einer Überlagerung dieser Energiefreisetzungsmechanismen, was schließlich in einem modifizierten Harz mit ungewöhnlich gutem Eigenschaftsprofil resultierte.

Mit dem modifizierten Harz wurden glasfaserverstärkte Platten mittels RTM- Verfahren hergestellt. Die Imprägnierungsqualität der so gefertigten Faser-Kunststoff-Verbunde wurde mikroskopisch analysiert. Dabei wurden in der Regel faserverstärkte Platten ohne strukturelle Defekte und mit guter Oberfläche erzielt. Probekörper aus diesen Platten wurden mechanisch charakterisiert. Dabei wurde deutlich, dass die verbesserten Harzeigenschaften auch in den Faser-Kunststoff-Verbund übersetzt werden können.

Die hybrid-modifizierten Epoxidharze verbessern die Festigkeit im Faser-Kunststoff-Verbund um 15 %, die interlaminare Bruchzähigkeit sogar um 50 %.

List of Abbreviations and Symbols

Abbreviations

COD	Crack opening displacement
CT	Compression test
DCB	Double cantilever beam
DGEBA	Diglycidyl ether of bisphenol A
DMTA	Dynamic mechanical thermo analysis
EP	Neat epoxy resin
GFRC	Glass fiber reinforced composite
ILSS	Interlaminar Shear Strength
ROM	Rule of mixtures
RTM	Resin transfer molding
SEM	Scanning electron microscopy
SR	Silicon rubber
TEM	Transmission electron microscopy

Symbols

a	$[mm]$	Length of the pre-notched crack, CT Specimen
a_d	$[mm]$	Length of delamination, DCB Specimen
A_r	$[1]$	Arrhenius constant
A	$[m^2]$	Area
b	$[mm]$	Width DCB and ILSS specimen
B	$[mm]$	Specimen thickness, CT and ILSS specimen
C	$[1]$	Compliance calibration factor , DCB test
c	$[\mu m]$	Half of the interparticle distance

D_{50}	$[nm]$	Average fraction measurement (50 % of the particles are smaller than D_{50})
d_p	$[nm]$	Particle diameter
E	$[MPa]$	Young's modulus
E^*	$[MPa]$	Complex modulus
E_a	$[kJ/mol]$	Activation energy
$f(x)$	$[1]$	Shape factor of CT specimens
F	$[N]$	Force
G_{IC}	$[J/m^2]$	Critical energy release rate (Mode I)
G'	$[Pa]$	Storage modulus
G''	$[Pa]$	Loss modulus
h	$[\mu m]$	Indenter displacement, hardness test
h_c	$[\mu m]$	Hysteresis during hardness test
H	$[MPa]$	Indentation hardness
k_E	$[1]$	Generalized Einstein coefficient
K	$[1]$	Constant
K_{IC}	$[MPa*/m^{1/2}]$	Critical stress intensity factor (Mode I)
$K(T)$	$[Mol/s]$	Reaction rate constant
l	$[nm]$	Particle length
P	$[N]$	Maximum force
R	$[J/molK]$	Ideal gases constant
t	$[s]$	Time
t_{gel}	$[s]$	Gel time
T	$[K, °C]$	Temperature
T_g	$[°C]$	Glass transition temperature

V	$[1]$	Volume fraction
V_{max}	$[1]$	Maximum volume fraction of filler
W	$[mm]$	Distance from the test axis to the CT specimen end
x	$[1]$	Normalized crack length, CT specimen
α	$[mol]$	Cure grade
α_{gel}	$[mol]$	Cure grade at gel time
β	$[1]$	Modulus constant, Lewis-Nielsen model
δ	$[mm]$	Load point displacement
$Tan\ \delta$	$[1]$	Loss factor, mechanical damping
ε	$[\%]$	Mechanical strain
η	$[Pa*s]$	Viscosity
μ	$[1]$	Constant Lewis-Nielsen model
μ_t	$[1]$	Geometry correction factor modified ROM
μ_0	$[1]$	Orientation correction factor modified ROM
ν	$[1]$	Poisson ‘s ratio
π	$[1]$	Mathematical constant
ρ	$[1]$	Constant of Halpin-Tsai model
σ_y	$[MPa]$	Yield stress of the matrix
τ	$[MPa]$	Shear strength
ζ	$[1]$	Halpin-Tsai geometry shape factor

1 Introduction

Fiber-reinforced composites are high strength and high modulus materials which find wide acceptance for use as structural components in automotive applications, as components of buildings as well as in spacecraft and aeronautic industries. When used in structural applications the composites are typically formed of continuous fiber filaments or woven cloth embedded in a thermosetting or thermoplastic matrix. Such composites may exhibit considerable strength and stiffness, and the potential for obtaining significant weight savings makes them highly attractive to be used as metal replacement.

Epoxy resins are so versatile because of the large number of potential combinations epoxy prepolymer and curing agent, each one of them giving a different molecular structure to the final thermoset material. They have widespread application, but they are mainly used as matrices of reinforced composites. Epoxies have in general good mechanical and thermal properties, however highly crosslinked epoxy systems are usually brittle, which limits their utility in applications requiring high impact and fracture strength. As a consequence, the search for toughened epoxy matrices has become the subject of numerous recent patents and publications, and by these efforts some formulations have been developed to the composite industry [1,2].

Different mechanisms have probed to enhance the toughness of epoxy resins, either by chemical transformation, reformulation tending to reduce their cross-link density, or by modifying already available epoxy resins, through incorporation of a secondary dispersed toughening phase. The epoxy modifiers studied to improve the toughness include: rubbers, thermoplastics, and inorganic particles [3,4,5].

Epoxy resins can be substantially toughened by the addition of a rubbery phase, although the improvement in toughness appears commonly accompanied by a significant loss in elastic modulus, strength and glass transition temperature [6,7].

An alternative to toughen epoxy resins without detrimental of other properties, mainly thermal performance, is using engineering thermoplastics as a second phase [8,9]. The reported results show that thermoplastics improve only modestly the fracture

toughness and in some cases they may represent a problem of processability, caused by their poor compatibility with the epoxy matrix.

Rigid fillers such as alumina [10], titanium dioxide [11] and clay [12] have been added to the epoxies to increase their stiffness, strength and thermal properties; but they have also demonstrated a favorable toughening effect. It is possible to increase the toughness of an epoxy resin by up to 100% using selected rigid fillers, normally sized in the range of nanometers. However, this toughening effect seems so moderate when is compared with the toughness of epoxy matrices modified with rubber, and normally is not enough to cover the requirements of high demanding applications.

Considering the benefits reported from the rubber and rigid fillers epoxy modifications, recent researches converge on the formulation of hybrid modified matrices, containing rigid fillers and a rubber toughening phase, as a possibility to obtain toughened epoxy resins without loss of other important properties [13,14].

On this basis, the present work is concentrated on the obtaining of easy to be processed rubber toughened and nanoparticle reinforced epoxy matrices, with enhanced stiffness/toughness balance as well as good thermal properties.

Among the industrial methods used to produce fiber reinforced composites, Resin-Transfer-Molding (RTM) has been established in the past few years as an alternative to the prepreg autoclave technique. The significantly lower costs of the finished products are advantageous here when the production quantity justify the investment costs for the vacuum-tight, temperature-adjustable, pressure-stressed, and frequently very complex and heavy moulds. The RTM makes possible the production of large parts in series as demanded in automotive and aeronautic industries [15].

Therefore, a second goal of this work is that the toughened epoxy matrices were suitable to be processed by RTM technology in order to make fiber composites. During the manufacturing process, the modified matrices are not allowed to lose any of their unique reinforcing properties. In particular those intended to enhance the stiffness/toughness balance of the final composites.

Nanocomposites can be prepared by different technologies. In the present work two different methods to produce nanomodified matrices and hybrid compounds were used. The first one involves epoxy modified master-batches; obtained by sol-gel technology and the second one implies the direct incorporation of nanoparticles, in powder form, into the fluid epoxy resin. In both cases, the milling/mixing processes needed for obtain and thinning down the master-batches were examined in detail in order to achieve matrices with homogeneous particle distribution.

The systematical mixing of different types and amounts of fillers aims to find out the optimum matrix composition at which a simultaneous increase in fracture toughness, modulus and strength is expected to occur.

The rheology and curing behavior of the modified epoxy resins were analyzed to determine their suitability to be processed through RTM and to define the right composition and processing variables to manufacture glass fiber reinforced composites (GFRCs).

GFRCs were produced and properly characterized. The experimental results of the composites characterization were correlated with the matrix properties and also with theoretical models; treatment that allowed a better understanding of the internal changes induced by the fillers in the polymer structure and also of the effect of these structural changes on the macroscopic properties of the final composite product.

2 Basis and State of the Art

2.1 Epoxy Resins

According to the common chemical practice, epoxy resins are low molecular weight prepolymers characterized by the presence of epoxy or oxyrane functional groups, which consist of a three-membered ring containing two atoms of carbon and an oxygen [16].

Epoxy resins exist in wide range of molecular weights and can react with diverse curing agents to produce a crosslinked thermosetting material.

A wide range of starting materials can be used to prepare epoxy resins, providing a variety of resins with controllable performance characteristics. Most conventional epoxy resins are prepared from bisphenol A and epichlorohydrin, which is the case of the diglycidyl ether of bisphenol A (DGEBA) based epoxy.

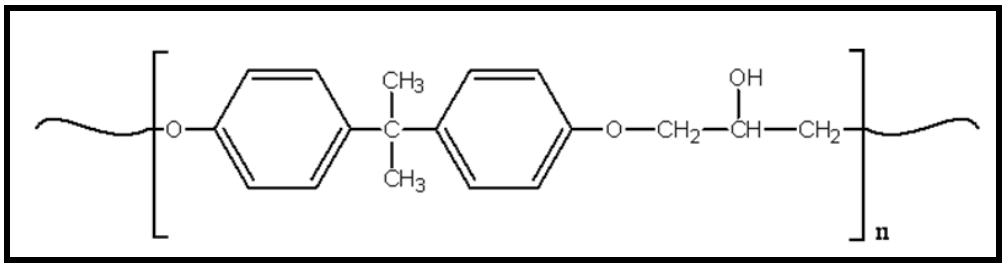

Figure 2.1: Chemical structure of diglycidyl ether of bisphenol A (DGEBA) epoxy.

The curing process is a chemical reaction in which the epoxy groups reacts with a curing agent (hardener) to form a highly crosslinked, three-dimensional network, which result into a hard, infusible, and rigid material.

A wide variety of curing agents for epoxy resins is available depending on the process and properties required. The right curing agent should be carefully selected because it will affect the type of chemical reaction, pot life and final material properties. The commonly used curing agents for epoxies include amines, polyamides, phenolic resins, anhydrides, isocyanates and polymercaptans [17,18]. The stoichiometry of the epoxy-hardener system also affects the properties of the cured materi-

al. Employing different types and amounts of hardener, which tend to control cross-link density, vary the final epoxy structure.

The epoxies used in composites are mainly prepared from the glycidyl ethers and amines. The material properties and cure rates can be formulated to meet the required performance.

Amines are the most commonly used curing agents for epoxy resins. Primary and secondary amines are highly reactive with epoxy. Tertiary amines are generally used as catalysts, commonly known as accelerators for cure reactions. Use of excessive amount of catalyst achieves faster curing, but usually at the expense of working life, and thermal stability. The curing process of the epoxy resin with an amine hardener is described in Figure 2.2.

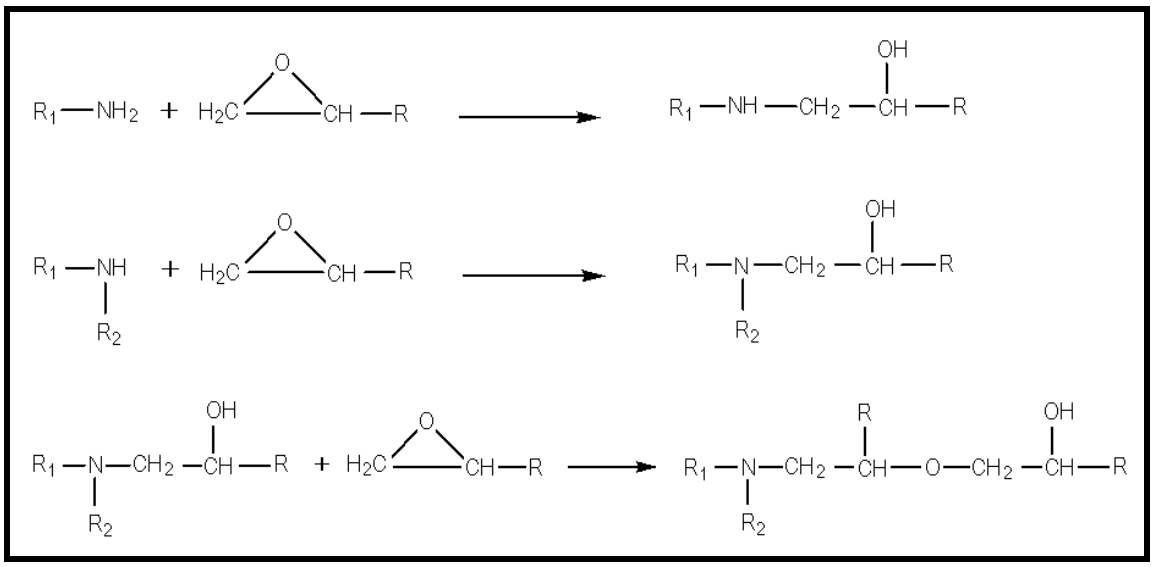

Figure 2.2: Curing reaction of epoxy resins with amine curing agent [19]

Curing cycles determine the degree of cure of epoxy resins and have an important effect on the mechanical properties of the final products. Although suppliers of commercial epoxy resins usually suggest curing cycles for customer applications, their curing cycles hardly ever are the optimal for a special application, mainly when the epoxy is modified by addition of a second phase. In order to optimize the curing cycles of the modified epoxy matrices, it is necessary to understand the cure kinetics and characteristics of the epoxy systems in detail.

2.2 Epoxy Nanocomposites

Fillers and additives are often added to the epoxy formulations to meet specific processing requirements or achieve desired materials properties. Whereas cheap extenders such as quartz sand are used to lower the formulation price, active fillers are applied to enhance certain properties of the basic epoxy system.

In its most basic form a composite material is formed by at least two elements working together to produce material properties that are different to the properties of the elements on their own. In practice, most composites consist of a bulk material (matrix), and a reinforcement of some kind, added to the matrix in order to improve its final performance. The reinforcing filler component can be chosen as particles for instance ceramic powders or as fibrous fillers.

The fillers commonly used for manufacturing thermosetting composites have relatively large diameters in between 1-50 micrometers. Typical powders may be glass, silicon carbide, aluminum oxide and similar materials [20,21]. These micro-fillers can be easily worked into an epoxy resin by using tools which generate relatively low shear forces. However, these microparticles have shown to weaken some mechanical properties of the resulting composite, especially under impact conditions [22,23].

Moreover, microfiller reinforced matrices may cause important processing problems, as the filtering effect. Relatively large fibers act as barriers blocking the way of the particles, which cannot pass and pile up instead of flowing freely into the fiber bundles together with the polymer. The polymer matrix loses its homogeneity because of the particle concentration fluctuates locally, and this effect decreases the mechanical properties of the final product.

A new approach aiming to overcome these problems takes advantage of the nanotechnology, using nano-sized fillers to reinforce polymer matrices. In case the ultrafine filler dimensions are maintained after matrix compounding, the large filler active surface, would lead to a very strong polymer-filler interfacial interaction. As the interfacial structure plays a critical role in determining the composite properties, it is expected that nanocomposites possess unusual properties [24,25].

Figure 2.3 shows comparatively the improvement in mechanical properties of an epoxy resin using micro- and nanofillers. It is observed that both types of fillers have similar effect on the matrix modulus. However in the case of fracture toughness the panorama seems quite different; although micro- and nano-sized fillers act as tougheners, the toughening effect of nanofillers is clearly superior, almost 2 fold higher than the one induced by micro-sized fillers. Then the nanocomposites show best stiffness/toughness balance.

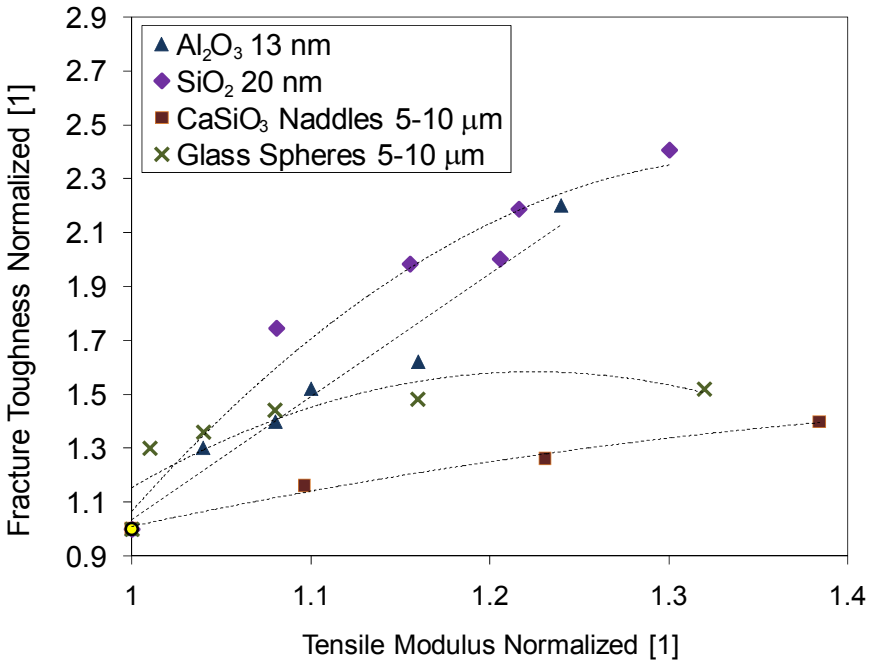

Figure 2.3: Epoxy properties improvement as function of the filler type and size. (Al_2O_3 and Glass spheres 1,2,3,5 and 10 vol.-% [26]; $CaSiO_3$ 3, 6.5 and 12.5 vol.-% [26]; SiO_2 2.5, 4.9, 7.1, 9.6 and 13.4 vol.-% [27]).

Polymer based nanocomposites present an additional challenge, because they are difficult to be produced using techniques applied to conventional composites, for example the addition of organically modified particles directly into a polymer melt or solution. This fact is due to the strong tendency of nanoparticles to agglomerate, phenomenon hard to be controlled only by application of shear force during the mixing process. Alternatively, chemical methods have been proposed to produce nanoparticles in-situ (directly inside the polymer). This technique overcomes the agglomera-

tion dilemma and can produce individual, surface-optimized, and homogeneously distributed nanoparticles with controlled size.

In-situ methods are commonly designed in two steps. Firstly the nanoparticles are added to the low viscous monomers and homogeneously distributed herein, and once that the desired distribution is obtained the polymerization takes place and as the reaction advances, the polymer chains encapsulate the nanoparticles [28,29].

Sol-Gel-Technology is one of the most recognized to produce in-situ modified polymer matrices [30,31]. During the sol-gel process, pre-polymers are incorporated into sol-gel glass, where both the organic and inorganic phases are simultaneously formed through the synchronous polymerization of the organic monomer and the sol-gel precursors. Under the right set of conditions, polymers can be kinetically trapped within inorganic matrices prior to significant phase separation. The limited species of polymers and monomers which are soluble in the tri-component sol-gel solution and the shrinkage associated with the drying process are disadvantages of this method.

2.3 Toughened Epoxy Matrices

In general epoxy matrices are classified as brittle materials having toughness typically below 1 $MPam^{1/2}$ [32]. To broaden the field of application of epoxy resins, it is necessary to enhance their fracture properties without sacrificing other mechanical properties. The fracture toughness is defined as the energy which is necessary to increase the fracture surface of a pre-notched material.

Epoxy resins may be toughened by diverse methods that can be divided in two categories: Chemical modification using reactive diluents and physical toughening by addition of a second toughening phase. Each toughening approach exhibits unique advantages over the others.

Reactive diluents are oligomers or small particle compounds having functional groups able to react with the epoxy resin to generate more flexible networks [33], by reduction of their crosslink density. Reactive diluents are particularly advantageous because the incorporation of modifiers into the epoxy network by chemical bonding results in homogeneous formulation and as consequence uniform properties, in con-

trast with the inclusion of unbonded particles [34]. Among the most useful reactive diluents are linear aliphatic diols, urethane, oligomers of ester and ether linkage [35,36,37]. Although an increment in toughness may be reached be this method, it is clear that the crosslink reduction has a negative impact in other properties as the strength.

Other important and efficient way to make the epoxy materials tougher is to modify the original epoxy resins, with a second phase component through physical blending.

Unmodified epoxy resins are usually single-phase materials, while the addition of modifiers turns the toughened epoxy resins into multiphase systems. When modifier domains are correctly dispersed in discrete forms throughout the epoxy matrix, the fracture energy or toughness can be greatly improved. The reason is that cross-linked epoxy resins have limited ability to deform especially in the triaxial stress field present inside the sample at the crack tip [38]. However, the addition of second phase modifiers changes this situation and can significantly improve the fracture toughness.

The toughening phases studied to modify cured epoxy resins, can be roughly classified as three types: liquid rubbers, engineering thermoplastics, and inorganic particles.

As mentioned in the previous section rigid inorganic particles have been added to the epoxies in order to enhance their stiffness but they are proved also to be polymer advantageous in improving toughness without compromising other properties as thermal behavior [39,40]. However, the toughening effect of rigid fillers seems to be quite moderate when it is compared with the superior toughness provided by other elastic particles.

As an alternative method, engineering thermoplastics have been used to improve the poor fracture properties of epoxy resins. Thermoplastic modifiers come into view, because they are tough, ductile, chemically and thermally stable, and have high T_g. Then it is expected that through this technology toughened epoxy resins without negatively affecting their thermal performance may be obtained.

The thermoplastics used as modifiers include Poly(ether-sulfone) [41] Poly (ether-imides) [42], Poly(ether-ketone) [43] . Various amorphous and semicrystalline thermoplastic polymers [8,9] have been tried to toughen epoxy systems. Even though some optimistic results have been reached using thermoplastic, oligomers or polymers, as epoxy resins toughening agents; in general, they could not bring significant improvement in fracture toughness and in some cases, the fracture toughness decreases, due to the poor adhesion filler-matrix [44]. Additionally, thermoplastic-epoxy systems have also processability problems, which are mainly caused also by poor compatibility with the uncured epoxy resin and the toughening phase [45].

Elastomeric modifiers have been proved to be a successful way of enhancing the fracture toughness of epoxy resins. The addition of a rubber modifier improves the fracture toughness, but it is usually at the expense of other important bulk properties, such as stiffness or thermal resistance. This is not unexpected since the modulus of the toughened modifier is much lower than the modulus of the thermosetting matrix.

The technology of rubber toughening has been applied to epoxy resins through the utilization of low molecular weight liquid butadiene-acrylonitrile copolymers having carboxyl (CTBN), amine (ATBN) or epoxy (ETBN) reactive end groups [46,47,48]. Other elastomeric modifiers that have been studied include acrylate elastomers and polysiloxanes.

Table 2.1, summarizes the properties of an epoxy resin when it is modified with a specific amount of different secondary toughened phases. It is shown that rubbers can effectively improve the fracture toughness of the resin, and the best results, by balancing with other properties; were reached by acrylic and core shell rubbers [49].

The phase separation of the initially miscible rubber, necessary for effective toughening, is governed by several parameters. In the uncured state, the modifier should be miscible with the matrix resin ensuring low viscosities and thus good processability. The compatibility between matrix and modifier depends, among others, on the chemistry and polarity of the resin system, the molecular mass and the functionality of the rubber as well as the temperature of the mixture. Good adhesion to the resin matrix is another requirement for effective toughening. Upon loading, stresses in the ma-

trix can be transferred to the rubber particles if strong interfacial interactions exist. Only then, the toughening mechanisms stemming from the separated particles can work [50].

Table 2.1: Properties of an epoxy resin modified with different toughening phases. (5 wt.-%) [51]

	Flexural Modulus [GPa]	Strength [MPa]	K_{IC} [MPa*m$^{1/2}$]	G_{IC} [kJ/m^2]	T_g [°C]
Epoxy	3.12	149.1	0.55	0.142	140.1
Acrylic Rubber	2.74	127.8	0.87	0.299	143.4
Core shell Rubber	2.94	108.4	0.93	0.358	142.5
CTBN	3.08	122.9	0.74	0.259	134.2
ABS	2.92	122	0.79	0.323	143.8
PDMS	2.57	122.7	0.72	0.259	137

Besides the use of soluble liquid rubbers, another form of rubber toughening of epoxy resins is attained by the application of pre-formed elastomeric particles. Via mechanical mixing, finely dispersed particles with defined diameters can be incorporated into the resins. The mixing process, however, is impaired by the usually high viscosity of the mixtures. If sedimentation is prevented, the rubber dispersion is fixed during matrix cure [52].

Core-shell microparticles are prepared to enhance the interfacial adhesion of non-compatible rubber particles by grafting a compatible polymeric shell onto an elastomeric core. Versatile core-shell toughening modifiers consist of a polybutadiene core and a thermoplastic shell of either styrene/acrylonitrile or styrene/methyl methacrylate. Depending on the acrylonitrile or methyl methacrylate content, the compatibility and thus the interfacial adhesion between shell and thermosetting matrix can be varied over a wide range [52].

The toughening processes which contribute to the energy dissipation in a strained sample stem from the multiple localized plastic deformations initiated by the dis-

persed particles. They involve internal cavitation and interfacial debonding of the rubber particles as well as localized shear yielding in the matrix. Rubber particle bridging behind the crack tip and crack pinning are other toughening mechanisms active in rubber toughened thermosets. If the adhesion of the rubber to the matrix is strong, the particles are first deformed and finally cavitate internally when a load is applied. If the adhesion is poor, though, debonding at the Interface occurs. In both cases energy is dissipated and voids are formed [53].

2.4 Fiber Reinforced Composites

As mentioned, a composite material is a complex solid composed of two or more constituents. On macroscopic scale, composites have structural and functional properties not present in any their individual components, and generally they are designed to exhibit the best properties or qualities of its constituents.

Polymer resins have limited use to manufacture structures on their own, since their mechanical properties are not so good when compared to metals. However, they have desirable properties most notably their ability to be easily formed into complex shapes. On the other hand materials such as glass, aramid and boron exhibit extremely high tensile and compressive strength especially when they are produced in fibers. However, fiber alone can only exhibit unique properties along the fiber's length. It is only when resin systems are combined with fibers that exceptional properties can be obtained. High strengths, high stiffness, ease to mold complex shapes, high environmental resistance and low densities, make the resultant composite superior to metals for many applications [54].

A fiber-reinforced composite is a system made of fibers embedded in a matrix, most of the times coupling agents are used to ensure the adhesion of such dissimilar materials as polymers and glass, establishing chemical bonds between the two composite phases.

Since polymer matrix composites combine resin and fibers, the properties of the resulting composite are determined mainly by the properties of the fiber, the properties of the resin, the ratio fiber to resin in the composite (fiber volume Fraction) and the geometry and orientation of the fibers. Thus, strength, tensile modulus and impact

toughness as well as dimensional stability are mainly governed by the fiber forming material, the fiber sizing as well as the orientation of the fibers [55,56]. On the other hand, the polymeric matrix is responsible for chemical stability, scratch resistance, electrical properties and shrinkage during cure. Density, thermal conductivity and thermal expansion depend mainly on the fiber volume content.

The geometry of the fibers in a composite is important since, as mentioned, fibers have their highest mechanical properties along their lengths, rather than across their widths. This leads to the highly anisotropic properties of composites, which means, that the mechanical properties of the composite are likely to be very different when tested in different directions. Therefore it is important when considering the use of composites to understand at the design stage, both the magnitude and the direction of the applied loads.

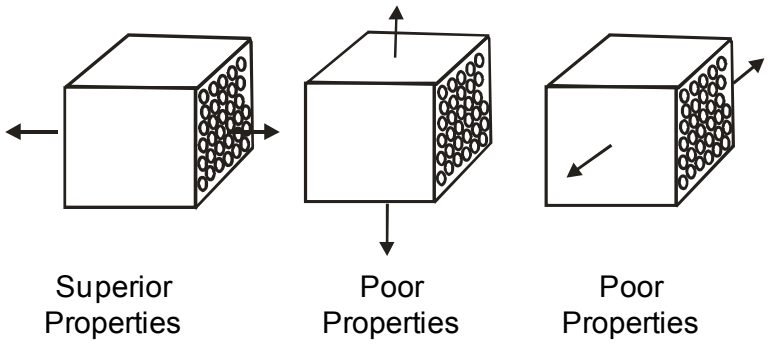

Figure 2.4: Composite properties as function of the load direction [55]

It is also important to note that a composite material is formed at the same time as the structural part is being fabricated. This means that during their molding are being defined the properties of the final product, and so the manufacturing processes play an unusually critical role in determining the performance of the resultant structure.

There is a very large range of mechanical properties that can be achieved with composite materials. Even when considering one fiber type on its own, the composite properties can vary by a factor of 10 with the range of fiber content and orientation that are commonly achieved.

Table 2.2 shows comparatively the properties of different types of composites and other common structural materials. The range of physical properties for the composite materials derives obviously of their composition but also of their manufacturing processes. Hence, the lowest composite properties are normally associated with simple manufacturing processes and material forms (e.g. spray lay-up glass fiber), meanwhile higher technology manufacture (e.g. autoclave molding of unidirectional glass fiber prepreg) usually leads to higher properties.

Table 2.2: Composite materials properties compared with other structural materials [56].

	Tensile Modulus [GPa]	Tensile Strength [MPa]	Density [g/cm^3]
Wood	5-15	50-250	0.3-0.8
Al Alloys	70-75	100-400	2.6-2.7
Titanium	110-115	850-1000	4.4-4.5
Steels	190-205	300-1200	7.6-7.7
E-Glass Composites	15-45	150-1100	1.4-1.9
S-Glass Composites	25-50	500-1800	1.7-1.9
Aramid Composites	35-70	400-1700	1.2-1.4
HS Carbon Composites	75-150	700-2200	1.4-1.6
IM Carbon Composites	100-175	900-2700	1.4-1.6

The data presented in Table 2.2 clearly show the range of properties that different composite materials can display. These properties can best be summarized as high strength and high stiffness combined with low density. This singular combination makes composite structures ideal for so many applications, even over metals. This is particularly true to applications which involve movement, such as in automotive, aviation, and aircraft industries, since lighter structures in such applications are always associated with a higher efficiency.

2.5 Resin Transfer Molding

There are three basic manufacturing techniques to produce composite structural products, with many variations and patented processes: 1) Pultrusion process in-

volves a continuous pulling of the fiber roving and mats through a resin bath and then into a heated die. The elevated temperature inside the die cures the composite matrix into a constant cross-section structural shape. 2) The filament winding process can be automated to wrap resin-wetted fibers around a mandrel to produce circular or polygonal shapes. 3) The layup process engages a hand or machine buildup of mats of fibers that are held together permanently by a resin system. This method enables numerous layers of different fiber orientations to be built up to a desired sheet thickness and product shape. Currently, the prepreg method is the most widely used industrially to produce high-quality, continuous fiber-reinforced components. Lately, however, rising production costs have led to more intense research on other methods as Liquid Resin Infusion and Resin Transfer Molding, which promises a significant reduction in production costs [57].

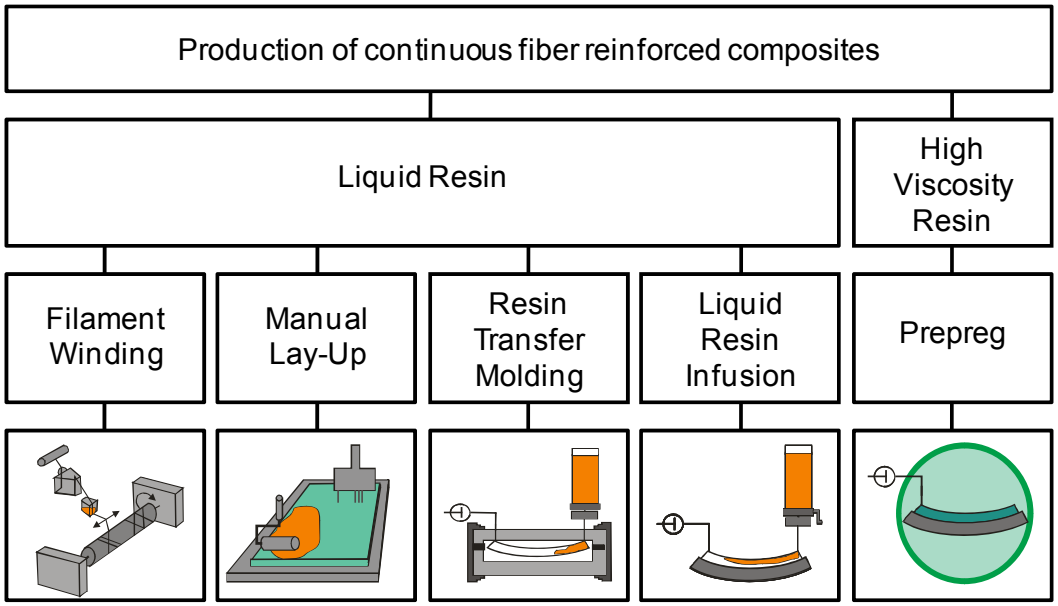

Figure 2.5: Techniques to production fiber reinforced composites [58].

Resin transfer molding has been used to produce polymeric composites for the automotive industry and aerospace applications since the early 1970s.

During the RTM process, the uncured liquid resin/hardener mixture is injected into the tempered mold which contains dry fibers by pressure (see Figure 2.6). The reinforcing structures (fiber fabrics) have been placed inside the mold in advance. The

curing process starts by applying heat to the mold. After curing, the finished composite part can be gained directly out of the mold.

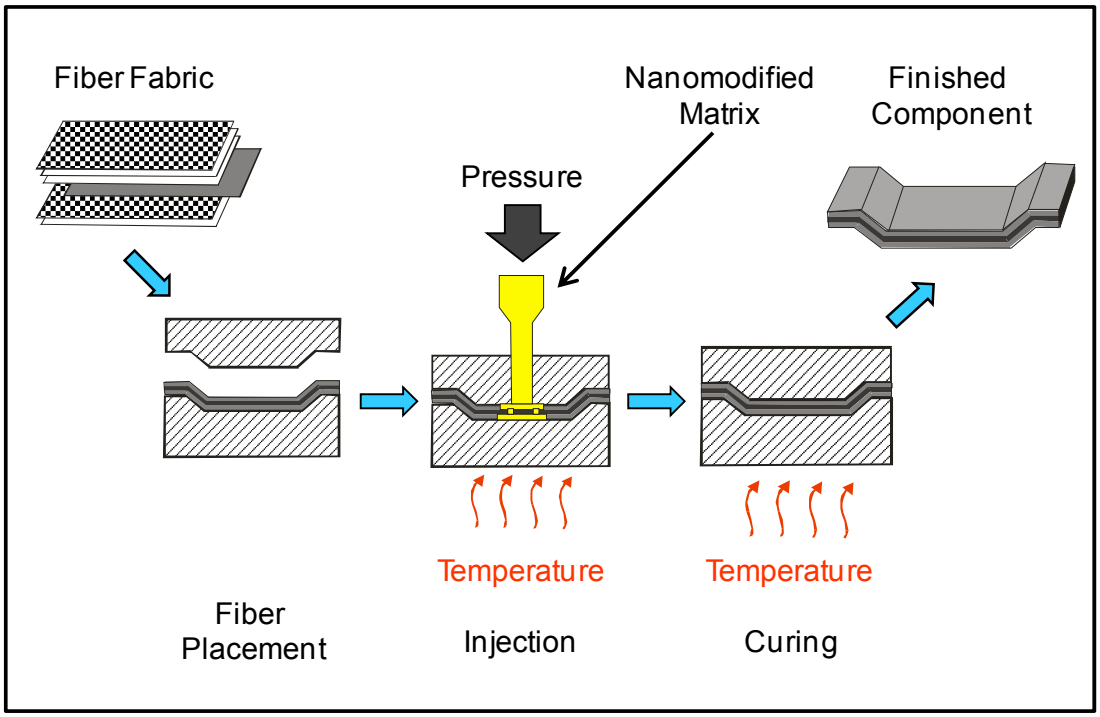

Figure 2.6: Manufacturing of fiber reinforced composites by RTM.

For the injection process, several fundamental parameters have to be controlled, the most important: Injection pressure, viscosity of the resin, processing temperature (tool, resin etc.), permeability of the reinforcing structures (resistance of fibers against resin flow)

From many experiments the optimum resin viscosity was elucidated to range between 200 and 500 mPa·s. Higher viscosities require high injection pressures with the risk of fiber displacement into the mould. Lower viscosities, on the other hand, can lead to increased air entrapment and can lead to pin-holing. Other prerequisites for RTM resins are sufficient fiber adhesion, low shrinkage as well as a pot-life of several hours and a simple cure schedule to ensure good processability [59].

The injection pressure can be controlled and suited to the requirements. The same can be done for the process temperatures. Specially placed sensors in the mold are able to detect temperature and pressure as well as the flow itself. Injection times and

the maximum way of flow are in-situ controllable. Furthermore, the whole RTM processing can be simulated in advance by a special software, if the viscosity of the resin and the permeability of the fabric are known.

The automatizable and cost efficient RTM processing offers important advantages in comparison to other technologies. The main advantage of RTM is that, once the mould has been constructed, even complex components can be produced in semi-automated processes meeting tight tolerances. Furthermore, cost savings result from the use of lightweight moulds, low tooling costs and reduced energy consumption. Large area and complex parts can be produced in large number of pieces at low cycle times, e.g. tail units (Airbus) or screw rotors for air compressors. A wide range of reinforcement types (glass, carbon as well as aramid) and forms (unidirectional material, fabric etc.) can be used. Since no volatiles leave the airtight mould, the RTM process can even be considered environmentally friendly [15,59].

3 Experimental

3.1 Materials

3.1.1 Epoxy Resins

The used epoxy resins are all Diglycidyl ether of bisphenol A (DGEBA), modified with Hexadioldiglycidyl ether; their mainly properties are summarized in Table 3.1.

Cetepox VP 823-30 R

Neat epoxy resin (EP), by Chemicals and Technologies for the Polymers GmbH [60].

Cetepox VP 823-33 R

Master batch epoxy resin is a suspension containing SiO_2-nanoparticles by Chemicals and Technologies for the Polymers GmbH. The disperse phase consists of surface-modified, spherical nano-SiO_2 with diameters under 50 nm and an extremely narrow particle size distribution, obtained from sol-gel chemical process on water [61]. The particles are agglomerate-free and homogeneous distributed in the epoxy resin. This behaviour permits that the resins maintain low viscosity also at high filler content [62].

Albidur EP 2240 A

Master batch epoxy resin modified with reactive silicone rubber micro-particles by Nanoresins GmbH. The elastomer fraction is a special silicon rubber addition obtained (Type A) with particle size 0.1-3 µm, that present a fine distributed separate phase in the fluid resin. Albidur EP 2240-A is totally compatible with other epoxy resins and also with the most diverse cured agents. The silicone elastomer particles have an organic shell structure comprising reactive groups. The reaction curing to rubber obtaining rules the hydrophobicity of the final particles and can be used to adjust the polarity of the formulation [63,64].

Table 3.1: Properties of epoxy resins

	CeTePox VP 823-30R	CeTePox VP 823-33R	Albidur EP 2240 A
Aspect	Transparent fluid	Whitish fluid	White fluid
Equivalent weight Eq./100g	0.581	0.485	0.318-0.345
Density g/cm^3	1.148	1.249	1.08-1.12
Particle content wt.-%	0	19.125	40
Viscosity 25°C mPas	1160	1330	30000-45000

3.1.2 Nanoparticles

Nanoparticles of ZrO_2 were also used to modify the pure epoxy matrix. They were provided under the trade name VP Zirconium Dioxide PH by Degussa AG. The properties of zirconia are summarized in Table 3.2 [65].

Table 3.2: Properties of zirconia nanoparticles

Molecular weight	g/mol	123.22
Density	g/cm^3	5.89
Particle size	nm	12
Chemical purity	wt.-%	97
Superficial area	m^2/g	60±15

Supplied zirconia is a light, dry powder consisting of needle shape nanoparticles sticked together, due to secondary intermolecular electrical forces, forming clusters which average size in range 2-3 μm. Microscopical aspect of the zirconia powder is shown in Figure 3.1.

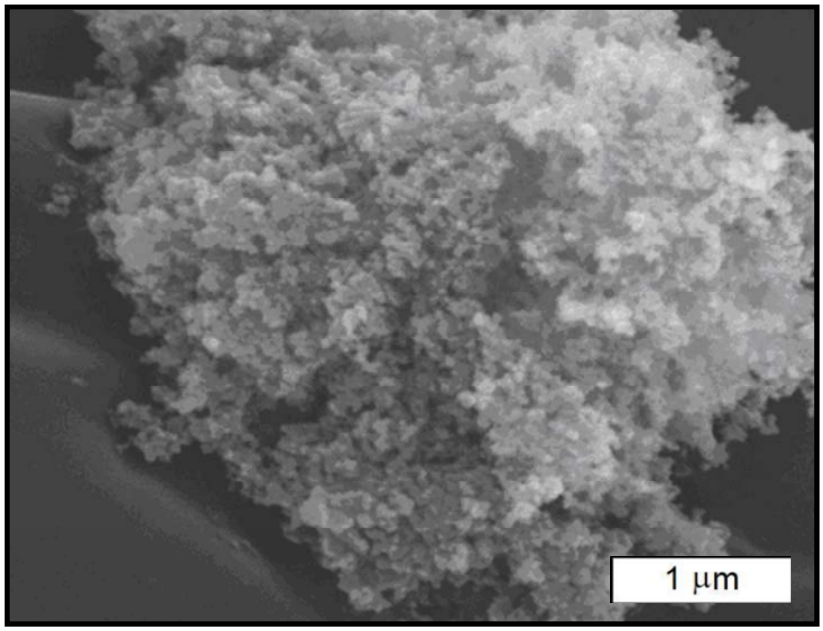

Figure 3.1: SEM image of zirconia powder

3.1.3 Curing Agent

Cetepox VP 823-2H

It is a curing agent based on cycle aliphatic polyamine; also supplied by Chemicals and Technologies for Polymers GmbH [66].

Table 3.3: Properties of the curing agent

Aspect		Clear colorless liquid
H equivalent weight	Eq./100g	50.7
Boiling point	°C	240
Density	g/cm^3	0.931

All the materials are grade industrial products and they were used directly as they were supplied, without any additional treatment.

3.1.4 Glass Fiber

The fiber reinforcement used to laminate composites production is a glass fabric style 92111 by Interglass, which properties are listed in Table 3.4 [67].

Table 3.4: Properties of the Interglass 92111 glass fabric

International style		7628
Weight	g/m^2	200
Warp/weft yarn	tex	EC 9-68
Warp ends	1/cm	17.3
Weft picks	1/cm	12
Weave pattern	tex	Plain
Thickness	mm	0.19

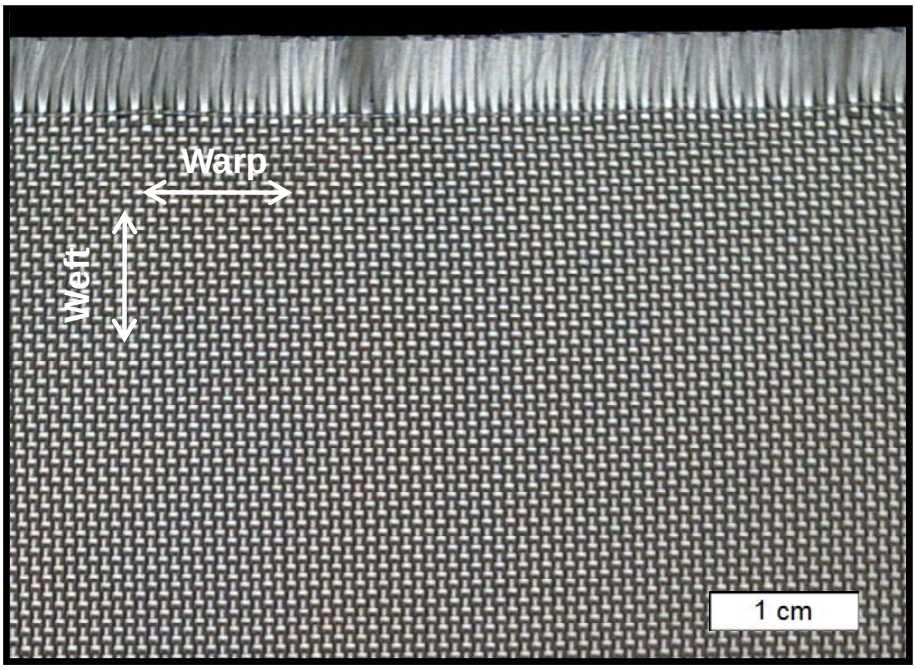

Figure 3.2: Aspect of the Interglass 92111 glass fabric

3.2 Compounding

Series of nanocomposites and hybrid compounds, with variable content of ceramic and rubber, were produced by dilution or mixing/dilution of the corresponding master batches with neat epoxy. As stated above, in the cases of SiO_2 and SR, the master batches were commercial products obtained by sol-gel technology; meanwhile, the ZrO_2 master batch was produced by direct incorporation of zirconia particles into the fluid epoxy, using exclusively mechanical shear forces (Torus mill). The detailed process and parameter to obtain the zirconia master batch is discussed in section 4.2.1.

Nanocomposites and hybrid compounds were prepared using a Dissolver, Wihelm Niemann GmbH, Germany; operated at 200 rpm, 60°C and vacuum during one hour.

Once that the epoxy mixtures were finished, the stoichiometric amount of curing agent was incorporated to the resin maintaining the temperature at 60°C and stirring at 50 rpm, during 10 minutes. After that the reactive mixture was placed into pre-heated steal molds (plates and test specimens) and cured in two stages, in order to minimize the internal stresses. The used curing program is schematically illustrated in Figure 3.3.

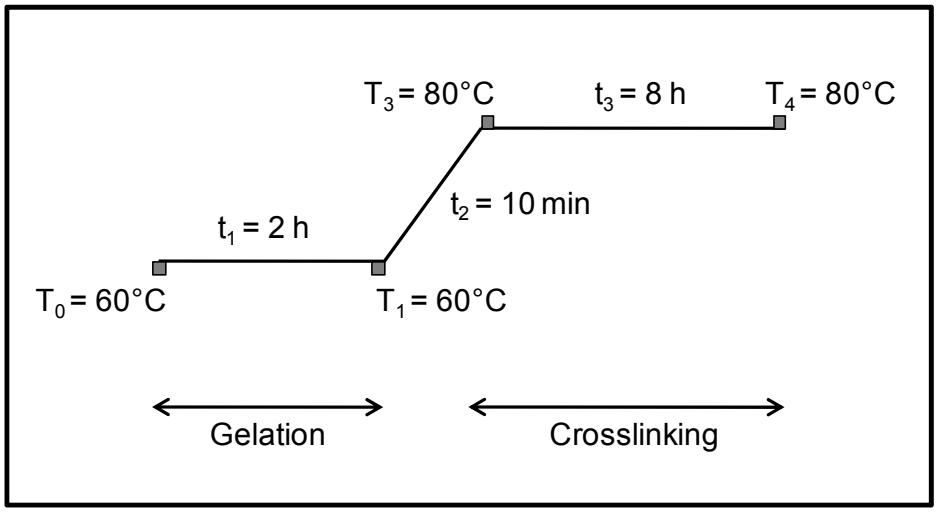

Figure 3.3: Curing program to EP and modified matrices.

3.3 Matrix Characterization

3.3.1 Rheology

The viscosity is one of the most important properties when a material has to be processed by RTM. Its value measures the resin ability to flow inside the mould and to produce final parts with homogeneous mechanical properties and good superficial finishing.

The viscosity of the modified resins was determined using a plate-plate rheometer ARES, Rheometric Scientific, USA; with 45 mm plates, in isothermal (25°C) and temperature sweep (25-60°C, rate 1°C/ min) modus, at frequency of 60 rad/s and 50% dynamic strain.

3.3.2 Density

The density of the obtained materials was determined using a balance Mettler ME 210250, Mettler Toledo, Germany; based on the Archimedean Principle. Small specimens (4x4x10 mm^3) were used to make the measurement and for statistic reasons, five specimens per material were evaluated.

3.3.3 Tensile Test

The test were performed on a universal testing machine Zwick 1474, Germany; with a 10kN load cell, 10 mm/min of cross head speed and precision sensor-arm extensometer to determine the specimen strain; according with the standard ISO 527 using molded specimens type 5A, in compliance with same standard.

3.3.4 Dynamic Mechanical Thermal Analysis

The viscoelastic response of the obtained materials was studies by Dynamic Mechanical Thermal Analysis; Eplexor 150N, Gabo Qualimiter, Germany. The test was carried out using rectangular prism specimens (50x10x4 mm^3) in tensile mode at 10 Hz frequency, temperature range -100 to 150°C and heating rate of 2°C/min.

3.3.5 Fracture Toughness

Fracture behavior of the modified epoxies was investigated by means of the compact tension (CT) specimens according with the standard ISO 17281. The configuration of the CT specimen is presented in Figure 3.4

The machined notch was sharpened by tapping on a razor blade, method that produces the smallest pre-crack tip radius and also low residual stresses around it. The fracture behavior of epoxies is highly sensitive to pre-cracking methods [68].

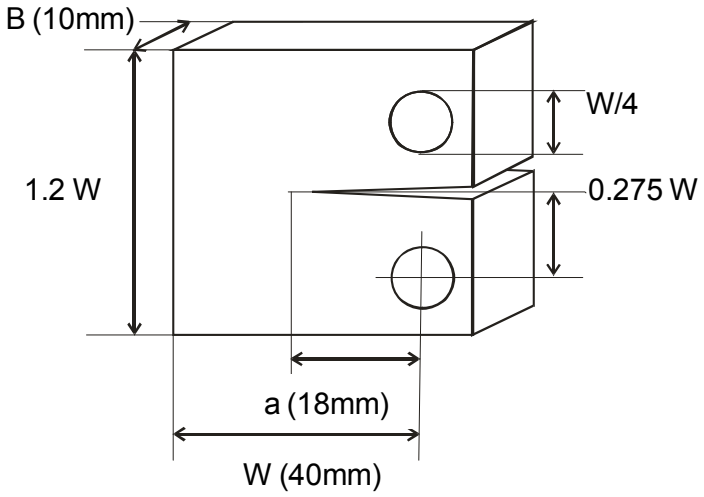

Figure 3.4: CT Specimen configuration and dimensions

The test was carried out on a universal testing machine Zwick 1445, Germany; using a 5 kN load cell and constant cross head speed of 1 mm/min. From the load vs. time curve plot the value for K_{Ic}, also referred to as the fracture toughness, can be calculated from the expression:

$$K_{IC} = \frac{P}{B\sqrt{W}} \cdot f(x) \qquad (3.1)$$

Where P is the maximum force in the load-displacement curve, B and W refer to the dimensions of the specimen, and f(x) is a shape factor defined from the ratio a/W, where a is the length of the pre-notched crack.

The critical stress energy release rate in a plane strain state, G_{IC} may also be calculated from K_{IC}, using the expression

$$G_{IC} = \frac{\left(1-\nu^2\right)K_{IC}^2}{E} \tag{3.2}$$

where E corresponds to the Young's modulus and ν is the Poisson's ratio, which was set to be a constant (0.35) for epoxy nanocomposites.

K_{IC} and G_{IC} are intrinsic parameters that do not depend on crack length and specimen size. They depend only on the test temperature and the strain rate. Normally, values of K_{IC} at room temperature range from 0.5 MPam$^{1/2}$ for very brittle materials to 2.0 MPam$^{1/2}$ for toughened thermosets. The values of G_{IC}, which depend also on the tensile modulus, are in the range of 100 J/m^2 to 2000 J/m^2 [52].

3.3.6 Hardness

Hardness has conventionally been defined as the resistance of a material to permanent penetration by another harder material. Instrumented indentation hardness is a technique that uses an electromagnetic force to press an indenter against a specimen. Pressing force is increased at a constant rate and the indentation depth is automatically measured. During indentation dynamic hardness is measured considering the hardness that corresponds to both plastic and elastic deformation. Figure 3.5 shows a typical load displacement hysteresis curve obtained from an elastic / plastic material as well as the schematic representation of the indent under load and in the unloaded condition.

The indentation hardness H is calculated from the test force, F, divided by the projected area of the indenter A in contact with the test piece at maximum load [69]:

$$H = \frac{F}{A\,h_C} \tag{3.3}$$

where h_c corresponds to the difference in depth between the surface profile under load and the one maintained once that load is removed.

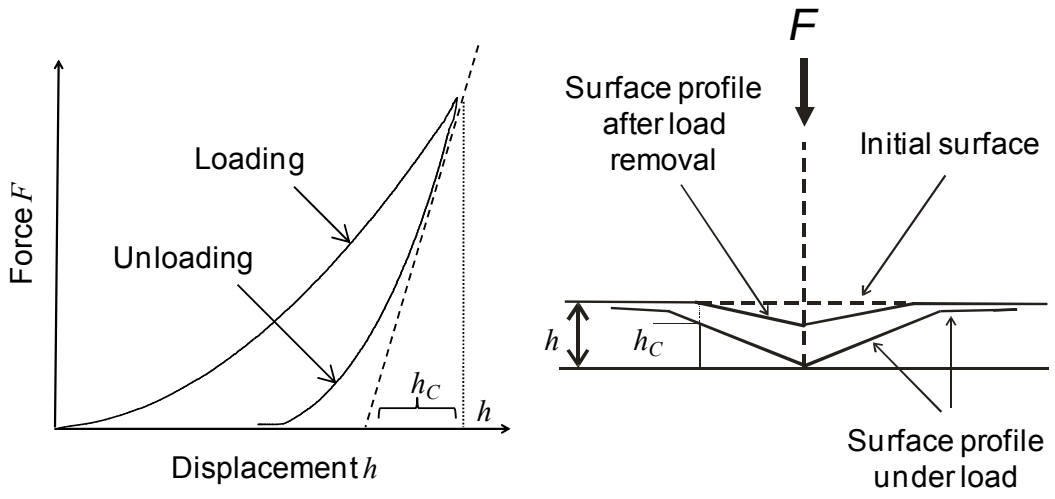

Figure 3.5: Schematic representation of the hardness measurement cycle.

Microhardness tests were performed using an ultra-microhardness tester DUH-202, Shimatzu Ltd. The test was conducted at room temperature under controlled loading of 1000 mN at a loading/unloading speed of 35 mN/s. Average values with standard deviations were reported from five measurements of each composition.

3.4 Composites Manufacture

Fiber reinforced plates were obtained according with the following steps. The glass fabric (32 plies) was placed into the mold, with dimension 300 x 300 x 5 mm^3. The mold was closed, and preheated at 60°C; vacuum (-1 bar) was also applied to eliminate the trapped air and create a negative pressure, that facilitate the resin flow. Epoxy resins was conditioned at 60°C, using a water bath, when the desired temperature is reached, the stoichiometrical quantity of curing agent was incorporated to the resin by stirring at 50 rpm during 10 min, air bubbles into the mixture were eliminated when required using an ultrasonic bath for no longer as 5 minutes. The reactive system (resin-hardener) was injected into a pre-heated mould at 60°C and 2.5 bars. The curing process of RTM plates was carried out following the program described to modified matrices (Figure 3.3). During the gelling phase the injection pressure was maintained but the crosslinking was completed at normal pressure.

3.5 Composites Characterization

3.5.1 Tension

Tensile properties of the composites were determined according to the standard ISO 527-4. Specimens type 2, with dimensions 250x25x5 mm^3, cut from the final RTM laminates at warp fiber direction, and using bonding were tested in a universal testing machine Zwick 1485, Germany; using 250 kN load cell, and 2 mm/min of cross head speed. Precision sensor-arm extensometers were used to measure the specimen strain during the test.

3.5.2 Compression

Fiber-reinforced composites are very sensitive to compression loads. The compressive behavior is much more critical than the tensile one for most of the service applications of this class of advanced materials [70]

The compression test was carried out according to the standard ISO 14126; using specimens type Celanese, with dimensions 110x10x 5 mm^3, cut from the final RTM laminates at warp fiber direction, without stocked tabs. A universal testing machine Zwick 1485, Germany; was used with 250 kN load cell, and 1 mm/min of cross head speed.

3.5.3 Interlaminar Fracture

The composites are anisotropic materials, and have different properties in different directions. The excellent properties of composites can be realized only if the loading direction coincides with the reinforcement direction. In many applications the loading is multidirectional and in these cases delamination, matrix cracking and other type of fracture can occur. The interlaminar fracture is commonly encountered in the form of delamination or interlaminar cracking, which is one of the predominant modes of damage in composite structures. The growth of delamination is resulted in stiffness degradation and eventual failure of the composite structure. The resistance to delamination is known as the interlaminar fracture toughness, it is an important composite property and widely acknowledged by designers.

Damage tolerance of composites was evaluated in unidirectional mode (Mode I), fulfilling the standard ASTM D 5528-01. Double Cantiliver Beam (DCB) test is conducted in a displacement controlled loading; it yields a stable crack growth which makes it well suited for energy release rate measurements. The DCB test simulates the delamination growth by interlaminar normal (peel) stress.

DCB specimens were prepared using aluminum piano hinges. The test was carried out in a universal testing Zwick machine with load cell of 1 kN and cross head speed of 1 mm/min.

The compliance calibration method was used to calculate the mode I interlaminar fracture toughness [98]. The compliance method uses the visually observed crack onset and the corresponding compliance to develop $Log\ C$ versus $Log\ a$ plot; the slope of this plot, n, can be used to calculate G_{IC}.

$$C = K\, a_d^n \tag{3.4}$$

where $C = \delta/P$; K is a constant, and a_d is the length of delamination. Then G_{IC} is determined by:

$$G_{IC} = \frac{nP\delta}{2b\, a_d} \tag{3.5}$$

Where δ is the load point displacement; P is the load; and b is the width of the specimen.

3.5.4 Interlaminar Shear Strength

The interlaminar shear strength test (ILSS) was carried out in accordance to the standard ISO 14130 using specimens short-beam with dimensions 20 x 10 x 2 mm^3, cut from the final RTM laminates at warp fiber direction. The test was performed in a universal testing machine Zwick 1485, Germany; at 1 mm/min of cross head speed.

The interlaminar shear strength, in MPa, was calculated from the equation:

$$\tau = \frac{3}{4}\frac{P}{bB} \tag{3.6}$$

Where P is the load at break or the maximum load, b is the specimen width and B the specimen thickness.

3.6 Microscopy

3.6.1 Transmission Electron Microscopy (TEM)

TEM images were taken in LEO 912 microscope, Omega GmbH, Germany; with accelerator voltage of 120kV. Thin sections (app. 100 nm) of the specimens were cryo-cut with a diamond knife at -120°C and used without staining.

3.6.2 Scanning Electron Microscopy (SEM)

The fractured surfaces of the samples were studied in a scanning electron microscope SEM JSM 5400, Jeol Ltd, Japan. The surfaces were sputtered, at a device SCD-050 Balzers, Liechtenstein; for 150 sec with a Pt/Pd alloy, prior to SEM investigation. The use of SEM was effective in order to investigate the filler distribution as well as the fracture mechanisms on the obtained materials.

4 Results and Discussion

4.1 Silica-Rubber Modified Matrices

4.1.1 Rheology

As mentioned, the viscosity of a resin employed in the RTM process is of supreme importance. As a prerequisite, the resin viscosity has to range between 200-500 mPa·s throughout the whole impregnation process, to ensure easy processability and complete wetting of the fabric inside the mould.

In general the addition of fillers to the epoxy resin produces an increment in its viscosity; owing to the particles represent an extra resistance to flow, independently of their nature. The viscosity change of the epoxy resin as function of the filler content is presented in Figure 4.1. It is observed that in the case of SiO_2 nanocomposites, the viscosity increases almost in direct proportion at rising particle content. Thus, the resin containing 3 vol.-% SiO_2 records a viscosity 13% higher than EP (η_0 = 450 mPa*s), while the addition of 8 vol.-% SiO_2 to EP increases its viscosity almost 50% up to 670 mPa*s.

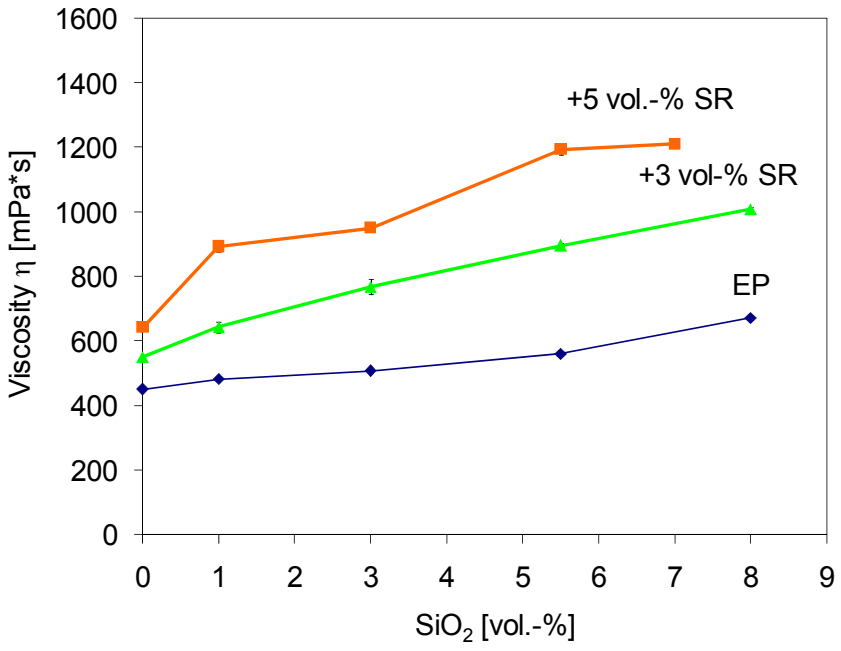

Figure 4.1: Dynamic viscosity of silica-rubber modified epoxy resins at 25°C

The addition of micro-sized silicone rubber to EP has stronger impact on its viscosity than the rigid silica nanoparticles. EP containing only 3 vol.-% SR records a viscosity increased in more than 20%, and the addition of 5.5 vol.-% SR to EP means a viscosity increment of almost 50%. The effect of SR on the viscosity of nano-modified epoxy resins is also higher that on the EP one. Hybrid compounds with 3 vol.-% SR have viscosities around 50 % higher than the nanocomposites with same silica content; and the addition of 5.5 vol.-% SR to the nanocomposites increase their viscosity approximately in 90%.

The changes in the epoxy resin viscosity, as a result of its modification with nanosilica and micro-rubber particles, can be better appreciated from the 3D representation shown in Figure 4.2

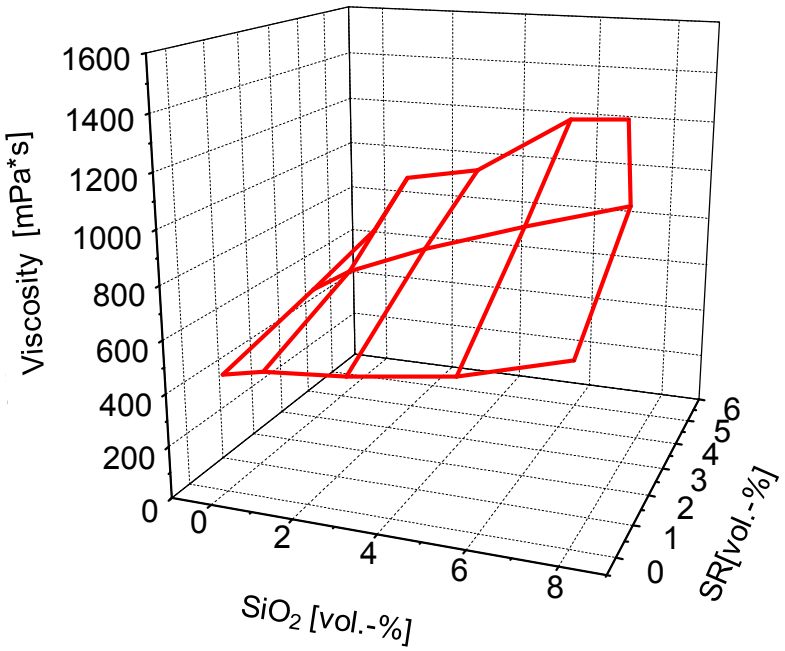

Figure 4.2: Dynamic viscositiy of silica-rubber modified epoxy resins at 25°C. 3D representation.

It is observed that the resin viscosity increases almost linearly as function of both filler content, but the slope of the lines parallel to y- axis (as function of the SR content) is considerably higher than the slope of the lines traced along the x-axis (as function of silica content).

Thus, the epoxy resin viscosity, may be approximated from its composition using the expression

$$\eta = \eta_0\left[1 + 0.06V_{f1} + 0.12V_{f2} + 0.02V_{f1}V_{f2}\right] \quad (4.1)$$

where V_{f1} and V_{f2} correspond to the volume fraction of nanosilica and silicone rubber respectively, and the proposed empirical constants have to be necessarily determined by the filler properties, but also by the filler-matrix bonding.

As mentioned, it is important to know the flow behavior of composite materials, because this property determines their processability. The theory defines polymer filled systems as suspensions of particles in liquids and their viscosity approximation starts with the Einstein equation [71], that only holds for rigid particles in extremely low concentrations. Many other equations have been proposed for the viscosity of suspensions but most of them are also limited by the particle form and concentration. Among the most useful equations, the Roscoe model fits experimental data of all kinds of suspensions, it is expressed as [72]:

$$\eta = \eta_m\left(1 - \frac{V_f}{V_{\max}}\right)^{-2.5} \quad (4.2)$$

where V_f is the volume fraction of filler and V_{max} is the maximum volume fraction that the filler can have [73]. It implies that the relative viscosity depends only on V_{max} for particles of any size, form, size dispersion and also of different materials.

To determine the Roscoe's viscosity of silica nanocomposites V_{max} =0.632, considering spherical particles, no agglomerated and in close packing. To the hybrid compounds V_f corresponds to the volume fraction occupied of both types of fillers and V_{max} =0.37 considering agglomerated spherical particles in close packing. It is because SR particles as much bigger than particles and physically can be considered as agglomerates that reduce considerably the maximum volume fraction that filler can occupy. Roscoe model results and obtained experimental data are compared in Figure 4.3.

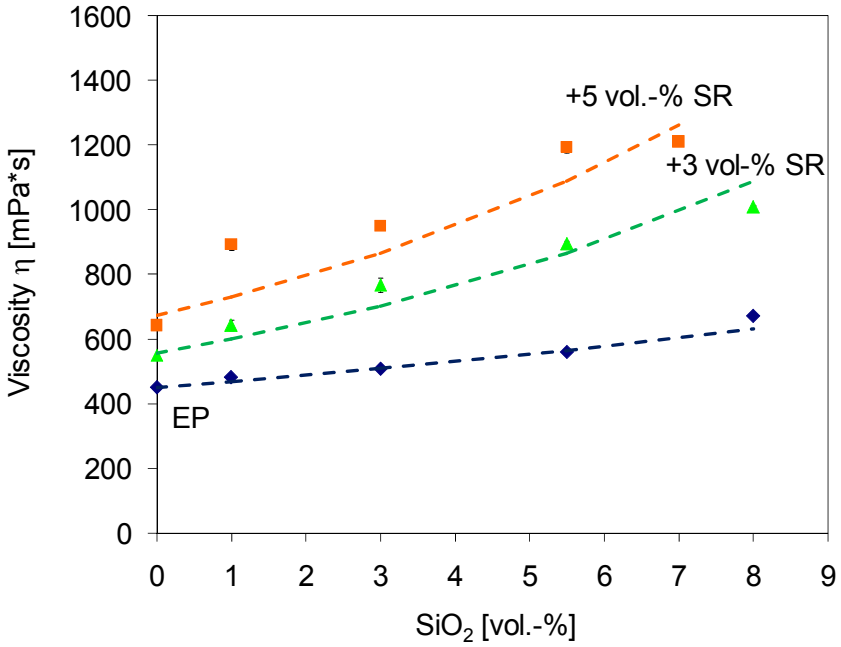

Figure 4.3: Dynamic viscosity from Roscoe's model (dotted lines) compared with experimental data to silica-rubber modified epoxies

No important deviation is observed between theoretical and experimental records, which means that the selected method is very good to approximate the viscosity changes induced to the epoxy resins, by addition of silica nanoparticles and micro-sized rubber.

From the obtained results it is clear that at room temperature, most of the obtained modified epoxies have viscosities much higher than the recommended to the RTM process. However, it is well know that the viscosity o a fluid depends directly on its temperature. Higher fluid temperature means higher molecular mobility and consequently the viscosity goes down. On this basis, changes on viscosity of the obtained epoxies were determined as function of the temperature. Figure 4.4 shows these viscosity changes of representative filled compounds.

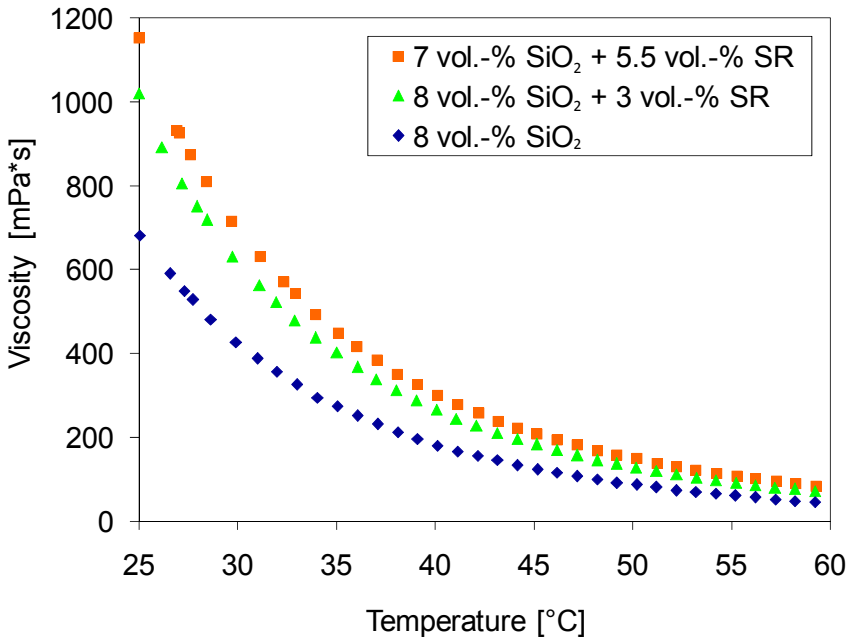

Figure 4.4: Viscosity change as function of the temperature to silica-rubber modified matrices.

It is obvious that once that the silica nanocomposites are heated over 30°C, and the epoxy hybrid compounds reach temperatures over 40°C, they might be successfully processed by RTM. However, their curing behavior has to be carefully evaluated before taking a decision about the right temperature of pre-conditioning and injection.

4.1.2 Curing

Rheological properties depend also on the curing behavior of the resins. During the curing process, the viscoelastic characteristics of epoxy resins change continuously. In the early cure stage, the epoxy resin is in liquid state, thus, cure reaction takes place initially in a continuous liquid phase. Whit the advance of the cure reaction, ramification occurs up to a critical extent, at which all the epoxy molecules are bonded together in a network, this critical value is called gel point. At the gel point, epoxy resin changes from liquid to a rubber state. It becomes very viscous and thus difficult to be processed. This process is schematically illustrated in Figure 4.5

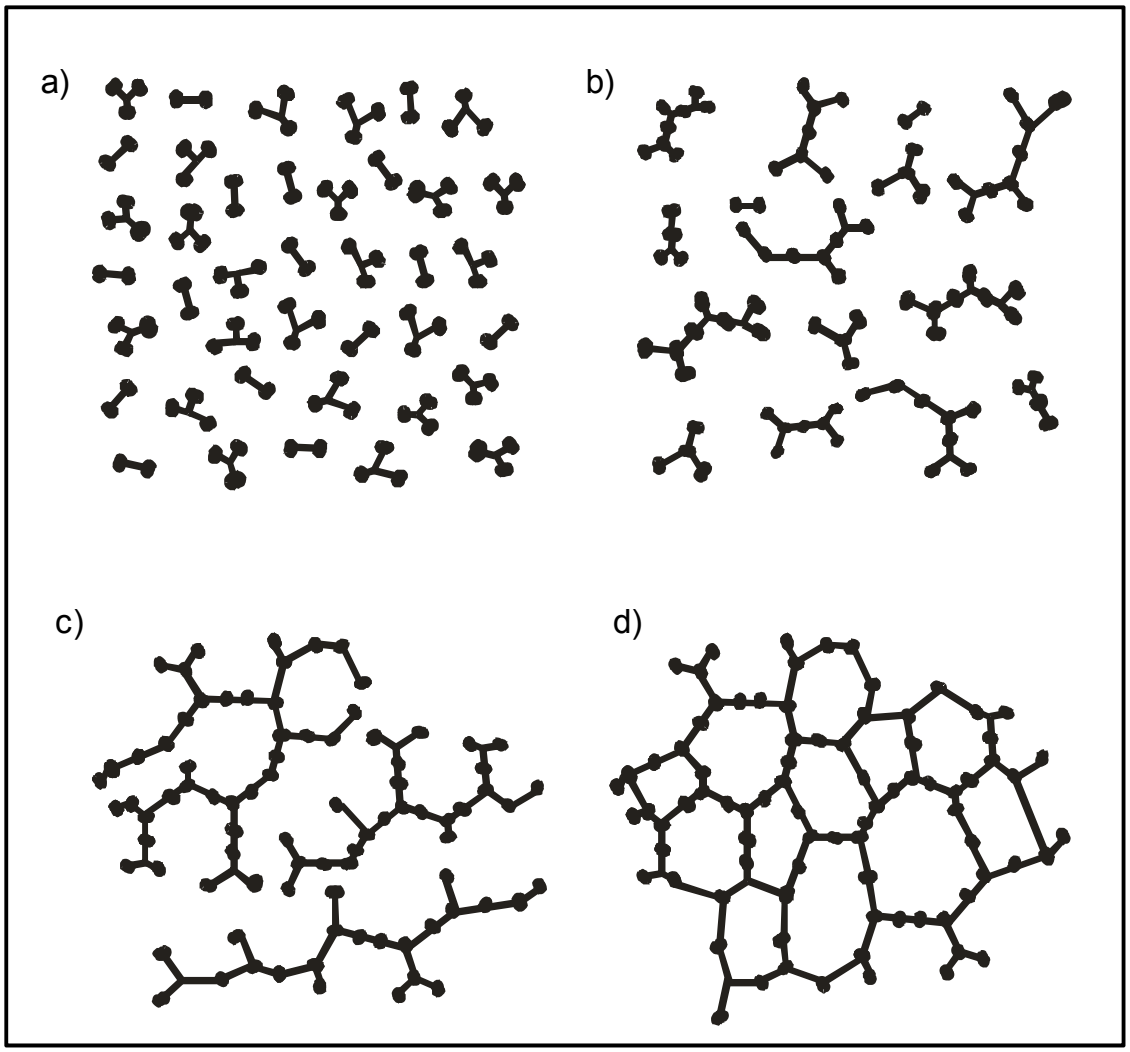

Figure 4.5: Schematic illustration of the cure progression due to a stepwise polymerization: a) Prepolymer and curing agent before curing; b) Reaction beginning, formation of oligomers; c) Gelation, all molecules are linked to a polymer chain; d) Fully cured system, crosslinked tridimentional network. [74]

The rheological behavior of a reacting system is governed by two effects; the first related to the molecular structural changes induced by the cure reactions and the second associated to the variation of the segmental mobility determined by temperature variations. At fixed temperature, any variation in viscosity is determined by changes in molecular distribution

The curing behavior rules the chemical structure of the final polymer net and determines in great measure the properties of the composite products. Thus, it is neces-

sary to determine the cure progression of the obtained modified epoxy resins, in order to define the effect of the fillers in the curing behavior of the matrix, and also to have a reference, to establish their optimal RTM molding parameters.

During the rheometry test it is measured the evolution of the viscosity of the reactive system as time function, up to the moment when the gel point takes place. Gel point is determined by the crossover between Storage modulus (G') and Loss modulus (G''), point at which the damping $tan\ \delta$ equals 1. The profiles of the viscosity at different isothermal cure temperatures for a representative epoxy formulation are presented in Figure 4.6.

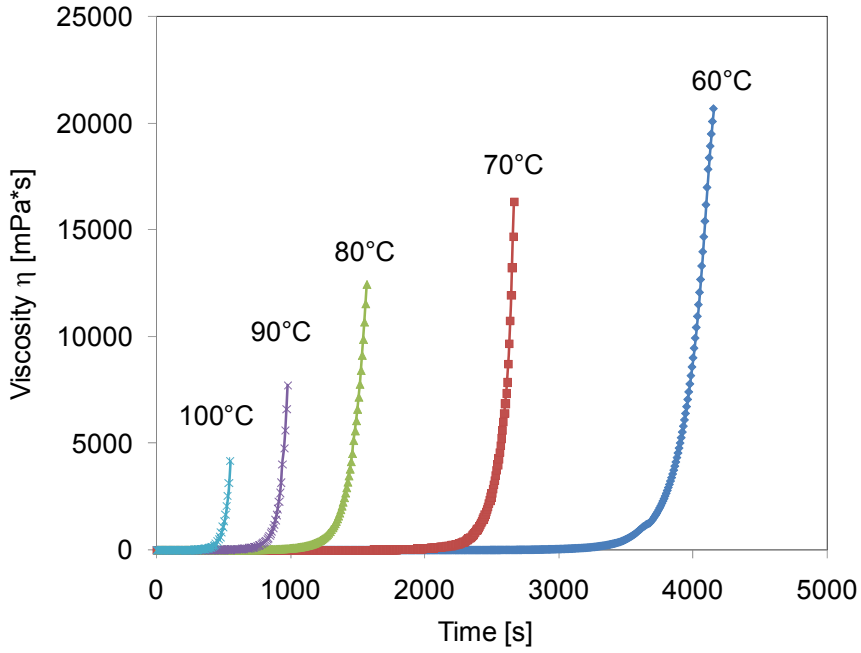

Figure 4.6: Viscosity profiles of the isothermal curing to the nanocomposite with 8 vol.-% SiO_2

Also the findings obtained from the isothermal viscosity profiles of some of the silica-rubber modified epoxies are summarized in Table 4.1.

Table 4.1: Gel properties as function of the cure temperature for representative silica-rubber modified epoxies.

EP					
Temperature [°C]	60	70	80	90	100
t_{gel} [s]	4860	2920	1768	955	605
Viscosity [Pa*s]	19.2	15.3	12.0	6.6	4.2
Modulus $_{gel}$ [Pa]	27.1	21.6	16.9	9.3	6.0
E_a [kJ/mol]	54.5				

3 vol.-% SiO_2					
Temperature [°C]	60	70	80	90	100
t_{gel} [s]	4495	2762	1625	947	599
Viscosity [Pa*s]	13.3	10.9	8.6	5.4	3.7
$Modulus_{gel}$ [Pa]	18.8	15.3	12.2	7.7	5.2
E_a [kJ/mol]	52.6				

8 vol.-% SiO_2					
Temperature [°C]	60	70	80	90	100
t_{gel} [s]	4186	2626	1570	979	553
Viscosity [Pa*s]	18.6	15.4	12.5	7.7	4.2
$Modulus_{gel}$ [Pa]	26.0	21.9	17.6	10.9	5.9
E_a [kJ/mol]	51.9				

8 vol.-% SiO_2 + 3 vol.-% SR					
Temperature [°C]	60	70	80	90	100
t_{gel} [s]	4224	2613	1537	955	588
Viscosity [Pa*s]	14.8	12.1	9.6	6.6	4.2
$Modulus_{gel}$ [Pa]	20.9	17.2	13.6	9.3	6.0
E_a [kJ/mol]	51.1				

7 vol.-% SiO_2 + 5.5 vol.-% SR					
Temperature [°C]	60	70	80	90	100
t_{gel} [s]	4187	2582	1576	926	564
Viscosity [Pa*s]	19.1	15.1	12.9	6.6	3.7
$Modulus_{gel}$ [Pa]	26.8	19.9	18.3	9.4	5.2
E_a [kJ/mol]	51.9				

As the isothermal temperature increases, the gel time decreases. The relationship between gel time and temperature is analyzed by cure kinetics. The kinetic model for a dynamic curing process with a constant heating rate can be expressed in the following form:

$$\frac{d\alpha}{dt} = K(T)\ g(\alpha) \tag{4.3}$$

where $K(T)$ is the rate constant, which depends on the temperature T, and $g(\alpha)$ is a function only of the cure grade α. It may adopt different forms, depending on the cure mechanism [75].

The rate constant $K(T)$ can be further expressed by an Arrhenius equation:

$$K(T) = A_r e^{-E_a/RT} \tag{4.4}$$

Gel time, which was detected by the rheological measurement, varies with the isothermal cure rate of reaction. By integrating the Eq. (4.3) from zero time to gel time t_{gel}, the relationship between the cure grade and cure rate is obtained,

$$t_{gel} = \frac{1}{K(T)} \cdot \int_0^{\alpha_{gel}} \frac{1}{g(\alpha)} d\alpha \tag{4.5}$$

where α_{gel} is the cure grade at gel time.

Substitute Eq. (4.4) into Eq. (4.5) and take logarithm on both sides to get the relationship between the gel time and isothermal cure temperature,

$$\ln(t_{gel}) = \ln\left[\frac{1}{A_0}\left(\int_0^{\alpha_{gel}} \frac{1}{g(\alpha)} d\alpha\right)\right] + \frac{E_a}{R}\frac{1}{T} \tag{4.6}$$

According to Flory's expression, the cure grade at gel time α_{gel} depends on the functionalities of the epoxy systems only. So it can be considered a constant for a given epoxy systems regardless the cure temperature.

By considering the first term on the left side of Eq. (4.6) as a constant c, a linear relationship is obtained:

$$\ln(t_{gel}) = c + \frac{E_a}{R}\frac{1}{T} \tag{4.7}$$

From Eq. (4.7), the apparent activation energy can be calculated from the slope of the curve of $ln(t_{gel})$ vs. $1/T$.

Depending on the cure temperature, the cure reaction presents different kinetic. On this basis, low cure temperatures are preferred because they result in slow polymerization rate and of course in a more appropriate cure cycle for the composite manufacture. Slow reaction allows processing times large enough to warrant the right filling of molds and permits a better control of the process, decreasing the probability of defects on the product and increasing consequently its mechanical properties. However, the use of too low temperatures have to be avoided, due to it results in very large cure cycles and also may reduce significantly the cure degree.

In the studied case, it is considered, that the fill up completely the RTM mould takes around 10 min, and considering the pre-conditioning of the resin and other possible delays (transport , right closure of the pressure chamber, etc.) it is estimated that the time required to whole process is around 30-40 minutes. Therefore, an injection temperature of 60°C was chosen, which warrant low resin viscosities over a sufficient processing time (approximately 60 minutes).

4.1.3 Morphology

The hybrid epoxy nanocomposite modified with SiO_2 and silicone rubber is a complex system which performance depends strongly of its morphology. Figure 4.7 shows the TEM photographs of the modified epoxy resins.

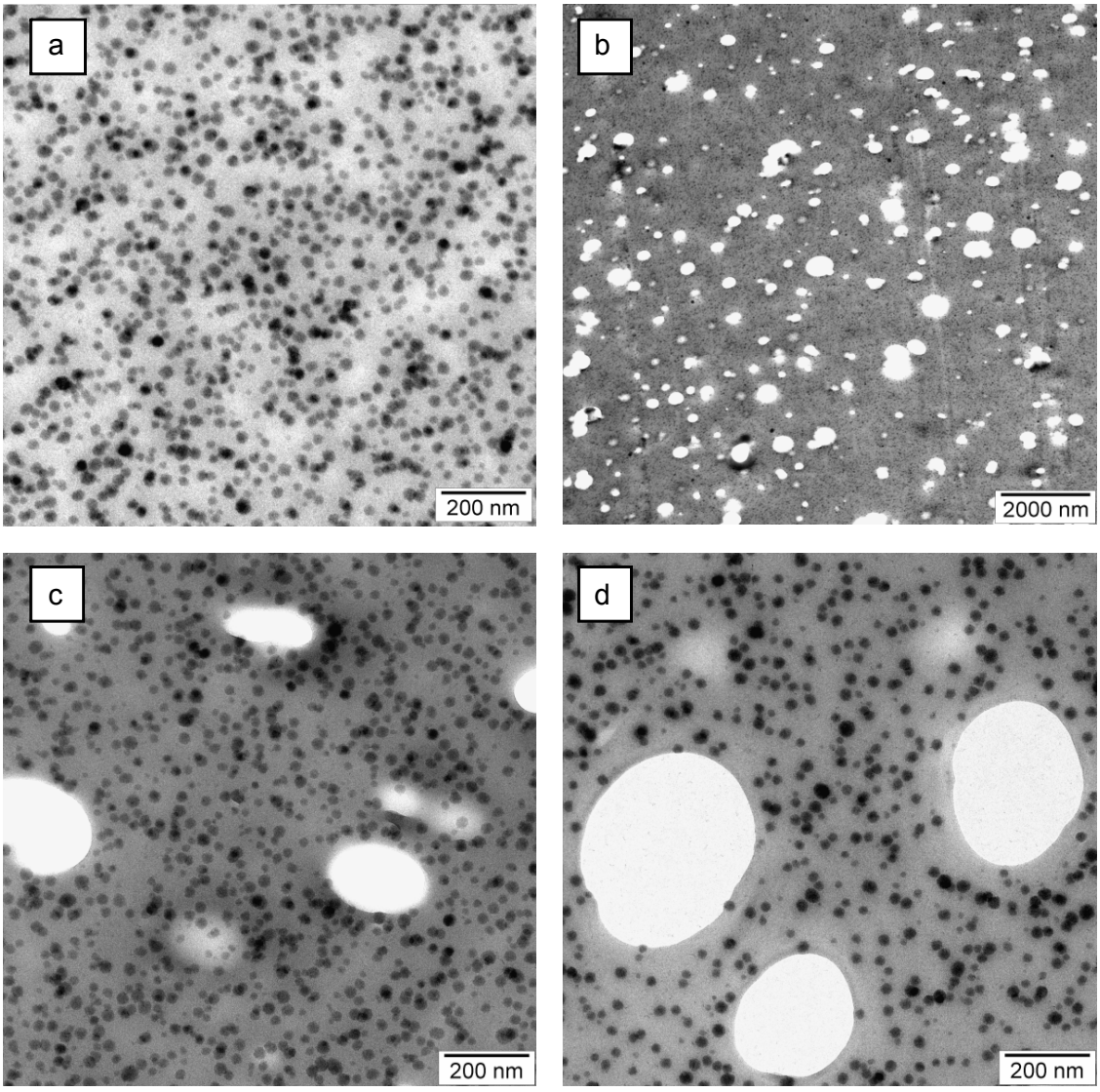

Figure 4.7: TEM photographs of the modified epoxy resins containing (a) 5.5 vol.-% SiO_2 and (b) 7 vol.-% SiO_2 + 5.5 vol.-% SR, c) and d) close up of b).

The nanoparticles are clearly evident in the specimens of both nanocomposite and hybrid compound. They are homogeneously distributed in the matrix bulk; neither agglomerates nor clusters are present, and the observed dark dots are the result of the overlapped particles in deep direction. The presence of rubber particles has no impact on the SiO_2 particle distribution.

It is no possible to see rubber particles, in Figure 4.7 (b), (c) and (d), because they were taken off of the matrix due to the shear forces during the specimen preparation (thin film cutting). However, the rubber particle distribution is evident from the location

of the micro holes inside the matrix bulk. Rubber particles are also uniformly distributed into the matrix, may be described as spherical formed and have a broad particle size distribution.

4.1.4 Density

The density is one of the most important properties of the cured epoxy resins, because it determines the weight of the final product, variable directly related with the cost of the energetic consume during its operation. The density of the epoxy resins modified with SiO_2 increases at rising nanoparticle content, because silica is denser than the polymer. Thus, the density of the pure epoxy resin is increased in more than 7% once that it is modified with 8 vol.-% SiO_2.

Table 4.2: Density of silica-rubber modified epoxy resins at 25°C

	EP		+ 3 vol.-% SR		+ 5.5 vol.-% SR	
Content SiO_2 [vol.-%]	Density [g/cm^3]	Std. Dev.	Density [g/cm^3]	Std. Dev.	Density [g/cm^3]	Std. Dev.
0	1.1524	0.0003	1.1479	0.0010	1.1432	0.0008
1	1.1637	0.0002	1.1636	0.0048	1.1564	0.0055
3	1.1841	0.0005	1.1921	0.0040	1.1741	0.0006
5.5	1.2053	0.0002	1.1992	0.0003	1.1968	0.0000
7	-------	-------	-------	-------	1.2102	0.0000
8	1.2339	0.0005	1.2230	0.0004	-------	-------

The addition of silicone rubber to the epoxy formulation, results in compounds with slightly reduced density. This is because the added particles are lighter than the polymer matrix. However, the effect of SR on the matrix density is less representative than the one induced by the hard silica particles. The addition of 5.5 vol.-% SR to EP and nanocomposites cause only a marginal reduction on their densities (lower than 2%).

4.1.5 Tensile Properties

The tensile properties of the materials are summarized in Figure 4.8 and Figure 4.9. It is observed that the tensile modulus for the nano-modified epoxy resins increases almost directly with their SiO_2 content. The improvement in the mechanical performance can be observed even at low filler content. The tensile modulus of the pure epoxy resin (E=3.1 GPa) is increased by almost 9%, in the epoxy containing 1 vol.-% SiO_2 and for the nanocomposite having 8 vol.-% SiO_2, the tensile modulus is increased by more than 30%.

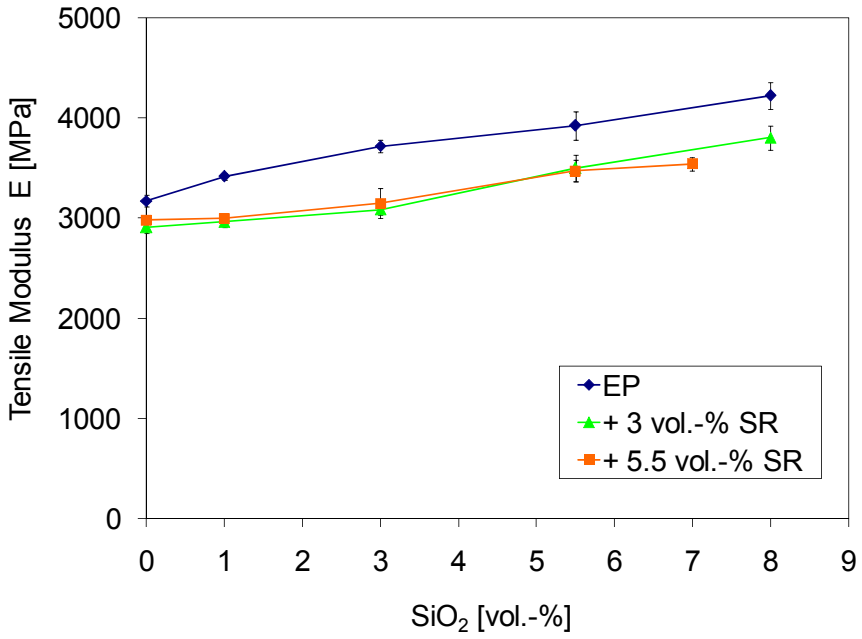

Figure 4.8: Tensile modulus of silica-rubber modified epoxy matrices

The addition of micro-silicone rubber, to the neat epoxy as well as to the nanocomposites, decreases their tensile modulus. However, the effect of the rubber on the epoxy modulus is lower regarding to the SiO_2. The modulus of the epoxy matrices is reduced by almost 9%, when 3 vol.-% of rubber is added. Meanwhile, the addition of 5.5 vol.-% of rubber represents an average reduction of 10% on the modulus. The reduction on the modulus of the hybrid compounds only depends on the amount of rubber present in them and occurs in the same proportion for all, neat and nanomodified, epoxy resins.

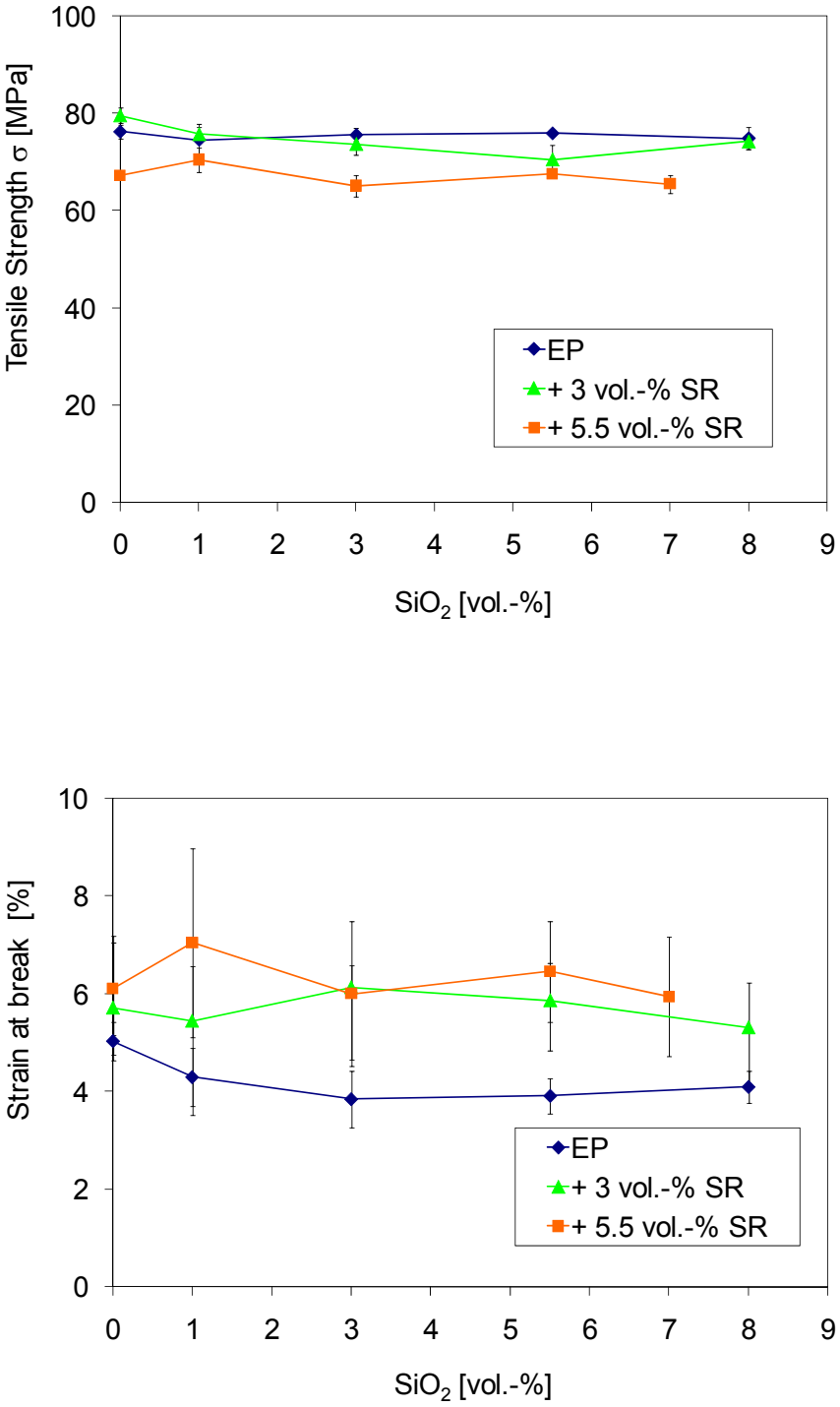

Figure 4.9: Additional tensile properties of silica-rubber modified epoxy matrices

The tensile strength seems to be independent of the nano-SiO_2 content. It remains almost constant for all silica nanocomposites. Only marginal reduction on strength is recorded, but no clear decreasing tendency is observed. Considering that the ceramic particles have much higher strength that the polymer matrix and their size generates a wide interfacial area per unit of unit volume, it was expected an increment in strength. This suggests the interfacial bonding between particle and matrix is not strong enough to permit a good stress distribution in both composite phases.

The modification of EP and nanocomposites with rubber leads to a decrease of their tensile strength. The addition of 3 vol.-% SR results in an average reduction of 2% on the tensile strength, and the addition of 5.5 vol.-% SR means a fall in 10% of the same property. This phenomenon is due to the fact that, rubber domains act as stress concentrators and weak the epoxy matrix.

It is known that the addition of rigid fillers, to a polymer matrix, results in a detrimental of the strain at break; that is because of the hard particles practically do not elongate under load. In the studied nanocomposites this effect is clearly appreciated. The elongation at break of the neat epoxy and nanocomposites increases once that they are added with silicone rubber, due to the inherent extensibility of the rubber domains.

Scanning electron microscopy fractographs of tensile specimens reflect the fracture mechanisms of the obtained composites. Figure 4.10 shows that the fracture surface of the EP specimen presents some ribbons and fracture steps but also rather smooth areas in between, which are typical in brittle fracture. However, the addition of silica yields in a rougher surface. Large dimples with irregular shape are observed. These fracture is explained considering that, although the silica is very well dispersed into the matrix bulk it may exist regions where several individual nanoparticles are quite close to each other. These regions may cause stress concentration and create weak sites, and further triggering the formation of dimples under load. In hybrid compounds, the fracture surface presents no more dimple evidence but larger fracture paths, as result of a higher plastic deformation; sites of rubbers cavitation are also observed.

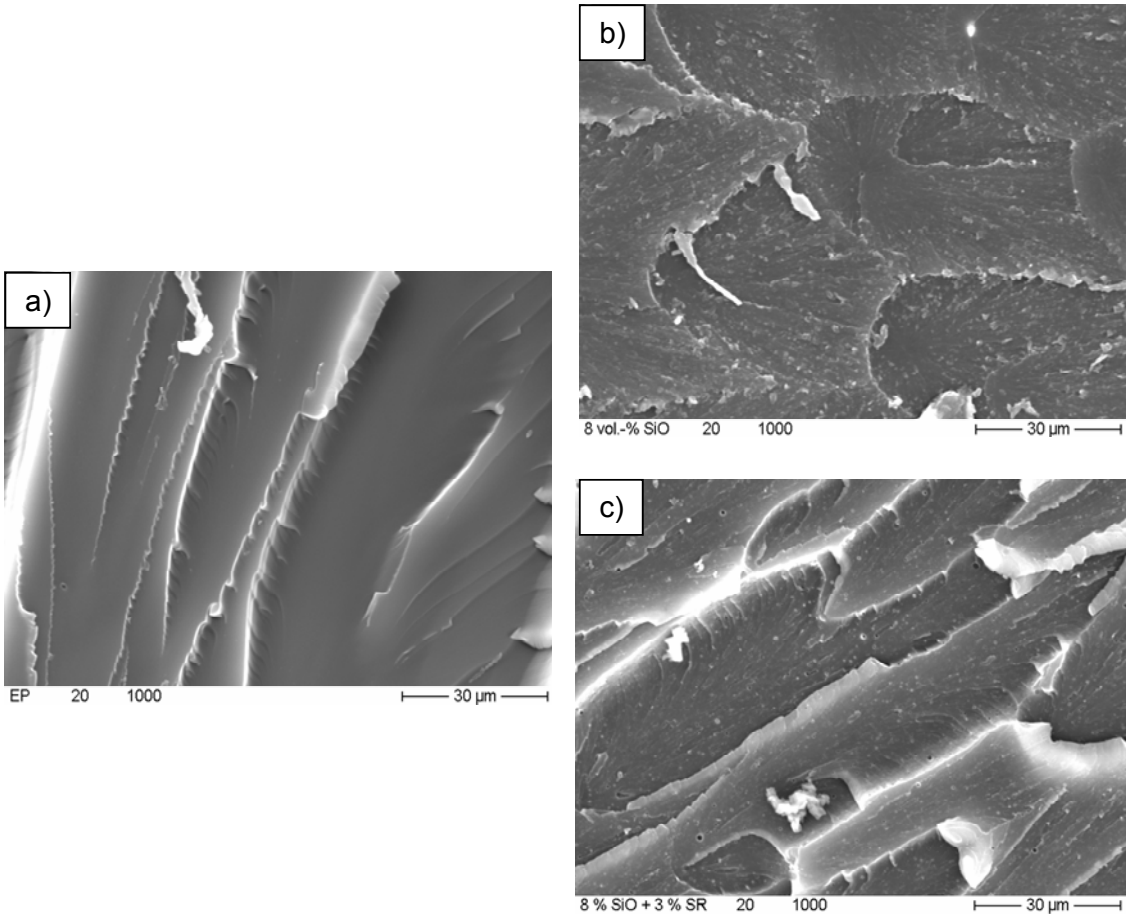

Figure 4.10: Fracture surfaces of tensile specimens a) EP, b) 8 vol.-% SiO_2, c) 8 vol.-% SiO_2 + 3 vol.-% SR

There are many theoretical models that can be used to predict the moduli of particle modified polymers among the most representative, simple and generalized are the Modified Rule of Mixtures, Halpin-Tsai and the Lewis-Nielsen ones [76,77].

The modified rule of mixtures, adjusted specifically to determine the stiffening efficiency of short fibers and particles, predicts the composite modulus as a function of the modulus of the polymer matrix E_m, the modulus of the filler E_f, and the volume fraction of filler V_f, including two correction factors [78].

$$E_c = \mu_t \, \mu_0 V_f E_f + (1 - V_f) E_m \tag{4.8}$$

The first one μ_t given by Cox [79] implies that the stiffening effect of the filler is mainly determined by its geometry, and is defined from of the particle dimensions (diame-

ter/length) and distribution, as well as the shear factor of the matrix and again the filler modulus. The value μ_o gives the correction of non unidirectional reinforcements depending on their degree of orientation and for all the studied systems equals 1.

The theoretical moduli obtained from Eq. (4.8) are shown in Figure 4.11 compared with the ones obtained experimentally.

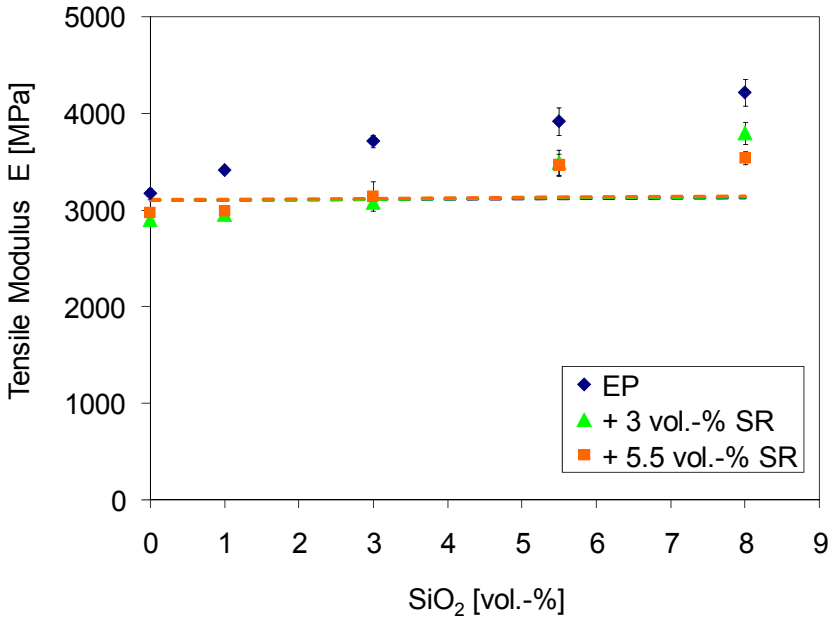

Figure 4.11: Experimental tensile modulus vs. modified ROM to silica-rubber modified matrices. The theoretical values (dotted lines) of the three compound series are superimposed.

The modified ROM underestimates markedly the experimental data. This is because of the spherical geometry of the silica and rubber particles ($l/d_p=1$) and their distribution, considered as a cubic system, generate very stumpy values of μ_t. Cox factor was maintained around 0.003 for both nanocomposites and hybrid modified matrices, along the analyzed range of volume fractions. In this manner the filler contribution to the compound modulus is practically ignored.

The Halpin-Tsai model predicts the composite modulus according to the expression:

$$E = E_m \left(\frac{1 + \varsigma \rho V_f}{1 - \rho V_f} \right) \tag{4.9}$$

where ζ is a shape factor defined from the reinforcement dimensions by the ratio w/t, where w is the particle length and t its thickness, but also depending on the loading conditions, and ρ is a constant described as function of the filler and matrix modulus as well as the shape factor.

To calculate the contribution of the SR to the hybrid compounds modulus, the nanocomposites with same content of silica were used as reference matrix. That means, the moduli of the nanocomposite, with the same volume fraction of ceramic than the corresponding hybrid compound, was substituted as E_m.

The parameters incorporated to the model were E_m=3.1 GPa [60], E_{Silica}=73 GPa [80], E_{SR}=0.5 GPa [81]. Both particles are spheres (see section 4.1.3), than w/t=1 and ζ=2.

The moduli calculated from Equation (4.9) for silica-rubber modified epoxies are presented in Figure 4.12 as dotted lines.

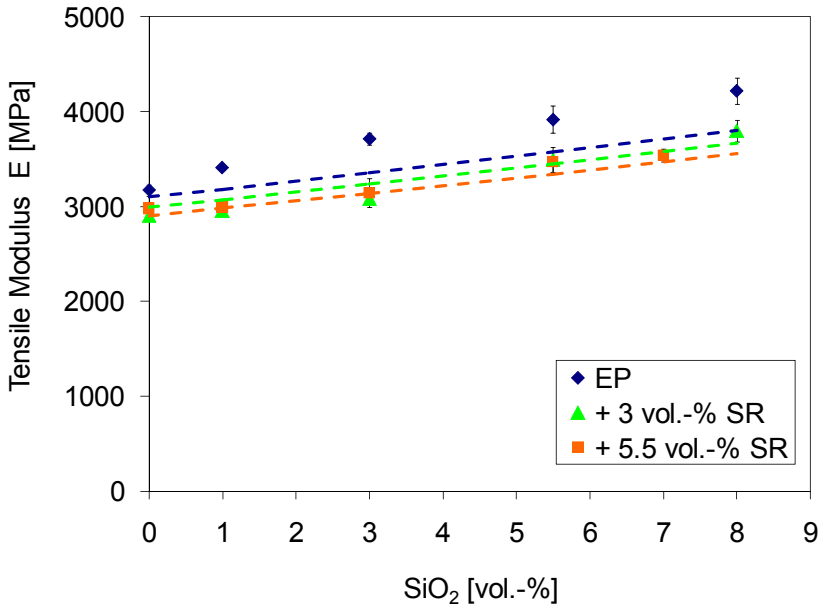

Figure 4.12: Experimental tensile modulus vs. Halpin-Tsai model to silica-rubber modified matrices.

The Lewis-Nielsen model predicts the composite modulus from the expression:

$$E = E_m\left(\frac{1+(k_E-1)\beta V_f}{1-\beta\mu V_f}\right) \qquad (4.10)$$

where k_E is the generalized Einstein coefficient (or intrinsic viscosity), β is a constant defined from the matrix and filler moduli and k_E , and μ is a function of V_f and V_{max}, (see section 4.1.1).

For both silica and rubber particles these constants were selected as V_{max}= 0.632, corresponding to random close packing nonagglomerated spheres; and k_E=2.1675, that is the Einstein coefficient for dispersed spheres with no slippage at the interface (2.5), reduced by a factor 0.867. This last because the Einstein coefficient have to be corrected when Poisson's ratio (ν) is lower than 0.5. For epoxy resins ν= 0.35.

The moduli calculated from Equation (4.10) for silica-rubber modified epoxies are presented in Figure 4.13 as dotted lines.

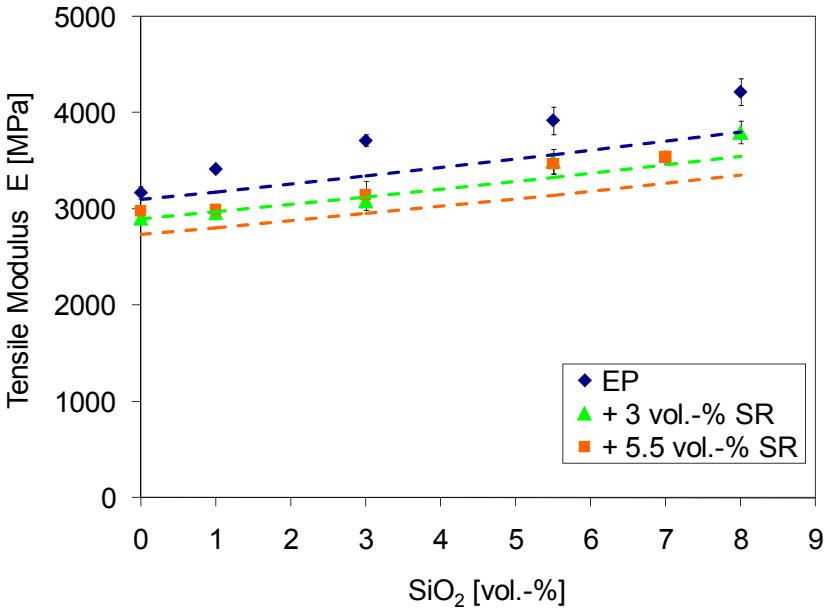

Figure 4.13: Experimental tensile modulus vs. Lewis-Nielsen model to silica-rubber modified matrices.

It is observed that Halpin-Tsai and Lewis-Nielsen models underestimate slightly the silica nanocomposite modulus. The difference between theoretical and experimental values in no case is higher than 10%. Both models predict also the hybrid compound moduli fairly accurately.

4.1.6 Dynamic Mechanical Thermal Analysis

The representative DMTA curves of the studied epoxy systems are summarized in Figure 4.14. It is observed that complex modulus of the epoxy resin increases by the addition of nano-SiO_2 and this effect is more pronounced at temperatures higher than T_g. Silica maintains its stiffening effect even in rubbery phase.

The hybrid composite containing 5.5 vol.-% SiO_2 + 3 vol.-% SR shows a complex modulus slightly lower than the nanocomposite with 5.5 vol.-% SiO_2 but clearly superior to the neat epoxy.

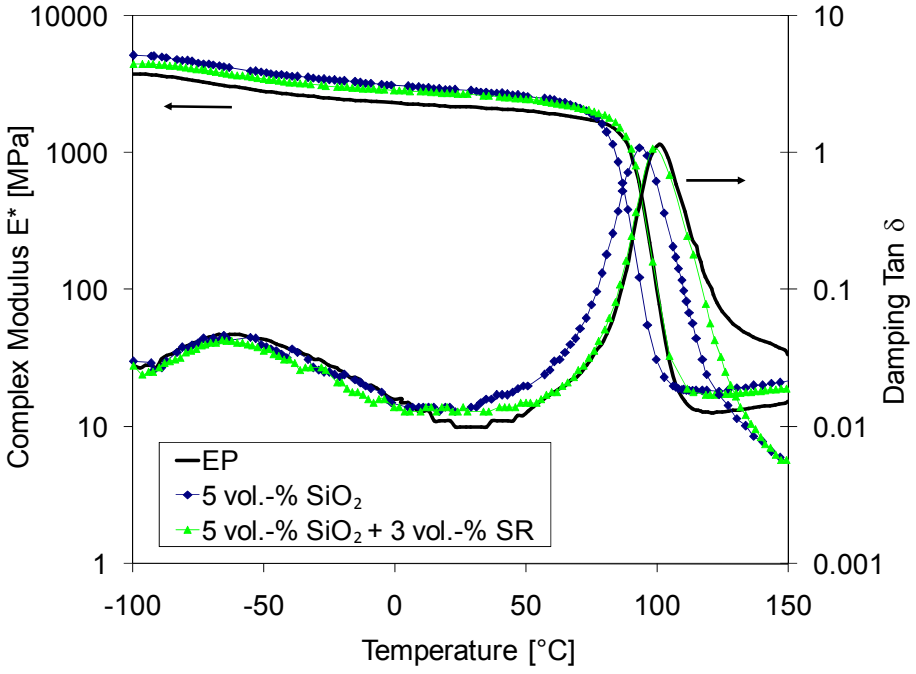

Figure 4.14: Complex modulus and damping as function of the temperature of silica-rubber modified matrices.

It is observed that complex modulus varies with the same tendency as elastic modulus, both of them increase at rising nanoparticle content, and they reduce when rubber is added. The rigid particles stiffen the polymer matrix and their effect prevails in the hybrid compounds, once the ratio of nanoparticles vs. rubber content is higher than one. Thus, the hybrid compounds with higher amount of nanoparticles, record moduli clearly higher than the neat epoxy.

Figure 4.15, shows the variation on T_g, defined as the maximum in the damping curve, as function of the filler content in the studied epoxy systems. The T_g, of the epoxy matrix is reduced due to the presence of nanoparticles. This reduction had been previously reported and is attributed to the plasticizing effect of the silica in the epoxy matrix [82,83]. The addition of rubber to the neat epoxy does not modify its T_g. However, the addition of rubber to the nanocomposites enhances their T_g and compensates the reduction on this property caused by the nanosilica. The presence of a thermo-stable rubber relieves the plasticizing effect of the nanoparticles on the polymer matrix.

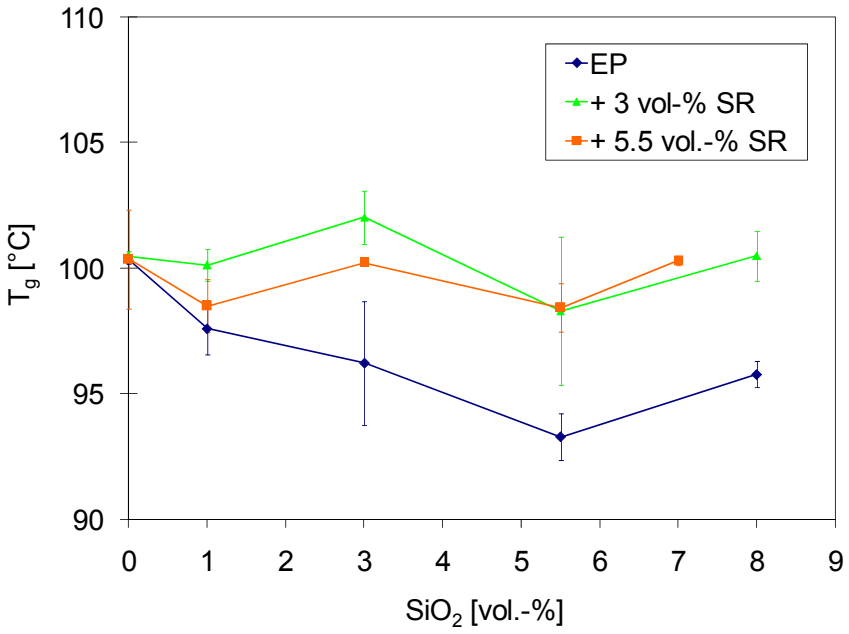

Figure 4.15: Glass transition temperature as function of the filler content of silica-rubber modified matrices

No important displacement is appreciated on the β-relaxation peak of the epoxy matrix, recorded approximately at -60°C.

4.1.7 Fracture Toughness

The characteristic load-displacement curves, from the fracture test, of neat and modified epoxy resins are comparative shown in Figure 4.16. The neat epoxy present initially abrupt fracture propagation and a second stage in which the failure propagates gradually up to total specimen breakage.

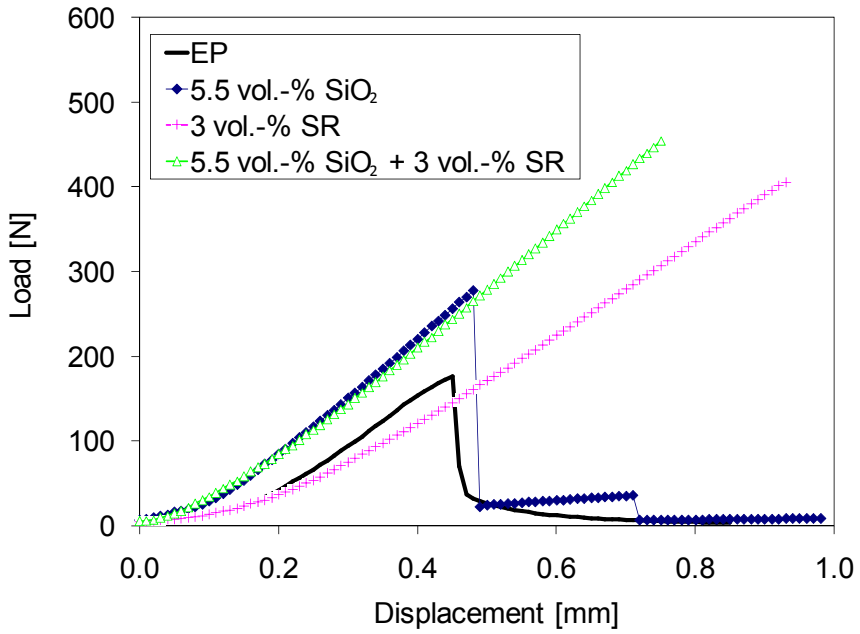

Figure 4.16: Characteristic load-displacement curves from the fracture test of silica-rubber modified matrices.

In the nanomodified epoxy, the fracture propagation begins at higher load than in the neat epoxy and present stick-slip steeps.

In the rubber modified epoxy resin and also the hybrid epoxy, the fracture propagation is also abrupt but total, once that the maximal force is reached. There is no evidence of plastic deformation previous the propagation begin. On this basis it is clear that the fracture process in the hybrid epoxy is dominated by the rubbery phase.

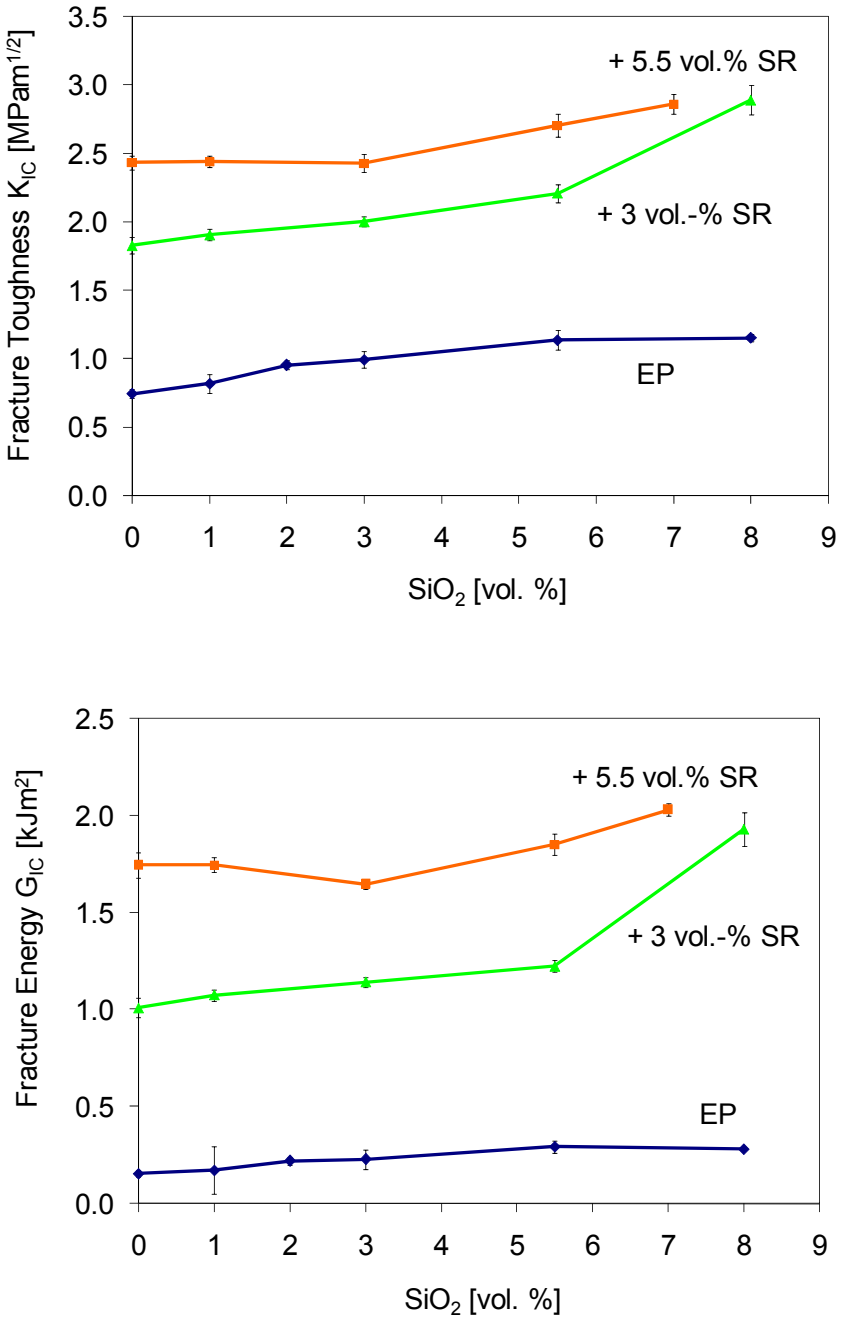

Figure 4.17: Fracture properties of silica-rubber modified matrices.

The improvement in fracture toughness and fracture energy of the epoxy matrix, as function of its filler content, is illustrated in Figure 4.17. The fracture toughness of the nanocomposites rises together with their silica content. The epoxy with 3 vol.-% SiO_2

records fracture toughness 35% higher than the EP, meanwhile for the sample containing 8 vol.-% SiO_2 the K_{IC} value has been increased in more than 55%.

The silicone rubber induces a superior toughness in the neat and nanomodified epoxy resins. The systems supplemented with 3 vol.-% rubber incremented their toughness around 150%, and the matrices added with 5.5 vol.-% rubber reach toughness three-fold higher in average.

The important increment of both fracture toughness and energy recorded by the hybrid epoxy systems containing higher proportion SiO_2 , appreciable for the change in curve directions, suggest the existence of a synergetic effect between the fillers. Hence, the epoxies, containing 7 vol.-% SiO_2 + 5.5 vol.-% SR and 8 vol.-% SiO_2 + 3 vol.-% SR, record fracture toughness nearly fourfold higher than EP, up to 2.86 and 2.89 $MPam^{1/2}$ respectively.

The nanocomposites log a simultaneous improvement of stiffness and toughness. However, their improved toughness seems to be so moderate compared with the toughness reached by the compounds containing rubber. On the other hand, the hybrid compounds exhibit a substantial increase in toughness but those who have low content of nanoparticles record moduli lower than the neat epoxy. However, the hybrid compounds containing higher proportion of nanoparticles fulfill the objective of having superior/toughness balance; they not only record no detriment in modulus, but also an appreciable improvement.

4.1.8 Fracture Mechanisms

The increase in the fracture toughness as a result of the particle modification can be explained analyzing microscopically the fracture surfaces of the pure and modified epoxy resins, Figure 4.18 and Figure 4.19.

The pure epoxy presents a smooth fracture surface with straight fracture lines parallel to the fracture propagation direction. This is the typical behavior of brittle materials.

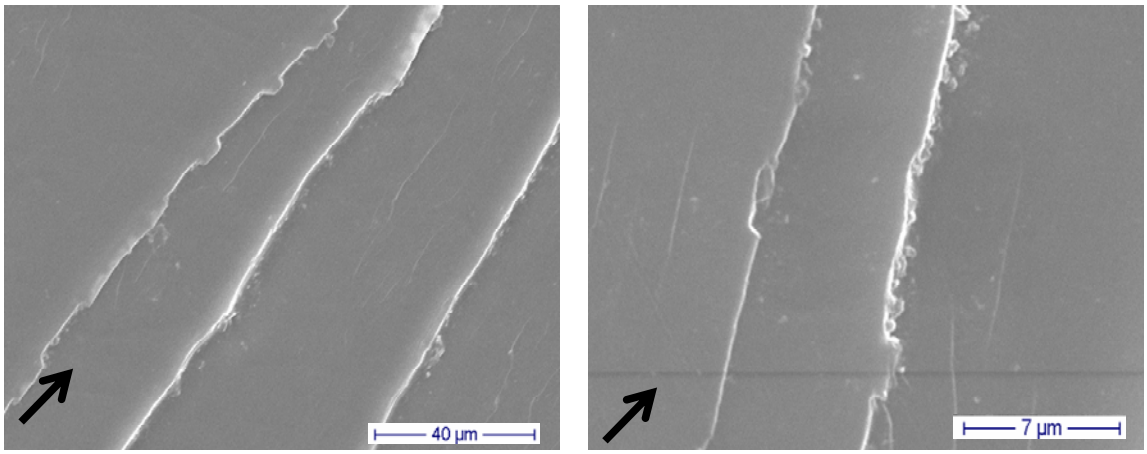

Figure 4.18: Fracture surfaces of a CT-specimen, Neat Epoxy.

Nanoparticle Toughening

The nanomodified epoxy, containing 5.5 vol.-% SiO_2, shows a textured surface with similar fracture features, but also with a variety of small paths, which reveal the existence of alternative fracture mechanisms attributed to the presence of particles [84].

Many researchers have shown that brittle polymers may be toughened by addition of rigid particles. The toughening effect of the particles has been explained in terms of specific fracture mechanisms, being the most recognized the crack pinning, crack deflection and plastic deformation [85,86].

Crack pinning and crack deflection

Crack pinning theory was first proposed by Lange [87] and further extended by Evans [88] and Green [89]. It proposes that a propagating crack trough a particle filled matrix will encounter the particles as obstacles and may be pinned. The crack front then moves on and extends by bowing, which leads to higher energy absorption before the crack propagation.

Crack deflection was described by Faber-Evans [90,91]. In this case it is assumed also that rigid particles act as obstacles to the crack propagation and the crack front is forced to move out of its initial propagation plane, by tilting or twisting.

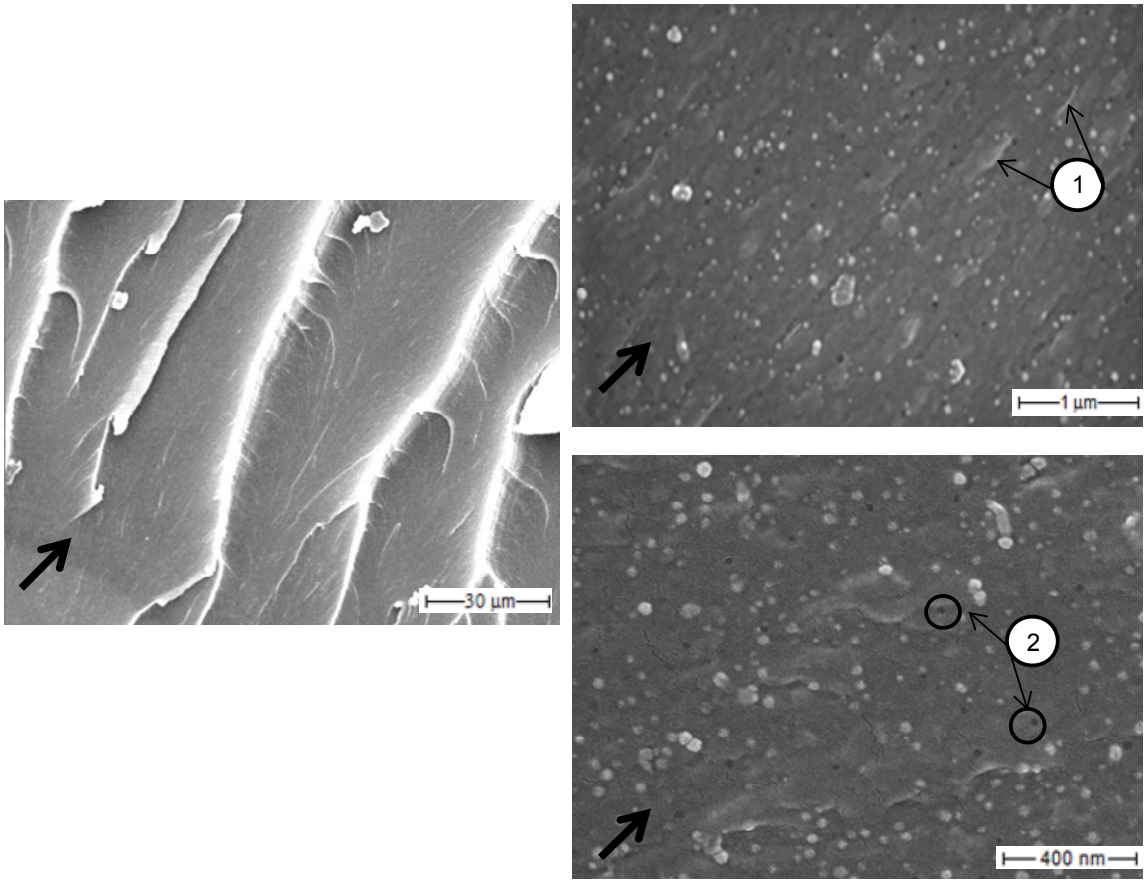

Figure 4.19: Fracture surfaces of a CT-specimen 5.5 vol.-% SiO_2 . Identified mechanisms: 1 Pinning, 2 Debonding

Both mechanisms assume that the filler particles are larger than the crack opening displacement (COD). The COD can be calculated from the expression [92]

$$COD = \frac{K_{IC}^2}{E\,\sigma_y}\left(1-\nu^2\right) = \frac{G_{IC}}{\sigma_y} \tag{4.11}$$

where σ_y is the yield stress of the matrix.

Crack deflection and pinning have been identified in epoxy resins filled with micro particles [93,94], but in nanocomposites their occurrence has been widely questioned. However, some authors have considered the presence of these mechanisms, based mainly on specific fractographic evidences [11,95].

For the silica nanocomposites, the COD falls in the range 2.1-3.8 μm, for the neat epoxy and the composite containing 8 vol.-% SiO_2 respectively, values those are much greater than the particle size. Hence, the existence of crack deflection and pinning is uncertain.

Higher magnification scanning electron micrographs, of nanocomposites fracture surfaces show characteristic paths, (tails) associated with crack pinning. Nevertheless, it is little probable that these mechanisms be the main responsible of the enhanced toughness of modified epoxies.

Plastic deformation

Epoxy resins, as most thermosetting polymers, are highly resistant to plastic deformation [96]. However, when they are modified with a second phase, the filler particles can induce shear yielding in the matrix by promoting a change in stress state. This may result from the formation of voids, cavities and debonding effects in the process zone at the crack tip state [97].

This effect is observed in silica nanocomposites. High resolution microscopy of the fracture surface of the matrix containing 5.5 vol.-% nanosilica, shows the presence of circular voids with average size 30 nm originated by particle debonding and due to its frequency it is most likely this mechanism to be responsible for the increase in toughness registered in silica nanocomposites.

Rubber Toughening

The hybrid composites show a typical fracture surface divided in two regions; the stress whitened and the fast-crack growth region. In the stress whitened region or plastic zone, ahead of the crack tip, the crack propagates slowly. It is characterized by a very rough fracture surface with numerous cavities and appreciable plastic deformation [98], Figure 4.20. The cavities in this region are larger than those in the fast crack section and massive shear bands connecting the cavitated particles are also observed.

The fast-crack growth region, located beyond the plastic zone, is characterized by rapid fracture propagation, smoother surface and some cavities of approximately same size as the undeformed rubber particles.

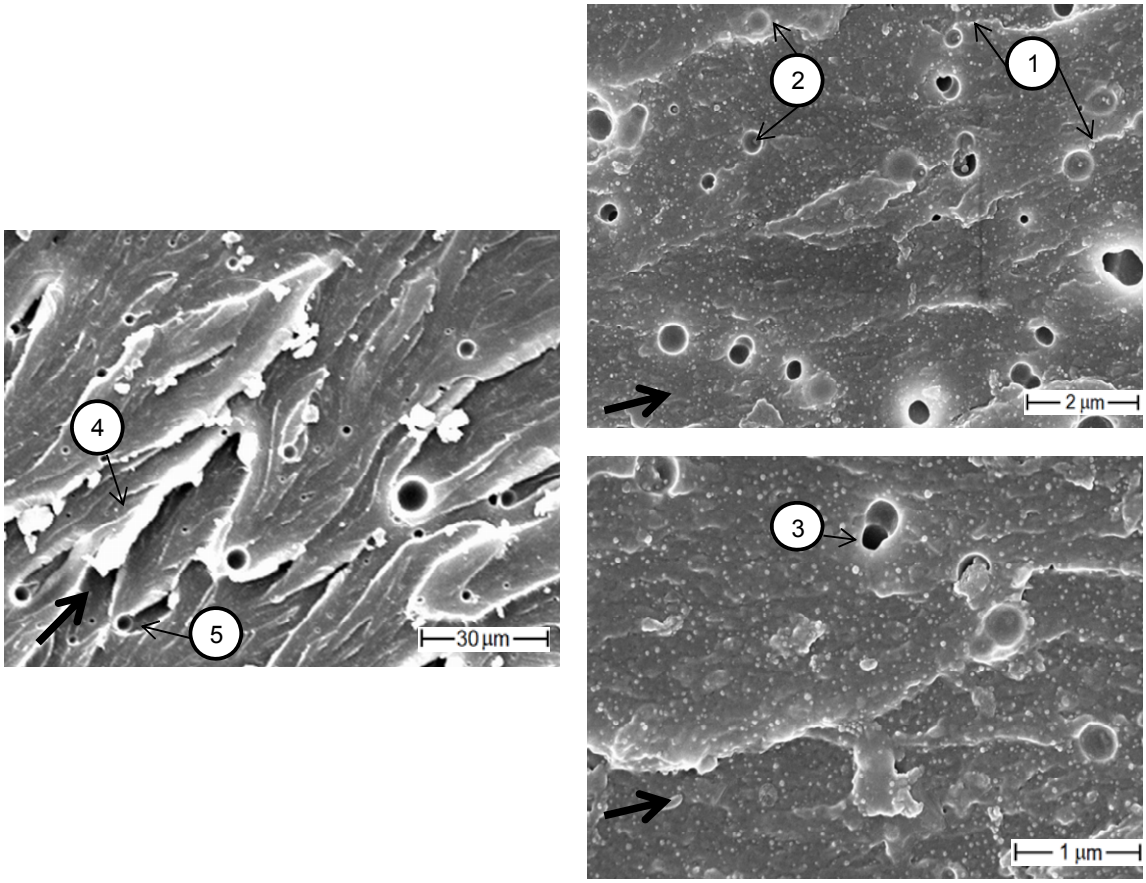

Figure 4.20: Fracture surfaces of a CT-specimen 5.5 vol.-% SiO_2 + 3 vol.-% SR. Mechanisms: 1 Pinning, 2 Debonding, 3 Cavitation, 4 Bridging, 5 Shear bending.

Similar behavior was reported in a CTBN rubber modified epoxy resin and is explained due to the rubber particles induce more localized plastic deformations around the crack tip increasing the size of the plastic zone leading to a somewhat rougher fracture surface [99]. Yee also suggested that the triaxial tension at the crack tip must be relieved before the crack propagates, so the deviatory stress can reach a critical value for yielding to occur [100]. This explanation justifies the load-displacement behavior illustrated in Figure 4.16. The plastic zone absorb the mayor fracture energy and once that the critical force is reached the total fracture take place.

Based on the above mentioned observations, Huang and Kinloch [101] developed a model, proponing that the greater fracture resistance in rubber modified epoxies results from the great energy dissipating processes that take place in the vicinity of the crack tip. The three main energy-dissipating toughening mechanisms are:

Cavitation

The formation of cavities is attributed to the dilatation of the rubber particles in presence of triaxial stress state around the crack tip. The localized cavitation of rubber gives rise to the stress-whitening that accompanies the crack growth and increase the toughness by obstruction of the propagating crack.

Shear bands

Rubber particles and existing micro voids and cavities induce massive shear yielding of the matrix. Shear bands are initiated by the stress concentration.

Bridging

This mechanism was first proposed by Kunz-Douglass [102] based on the concept that the fracture toughness is enhanced from the energy dissipated during the rubber particles tearing. Rubber particles span the crack and exert closure tractions in the crack surfaces, which reduces the applied stress intensity factor at the crack tip. Bridging is considered as a secondary fracture mechanism in rubber modified epoxies.

4.1.9 Hardness

Hardness is other of the properties usually affected negatively by addition of rubber as toughening agent to the epoxy formulation. It is not a surprising effect taking on account that, rubbers are considerably softer than thermoset matrices. Hardness is directly related to other important properties as abrasion and wear, which are especially important in application where loading motion is involved.

The results of the hardness test of the silica-rubber modified matrices are summarized in Figure 4.21. It is observed also that the nanocomposites hardness increases

with the particle content, due to silica is much harder than the epoxy resin. However, the increment seems to be so moderate. The maximum increase of hardness recorded by the nanocomposite containing 8 vol.-% SiO_2 was of only 6%. On the other hand, the addition of SR has a major impact on the matrix hardness. The addition of 3-5.5 vol.-% SR reduces the compound hardness in around 10-15%. Therefore, hybrid modified epoxies have lower hardness than EP, but to the matrices containing higher proportion of silica, the hardness reduction is not important. Hybrid compound containing 8 vol.-% SiO_2 + 3 vol.-SR has the same hardness than EP and the hybrid compound formulated with 7 vol.-% SiO_2 + 5.5 vol.-% SR has a hardness only 3% lower than the unmodified epoxy.

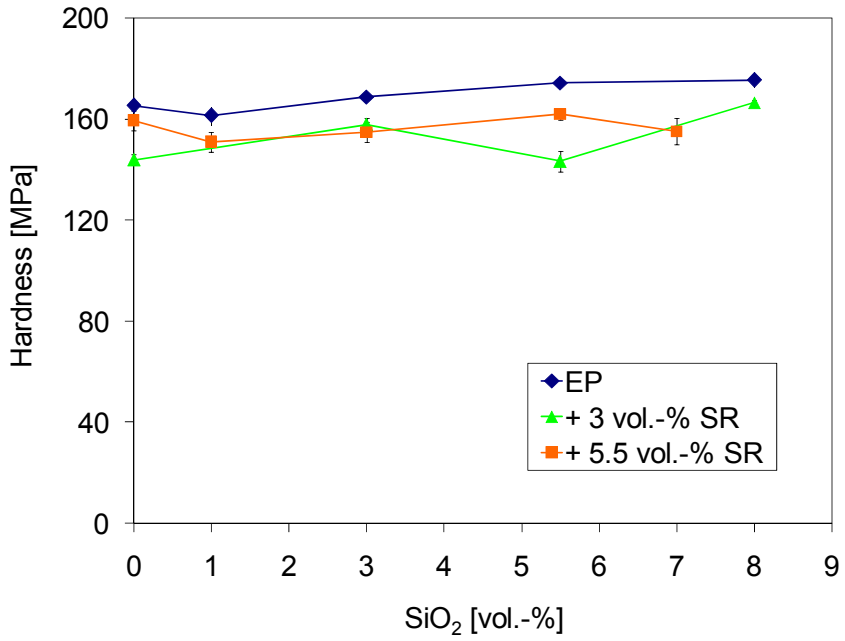

Figure 4.21: Microhardness of silica-rubber modified matrices

The measurement of hardness by micro indentation gives also important information about micromechanical properties of the studied matrices. Figure 4.22 shows the force-displacement for EP and the silica-rubber modified epoxy matrices. From the first part of the curve it is possible to approximate the E-modulus. The enhanced moduli of the both nanocomposite and hybrid compound result evident. It is also observed that the absolute indenter penetration, recorded by the modified materials is lower than the one reached by EP, and that fillers induce higher hyteresis in the ma-

trix, which limits the elastic recovery of the polymer net once that the force is suppressed.

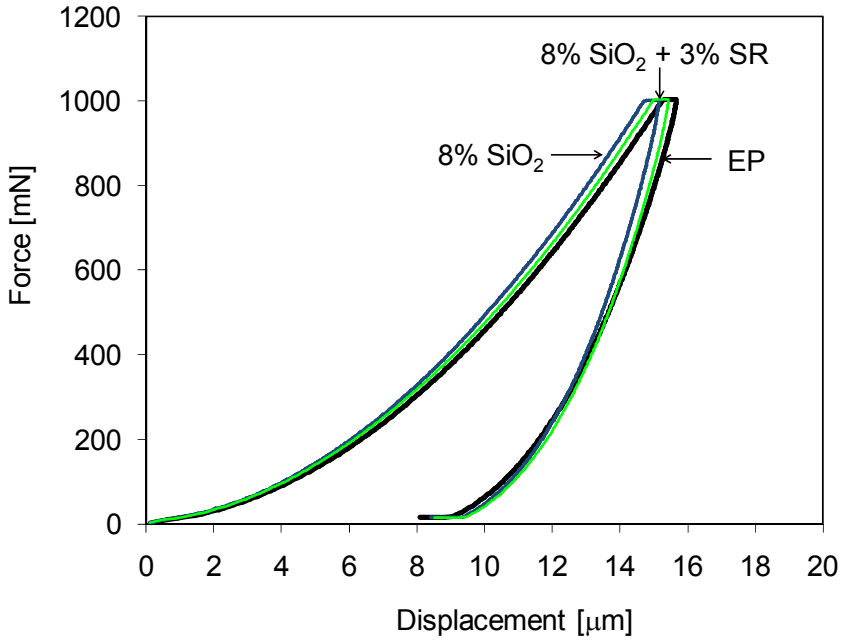

Figure 4.22: Microindentation force-displacement curve of silica-rubber modified matrices

4.1.10 Interparticle Distance

One of the main characteristics of the nanocomposites is their huge filler-matrix interface that can reach values up to several hundreds and even thousands m^2/g. As consequence of this fact, the properties of the nanocomposites become strongly dominated by the interface properties. The physicochemical properties of the interface are quite different from those of the bulk polymer matrix, because of several effects (crystallization, orientation, absorption) may exist in the immediate vicinity of the filler surface [12,95].

At increasing nanofiller content the interparticle distance is significantly reduced. Once that the interparticle distance reduces to a critical value, filler-filler interaction may occur. In this case, the interfacial layers around particles may overlap each other, forming a three dimensional network throughout the composite, affecting greatly the material properties, statement known as Percolation theory [103,104].

To determine if the nanocomposites and hybrid compounds object of the present research agreed the percolation theory, their main properties were examined as function of their particle distance, in order to establish the existence of a critical particle content beyond which the mechanical performance of the matrix will be controlled by the particle interfaces network.

The interparticle distance was determined using the Basal-Ardell equation, assuming spherical particles in perfect cubic arrangement [105]

$$2c = \left(\sqrt[3]{\frac{4\pi}{3V_f}} - 2 \right) \frac{d_p}{2} \tag{4.12}$$

where $2c$ represents the interparticle distance and d_p the particle diameter.

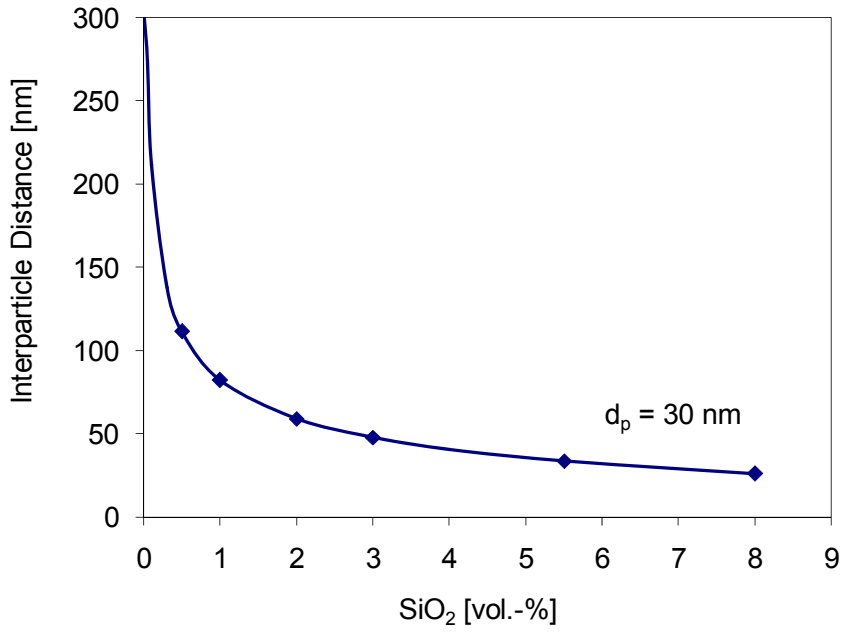

Figure 4.23: Interparticle distance silica nanocomposites.

According to Figure 4.23 the distance between particles equals the particle diameter around the 6 vol.-% nanoparticles ($2c/d_p=1$). This point is recognized by some authors as the generalized percolation critical interparticle [26,95].

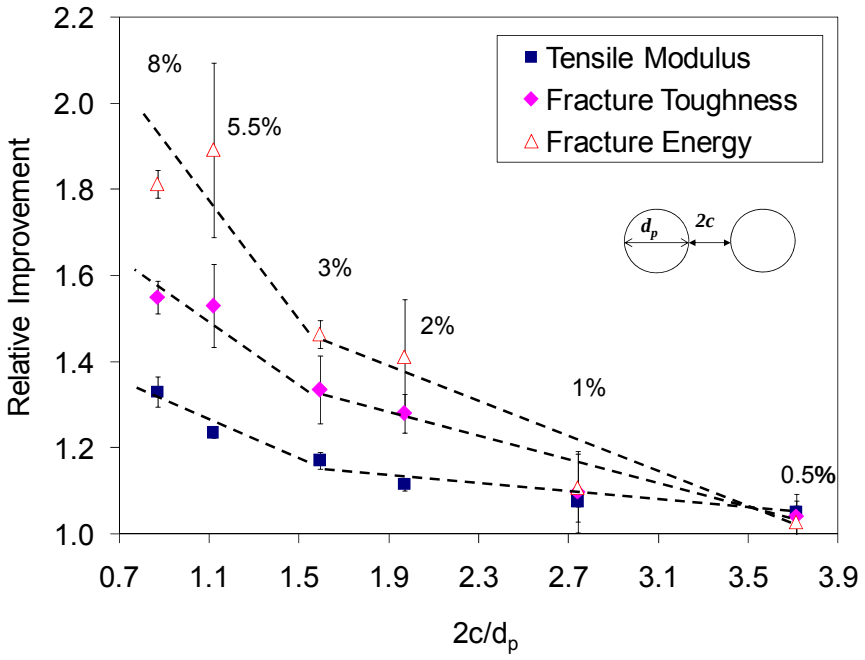

Figure 4.24: Relative improvement of mechanical properties as function of the inter-particle distance to silica nanocomposites.

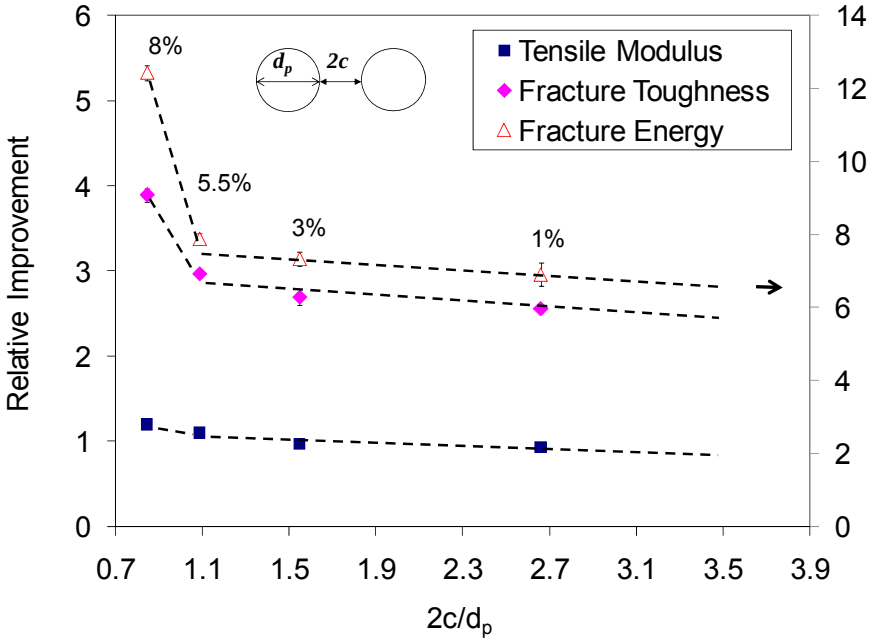

Figure 4.25: Relative improvement of mechanical properties as function of the inter-particle distance to silica-rubber hybrid compounds containing 3 vol.-%SR.

Figure 4.24 makes clear that this last statement is not a generality. It is observed that the critical interparticle distance by silica nanocompounds is registered at 1.6 times the particle diameter, at this point the trend of the lines turns abruptly to higher slopes and the matrix properties are enhanced more rapidly.

The especial reinforcement effect of the nanoparticles as function of their interparticle distance is also evident in hybrid compound, Figure 4.25. However, the presence of rubber displaces the critical interparticle distance to lower values. This result means that a closer distance between nanoparticles is required in order to the interfacial net become the ruler of the matrix properties. This can be explained from the fact that, rubber particles, with very different active surface and considerable bigger, act as obstacles to the interfacial net formation, and higher proportion of nanoparticles is required to compensate this effect.

4.2 Zirconia-Rubber Modified Matrices

4.2.1 Compounding of Zirconia Master Batch

The obtaining of the 12 vol.-% zirconia master batch took place in two steps. In the first one, a Dissolver was used to incorporate the ceramic powder into the fluid resin and in the second one a dipping mill was employed to break the particle agglomerates and generate a homogeneous particle distribution.

The particles were conditioned in an oven during 12 hours at 60 °C, to eliminate the humidity and to make easier their incorporation into the resin.

The neat resin was placed into a mixer and preheated up to 60°C to reduce its viscosity. This temperature was maintained during all the particle dispersion process. The preconditioned nanoparticles were added slowly into the matrix, approximately 10g/15 min., and incorporated into the resin using a dispersion disc of 50 mm diameter at 200 rpm. The air trapped in the system was eliminated by vacuum.

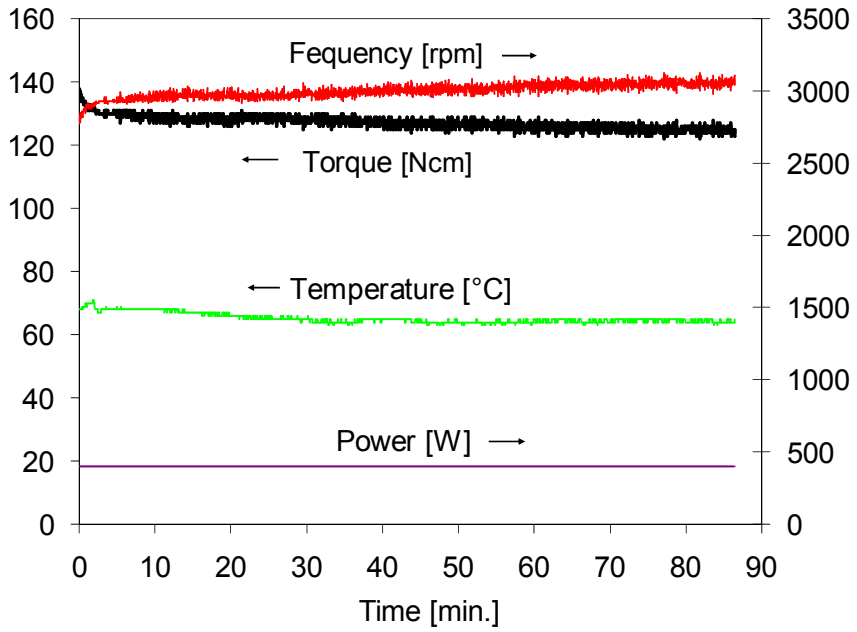

Figure 4.26: Control parameters of dipping mill process

Once that the total of particles were added to the epoxy resin, the mixture was placed into a dipping mill (Dispermat AE-3-C). The mill chamber is filled at 70% with ZrO_2 pearls of d=1.2-1.7 mm and is operated at constant power 400W, 65°C and with a cooling water flow of 1.95 l/min.

The control parameter to the dispersion of the system zirconia-epoxy is shown in Figure 4.26. It is observed that the process was stabilized during the first 10 minutes, after that, temperature and torque remain practically constants. However, the frequency is increased at longer operation time, which may be considered as evidence of the advance of the milling process. The reduction in particle size reduces the system viscosity and the resistance to the motor turn as well.

To define the quality of the mixture process, the particle size distribution into the fluid resin was determined by refractometry in a Horiba LB-550 device. The instrument measure the particle distribution in the range 1 nm – 6 μm, based on their Brownian movement and light scattering. The measurement takes place in a diluted solution of the filled resin, using Dichloro-methane as solvent [106]

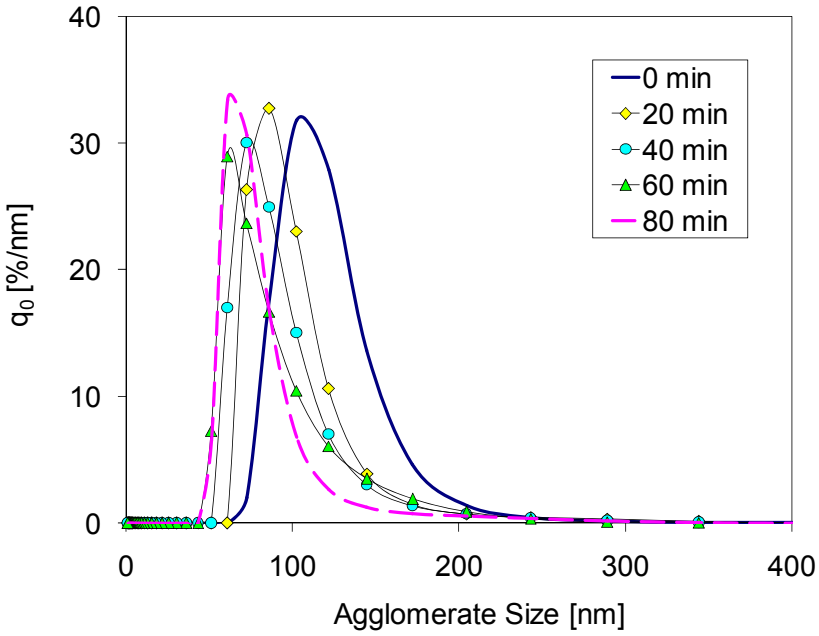

Figure 4.27: Particle size distribution of the zirconia master batch as function of the mixing time.

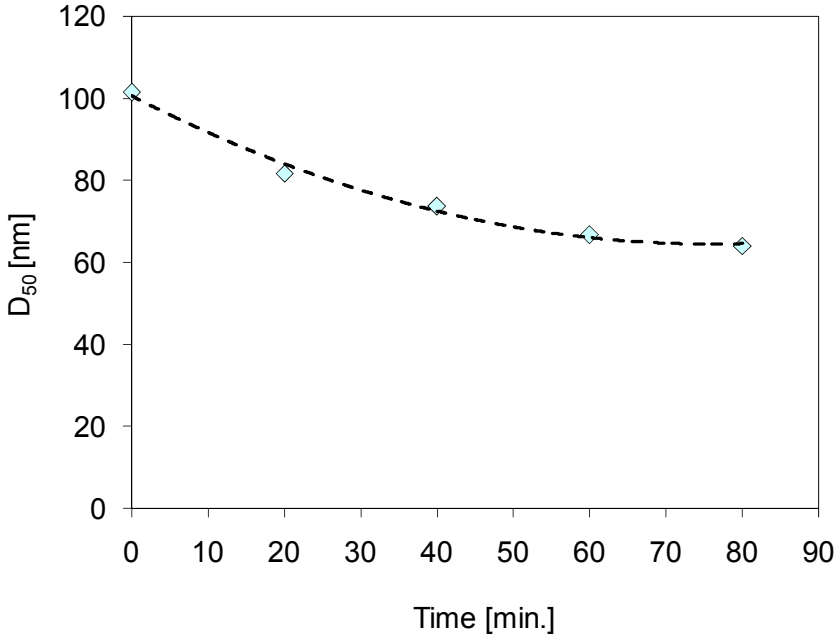

Figure 4.28: Maximum size of the 50% particle fraction.

Changes in particle size distribution of samples obtained at different mixture times are presented in Figure 4.27. Particle agglomerates at the beginning of the milling process were in the range of 70-220 nm and as expected their size is reduced when at rising milling time This effect continuously observed up to 60 minutes of milling, from this point on, the particle size does not go to lower values, only the size distribution is narrowed. On this basis, it was decided to stop the milling process at 80 min.

The final distribution show a distribution in range 40-150 nm with medium diameter around 65 nm, values much higher than the particle size declared by the supplier. It indicates that the shearing forces were not enough to break the secondary bonds that keep stuck the fine zirconia particles.

4.2.2 Rheology

For the mixtures containing ZrO_2, the relation between the viscosity increase exponentially with respect to the nanoparticle content, Figure 4.29. Hence, the resin containing 3 vol.-% of ZrO_2 reach a viscosity of almost 1000 mPas, whereas the epoxy containing 8 vol.-% zirconia has modified its original viscosity in more than eight times.

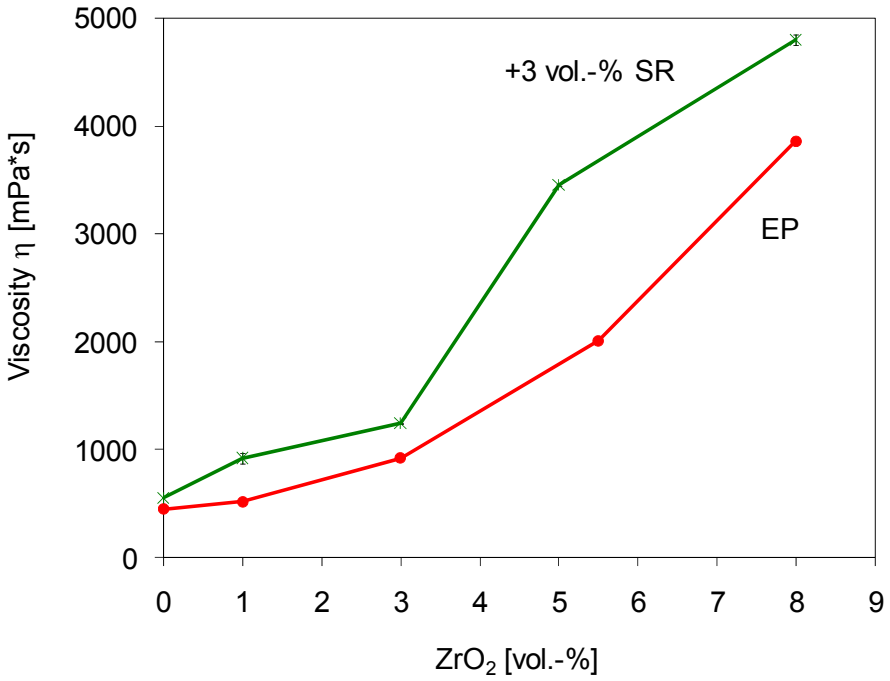

Figure 4.29: Viscosity of zirconia-rubber modified matrices at 25°C

The high viscosity of the epoxies containing ZrO_2 can be explained from their internal morphology. High quantity of agglomerates is present in the matrix bulks, which are irregular tridimensional particle arrangements, with wide size distribution and considerable denser than the epoxy resin, that act as barriers avoiding the free flow of the resin.

The viscosity of modified epoxy resins as function of both filler content is better illustrated in Figure 4.30. It is observed that the resin viscosity is mainly determined by the zirconia fraction included in its formulation. Epoxy viscosity increase also at rising rubber content, but in this case the increment is given as a lineal function (lines with small slope, parallel to y-axis).

Thus, the viscosity of the zirconia-rubber modified resins, in the studied interval, may be defined from the expression

$$\eta = \left(\eta_0 + 65.4 V_{f2}\right) e^{0.27 V_{f1}} \qquad (4.13)$$

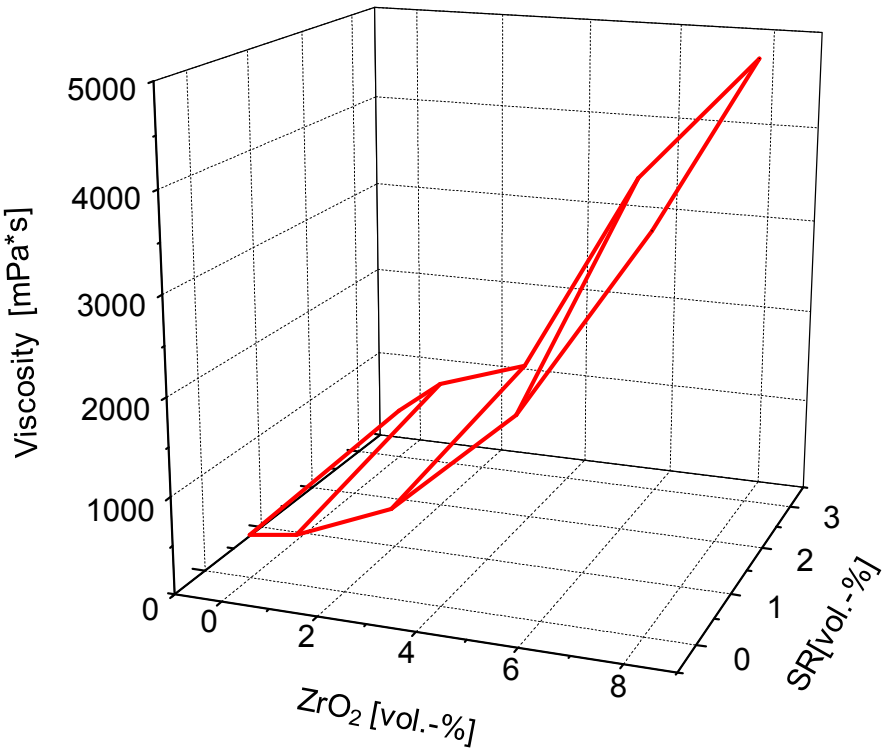

Figure 4.30: Viscosity of zirconia-rubber modified matrices at 25°C. 3D representation

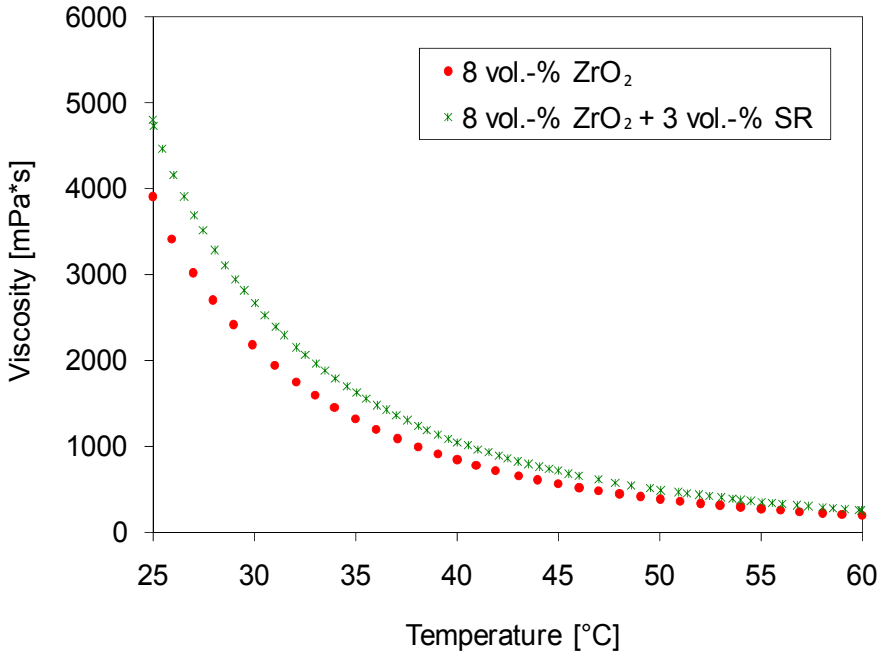

Figure 4.31: Viscosity of zirconia-rubber modified matrices as function of the temperature

The experimental viscosities of the zirconia-rubber modified epoxies seems to be much higher than those recommended by a resin to be processed by RTM. However, they are reduced considerably at rising temperature, Figure 4.31. This group of resins may be right processed by RTM only at temperatures over the 50°C

Therefore their curing process has to be also studied to determine their availability to be injected, as well as adequate conditioning and processing variables.

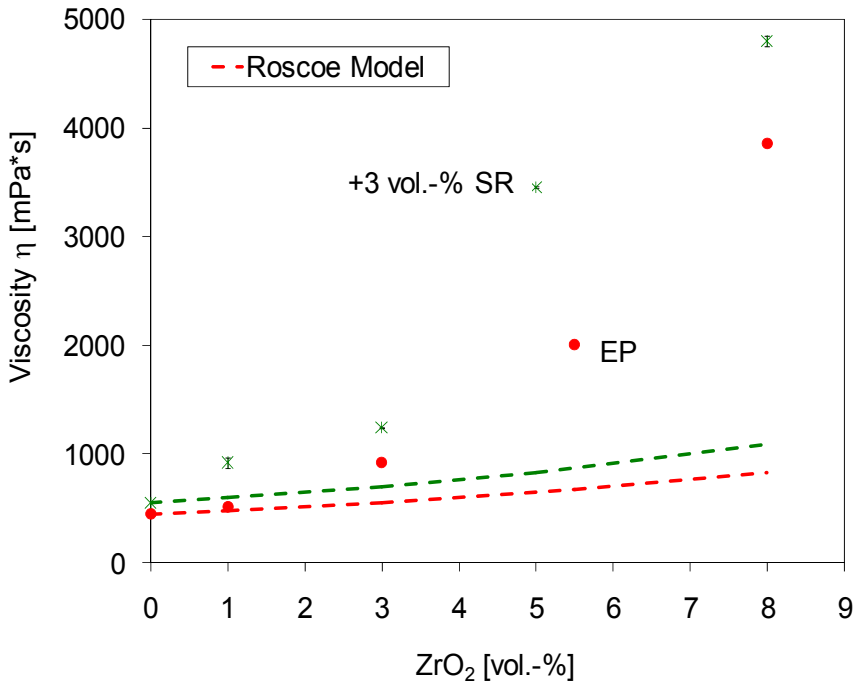

Figure 4.32: Theoretical viscosity curves from Roscoe's model compared with experimental data to zirconia-rubber modified matrices

Roscoe's model applied to zirconia-rubber modified epoxies, using V_{max}=0.37 corresponding to spheres in random close packing [73], results in theoretical values of viscosity much lower than the experimental ones, Figure 4.32,. The model considers particle characteristics that are not agree with the real ones. As stated, zirconia clusters have irregular form and dimensions, conditions both that may not permit their close packing; which, results in lower maximum volume fraction and higher viscosity. In addition, the theoretical expression does not consider the superficial interactions particles-matrix, which has been probed, play an important role on the suspension

viscosity. It is expected that at higher interaction particle matrix and/or particle-particle as high the viscosity. On this basis, the recorded results suggest a very high interaction of the zirconia particles/clusters with the epoxy matrix.

4.2.3 Curing

Table 4.3 shows that the gel point for representative epoxy systems containing zirconia, the increment in cure temperature is translated in lower gelling time, but also lower viscosity and modulus at gel point; which means that at higher temperature the cure reaction is faster but generate polymer chains with low ramification density.

The addition of zirconium dioxide reduces the time to reach the gel point; acting as a weak catalyzer. The apparent activation energy is reduced in more than 7% when the epoxy is modified with 8 vol.-% ZrO_2. The presence of zirconia has only marginal affect on gelling viscosity and moduli. Neither important changes in gelling time, viscosity or modulus where recorded by modification of the nanocomposites with 3 vol.-SR.

The viscosity of the zirconia-rubber modified resins remains in range 200-500 mPa*s during almost 40 minutes after they were mixed with the hardener. Than the selected injection temperature of 60°C was confirmed to be adequate.

4.2.4 Morphology

The obtained materials are opaque. The transparency, inherent to the epoxy resin, disappears once that nanozirconia is added.

TEM-analysis was carried out in order to study the particle distribution of the nanozirconia in the obtained composites. Figure 4.33 shows the micrographs obtained from the epoxy resins modified with 8 vol.-% of ZrO_2 and the hybrid compound containing 3 vol.-% ZrO_2 and 3 vol.-% SR. In both cases the presence of small zirconia agglomerates is evident. However, agglomerates are uniformly distributed into the matrix bulk.

Table 4.3: Gel properties as function of the cure temperature for representative zirconia-rubber modified epoxies.

EP					
Temperature [°C]	60	70	80	90	100
t_{gel} [s]	4860	2920	1768	955	605
Viscosity [Pa*s]	19.2	15.3	12.0	6.6	4.2
Modulus $_{gel}$ [Pa]	27.1	21.6	16.9	9.3	6.0
E_a [kJ/mol]	54.5				

3 vol.-% ZrO_2					
Temperature [°C]	60	70	80	90	100
t_{gel} [s]	4674	2670	1692	946	625
Viscosity [Pa*s]	17.9	12.3	12.0	5.7	4.8
Modulus [Pa]	16.6	15.9	11.6	7.6	5.2
Ea [kJ/mol]	52.3				

8 vol.-% ZrO_2					
Temperature [°C]	60	70	80	90	100
t_{gel} [s]	4150	2732	1631	960	597
Viscosity [Pa*s]	16.3	14.0	11.0	7.0	4.3
Modulus $_{gel}$ [Pa]	23.0	22.8	17.3	10.8	6.8
Ea [kJ/mol]	50.7				

3 vol.-% ZrO_2 + 3 vol.-% SR					
Temperature [°C]	60	70	80	90	100
t_{gel} [s]	4563	2596	1579	933	593
Viscosity [Pa*s]	17.1	11.0	7.7	4.2	4.5
Modulus $_{gel}$ [Pa]	14.5	13.0	10.8	6.2	5.9
E_a [kJ/mol]	52.7				

8 vol.-% ZrO_2 + 3 vol.-% SR					
Temperature [°C]	60	70	80	90	100
t_{gel} [s]	4291	2619	1397	942	609
Viscosity [Pa*s]	14.9	12.6	9.0	7.8	4.8
Modulus $_{gel}$ [Pa]	22.9	18.3	12.6	9.6	5.5
E_a [kJ/mol]	50.9				

The amount of clusters is obviously related to the nanoparticle content present. They appear like three-dimensional arrangements, considering that the dark dots on the micrographs correspond to overlapped particles in depth direction, which size may reach values around 100 nm; dimensions big enough to cause light scattering and form opaque materials. The number of single particles, whit dimensions near to the supplier specification (12 nm), is reduced.

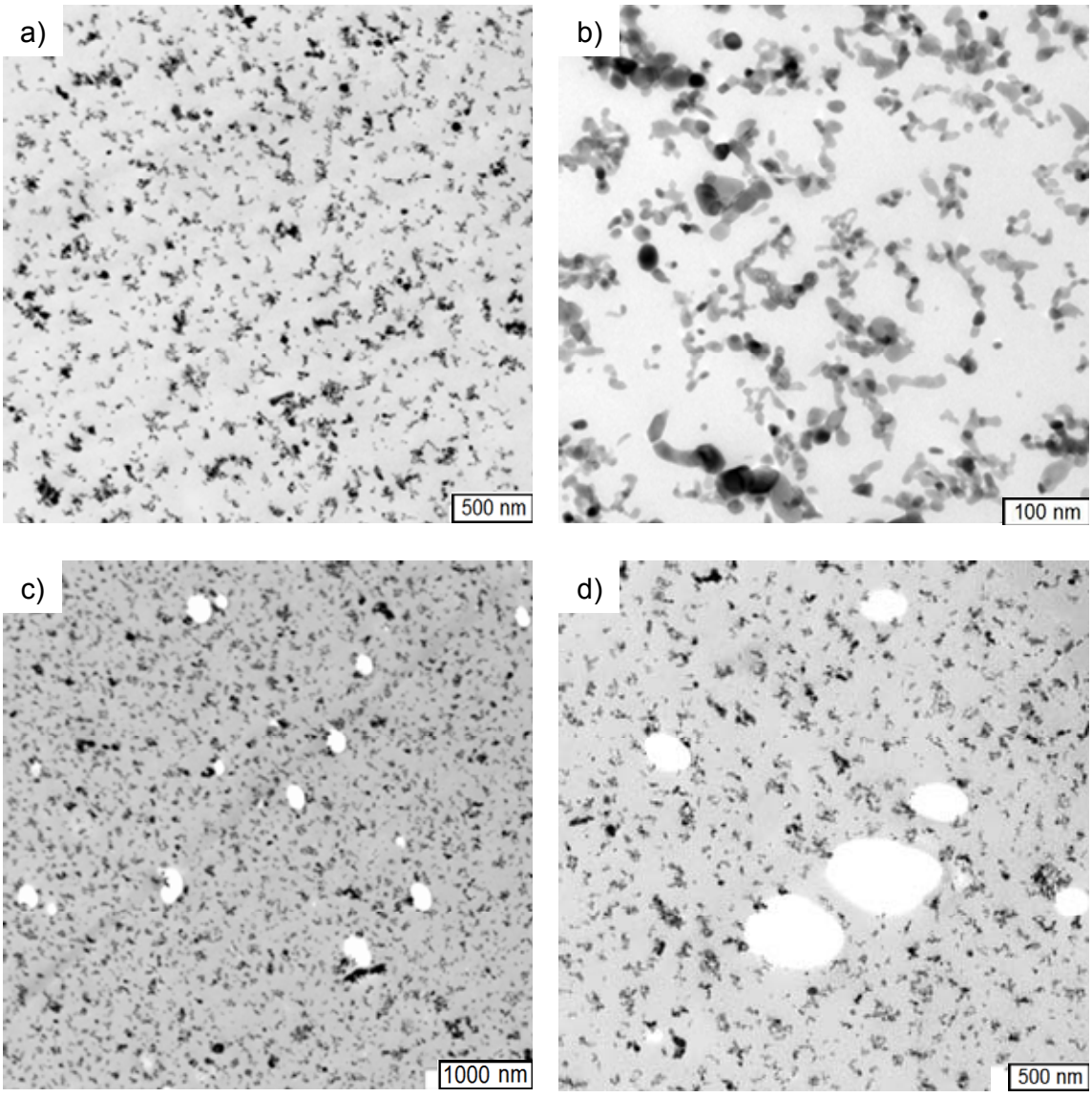

Figure 4.33: TEM photographs of the modified epoxy resins containing (a) and (b) 3 vol.- % ZrO_2 , (c) and (d) 3 vol.-% ZrO_2 + 3 vol.-% SR

As stated in section 4.2.1, the shear forces, applied during the milling and dispersion processes, were not efficient enough to break the small clusters. A detailed study of the mixing process should be done to find out the best mixing parameters and/or an alternative method to produce zirconia nanocomposites minimizing the presence of agglomerates.

The distribution of rubber particles in Figure 4.33 c) and d) is inferred from the position of the micro holes. It is observed again that rubber is well dispersed in the matrix and its broad particle size distribution is also evident.

4.2.5 Density

The changes in the epoxy resin density, as result of its modification with ZrO_2 and silicone rubber, are listed in Table 4.4. The addition of zirconia nanoparticles increases the matrix density, due to this ceramic is considerable denser than the epoxy resin (5 g/cm^3). Hence, the density of the pure epoxy resin is increased in more than 30% once that it is modified with 8 vol.-% ZrO_2.

The addition of 3 vol.-% SR to the neat epoxy as well as nanocomposites means only a marginal reduction (1-2 %) on their densities.

Table 4.4: Density of zirconia-rubber modified matrices.

	EP		3 vol.-% SR	
Content ZrO_2 [vol.-%]	Density [g/cm^3]	Std. Dev.	Density [g/cm^3]	Std. Dev.
0	1.1524	0.0003	1.1479	0.0010
1	1.2070	0.0054	1.1885	0.0053
3	1.2898	0.0187	1.2881	0.0093
5.5	1.4191	0.0013	1.3786	0.0073
8	1.5033	0.0098	1.4825	0.0052

4.2.6 Tensile Properties

Figure 4.34 and Figure 4.35 present the tensile properties of the zirconia-rubber modified epoxies. The tensile modulus of the epoxy matrix is increased by the addition of nanozirconia It is possible to see an important increment on the modulus even at low particle content. The elastic modulus of the pure epoxy resin was found to be 3.1 GPa, while the modified epoxy containing 0.5 vol.-% ZrO_2 reaches a modulus 18 % higher, up to 3.7 GPa (jump in graph). From this point on, the elastic modulus increases almost linearly, with the nanoparticle content. The elastic modulus of the epoxy matrix was increased by 37 %, up to 4.35 GPa, once it was modified with 10 vol.-% ZrO_2.

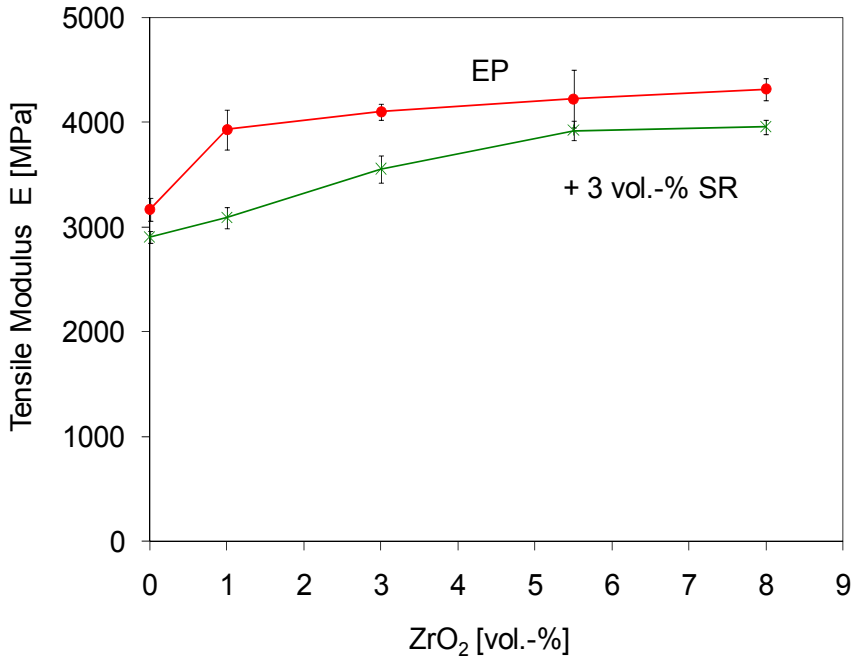

Figure 4.34: Tensile modulus of zirconia-rubber modified matrices.

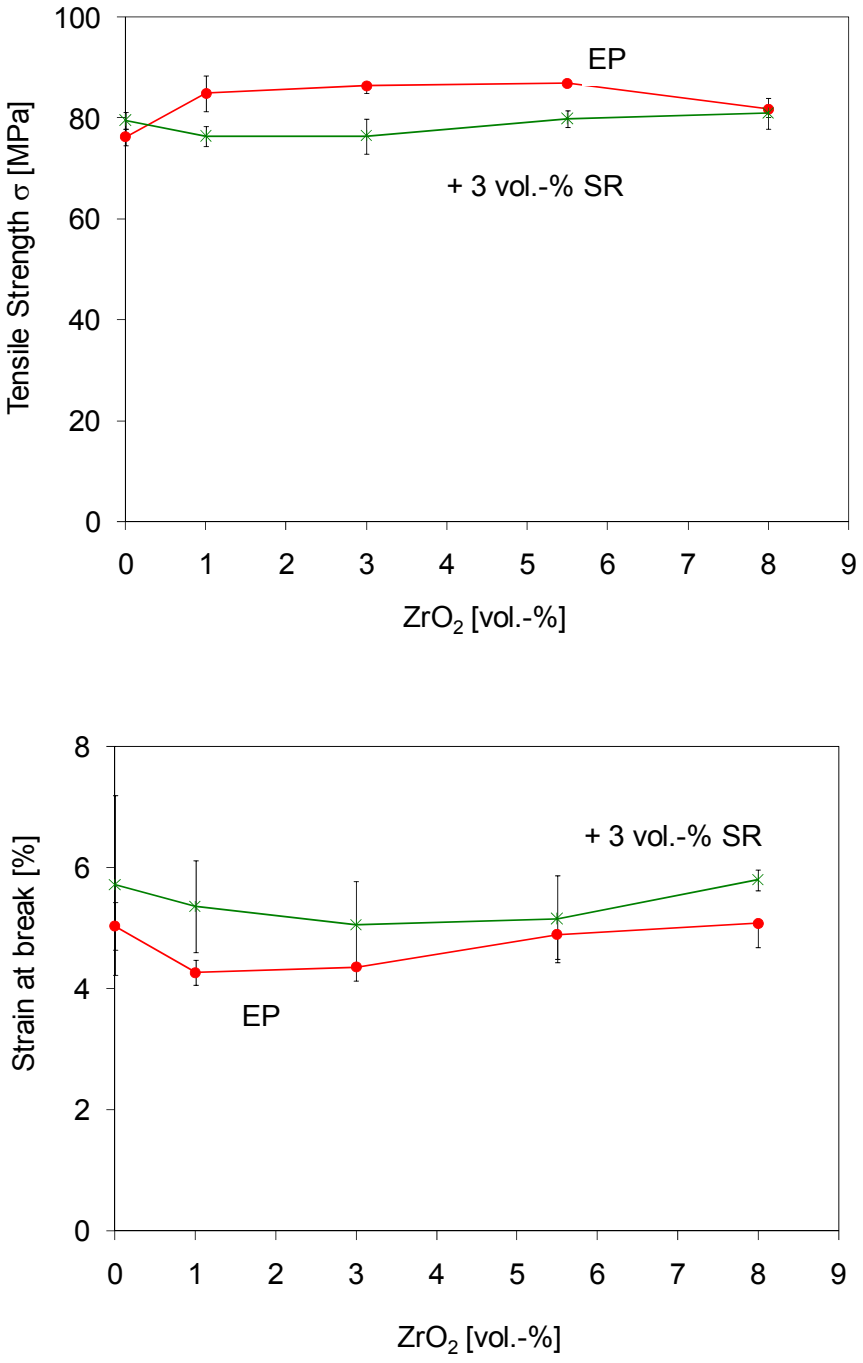

Figure 4.35: Complementary tensile properties of zirconia-rubber modified matrices.

The tensile strength of the neat epoxy was increased by the addition of nanoparticles. The nanocomposites record tensile strengths improved by around 20 %, but the composites containing 8 and 10 vol.-% ZrO_2, which record tensile strengths hardly 15 % higher than the neat epoxy.

The increment in strength is attributed to the fact that the ZrO_2 has a much higher strength than the epoxy matrix and also to the good bonding between filler and matrix, which permits the right stress distribution into both composite phases.

The reduction of strength at high filler content is due to the presence of the higher quantity of clusters. The agglomerates tend to reduce the strength, because even if they may be strong enough to increase the modulus, they constitute weak points, which break fairly easily when stress is applied.

The modulus calculated from typical models such as Halpin-Tsai rule and Lewis-Nielsen (Eqs. 4.9 and 4.10) are presented in Figure 4.36 and Figure 4.37.

The parameter used to the Halpin-Tsai calculus were E_m=3.1 GPa, E_{f1}=200 GPa [107], E_{f2}=0.5 GPa . The filler geometry was assumed as ellipsoidal, w/t=2, due to the aspect displayed by single zirconia particles in Figure 4.33.

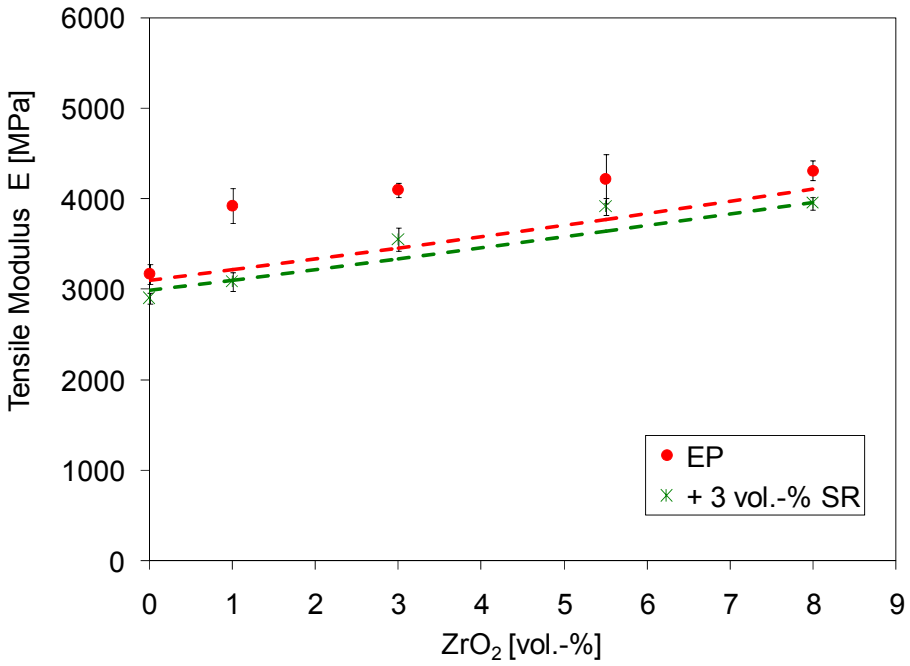

Figure 4.36: Experimental vs. Halpin-Tsai modulus to zirconia-rubber matrices

Additionally, it is clear that the particles have random orientation into the polymer matrix. Hence, the shape factor used to predict the composite modulus was ζ =3, which

corresponds to the average between both, parallel and perpendicular, particle orientations.

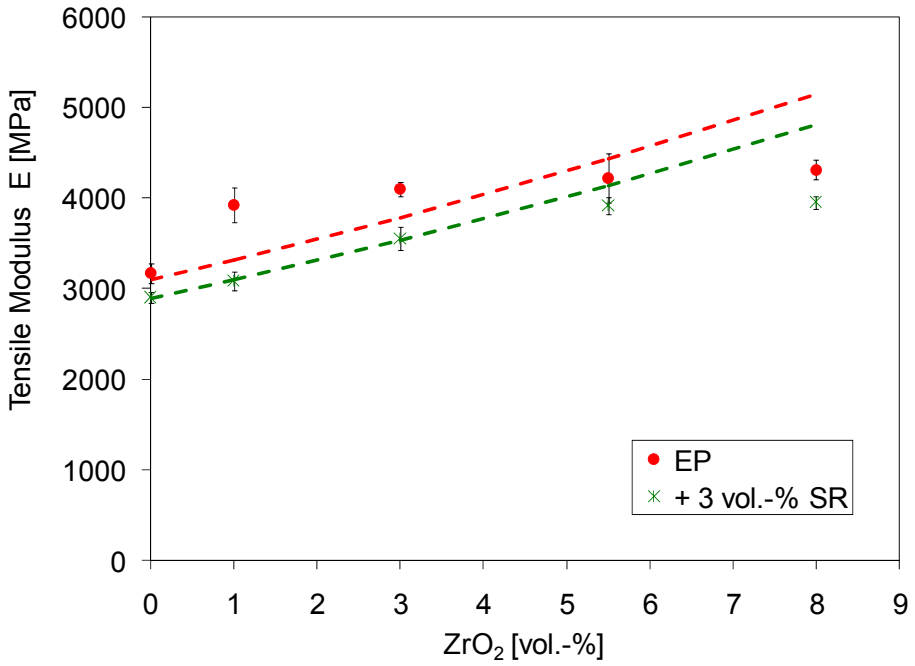

Figure 4.37: Experimental vs. Lewis-Nielsen modulus to zirconia-rubber matrices

For the Lewis-Nielsen model, the maximum volume fraction was defined as V_{max}= 0.37, corresponding to agglomerated spheres in random close packing; and k_E=5.86, resultant from the Einstein coefficient also for spherical particles agglomerated in random packing (6.76), reduced by a factor 0.867.

The Halpin-Tsai model underestimates again the nanocomposite modulus. This deviation may be explained also from the above mentioned interfacial phenomena particle-matrix (sections 0 and 4.1.9) but also considering that the selected geometrical values assume a generalized filler shape, which is not particularly true, because as mentioned the clusters have irregular form and very different dimensions.

On the other hand, the theoretical approximation by the Lewis-Nielsen model presents opposed deviations along the studied interval. At low zirconia content, it under estimates the tensile modulus of the composites, but at high filler content, the modulus is over estimated.

Both theoretical approximations establish a direct proportionality between filler content and modulus, which as shown in Figure 4.8 is not the case to zirconia nanocomposites. The moduli of these matrices can be better expressed using a second grade polinomial expression, as:

$$E = E_0(1 - 0.08V_f^2 + 0.1V_f) \tag{4.14}$$

where constants it is expected that be associated not only with the geometrical form and modulus of the filler, but also with the filler-matrix compatibility.

The SEM fractograms from the tensile specimens, Figure 4.38, show the different failure mechanisms of modified epoxy matrices. The fracture surface of the nanocomposites is characterized by the presence of small craters, in whose center, particle or cluster debonding marks are assumed. Under load, the nanoparticles and agglomerates act as stress concentrators. When the load is high enough, the particles are debonded forming little craters that grow radially until they meet another particle. The amount of debonded particles depends directly on the particle content. However, the failure surface is dominated by this mechanism even at low particle content. This fact explains the significant difference recorded between the tensile modulus of the neat and modified epoxy resins (jump in Figure 4.34).

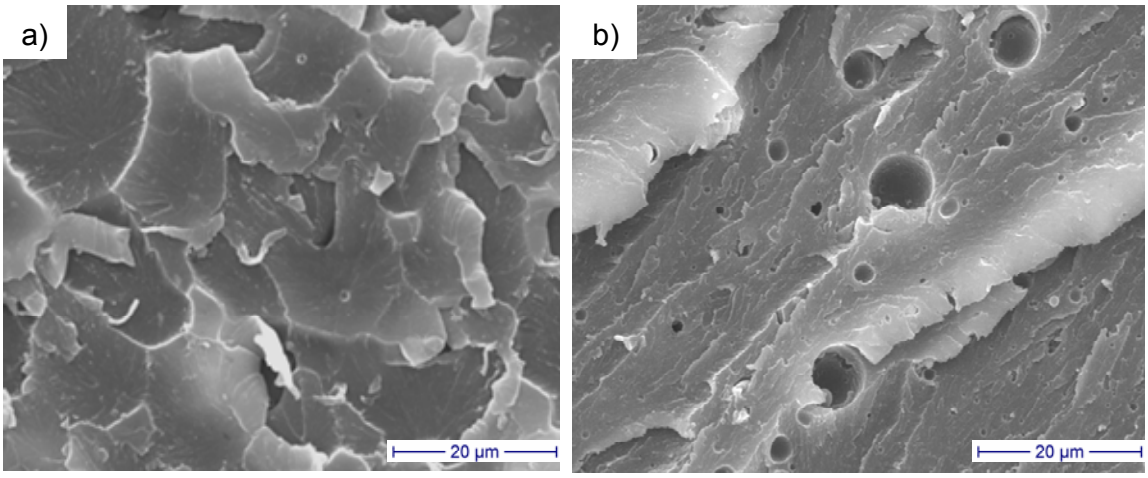

Figure 4.38: Fracture surfaces of tensile specimens a) 5.5 vol.-% ZrO_2, b) 5.5 vol.-% ZrO_2, + 3 vol.-% SR

The hybrid compound fracture surface presents no more dimple evidence but fracture larger fracture paths as result of higher plastic deformation; sites of rubbers cavitation are also observed.

4.2.7 Dynamic Mechanical Thermal Analysis

The DMTA results are summarized in Figure 4.39. The complex modulus of the epoxy resin increases, as expected, with the nanozirconia content. The stiffening effect of nanoparticles on the matrix is evident, and remains almost in the same proportion, along all the studied temperature range; inclusive at temperatures higher than T_g. This result can be associated also with a good bonding particle-matrix [11].

The addition of zirconia causes a gradual increase of the epoxy T_g, from 100°C of the neat epoxy, up to 108°C of the epoxy containing 8 vol.-% ZrO_2, Figure 4.40.This increment may be explained by the adsorption of polymer onto the particle surface, which reduces the polymer net mobility and modifies the conformation of chain segments.

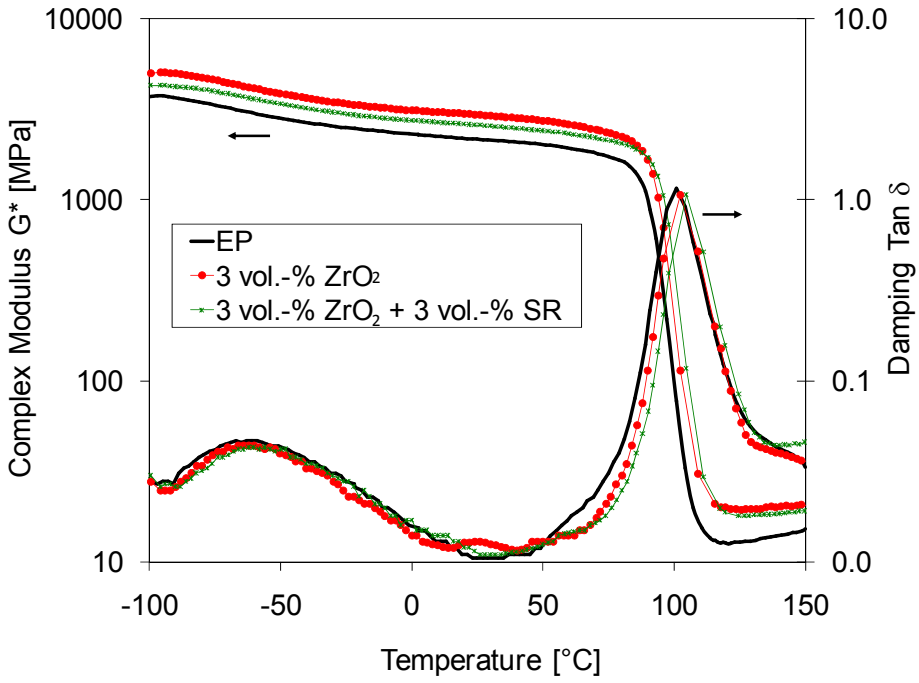

Figure 4.39: Complex modulus and damping as function of the temperature of zirconia-rubber modified matrices

The damping of the epoxy resin records no important change in the glassy stage (-100 to 35°C) due to the addition of nanofiller. It indicates that, storage and loss modulus, increase almost in the same proportion, along this temperature range.

On one hand the nanoparticles induce a higher stiffness on the epoxy resin, and by the other hand they induce new mechanisms of energy dissipation, as filler/filler and filler/matrix friction, which were suggested as main reason for damping in composites systems [73].

In the elastic zone (35 to 100°C), the damping of nanocomposites is lower than the damping of neat epoxy. In this stage the macromolecules start to move. The particles hinder the movement of the polymer chains resulting in lower energy dissipation.

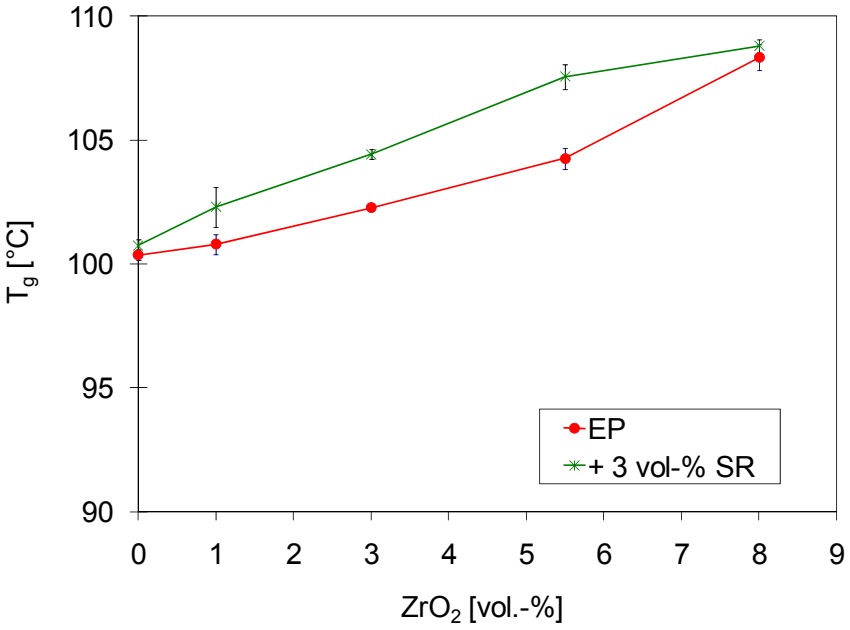

Figure 4.40: Glass transition temperature of zirconia-rubber modified matrices.

In the rubbery stage (100 to 150°C), the damping of nanocomposites is higher than for the pure epoxy. Nanoparticles maintain their reinforcement effect on the matrix. However, all polymer chains are in movement and the internal friction becomes more representative.

4.2.8 Fracture Toughness

The representative load-displacement curves, from the fracture test, of neat and modified epoxy resins are comparative showed in Figure 4.41. The curves show the improvement in mechanical properties of epoxy as well as important differences in fracture behavior, as result of its modification. The neat epoxy presents initially abrupt fracture propagation and a second stage in which the failure propagates gradually up to total specimen breakage.

The incorporation of nanoparticles increases the modulus as well as the fracture toughness. In the nanomodified epoxy, the fracture propagation begins at higher load than in the neat epoxy and present stick-slip steeps, phenomena normally related with the crack tip blunting [102].

The hybrid epoxy, containing nanozirconia and rubber, presents also higher modulus than neat epoxy and fracture propagation is abrupt and total once that the maximal force is reached.

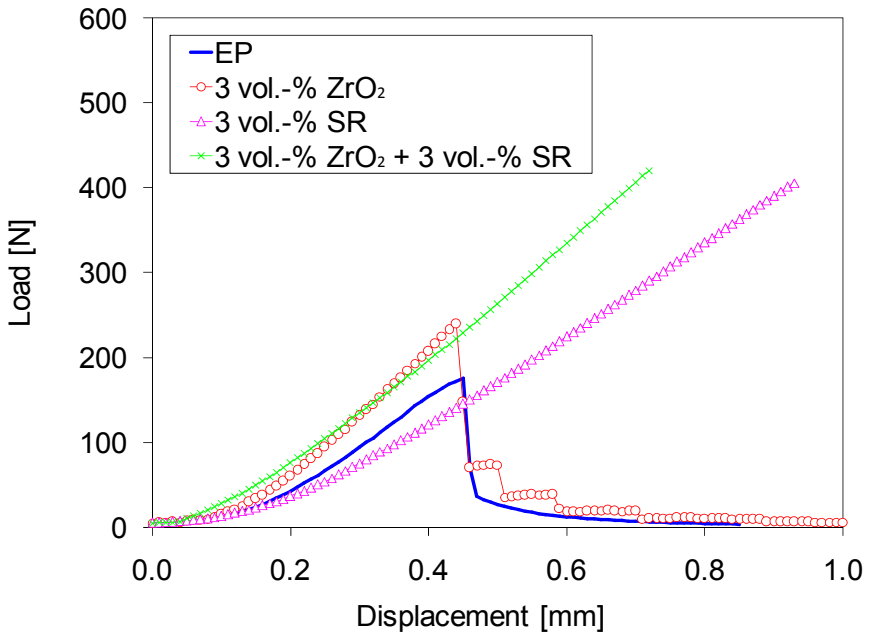

Figure 4.41: Characteristic load-displacement curves from the fracture test of zirconia –rubber modified epoxies.

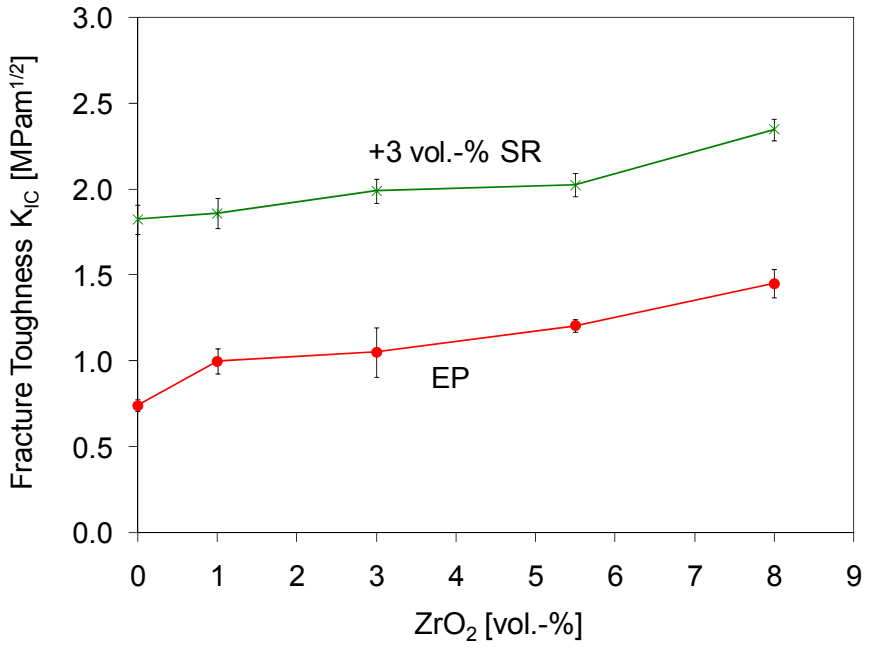

Figure 4.42: Fracture toughness of zirconia-rubber modified epoxies.

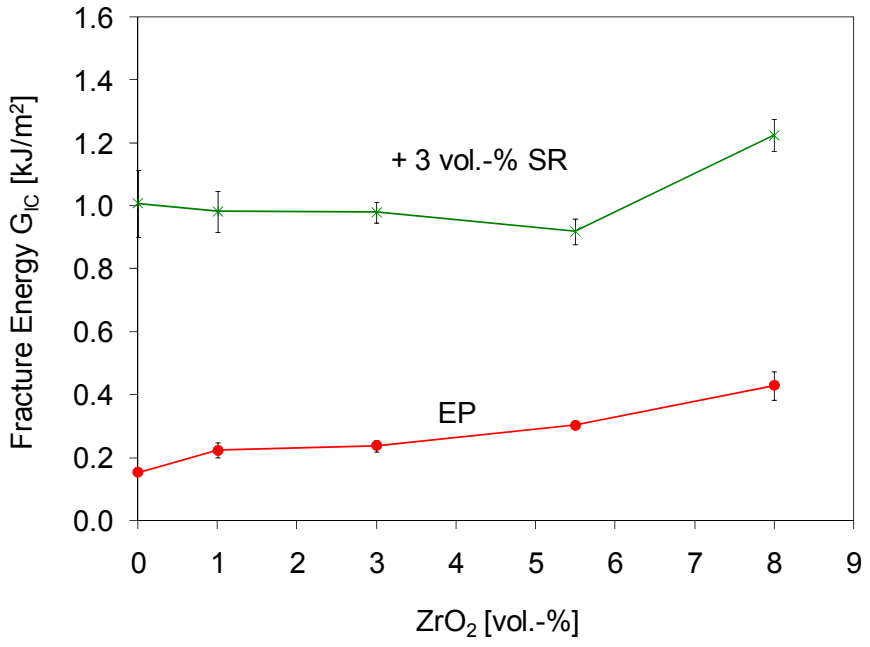

Figure 4.43: Fracture energy of zirconia-rubber modified epoxies.

Fracture toughness of nano-modified epoxy resins increases with particle content (Figure 4.42). The addition of 1 vol.-% ZrO_2, results in an approximately 35 % enhanced K_{IC} up to 1 $MPam^{1/2}$. While the nanocomposite with 8 vol.-% ZrO_2 shows a K_{IC}=1.45 $MPam^{1/2}$, almost two-fold higher than for EP (K_{ICo}=0.74 $MPam^{1/2}$).

The silicone rubber induces a superior toughness in the epoxy matrices. The hybrid epoxy resins containing 3 vol.% SR records fracture toughness around 120% higher than the analog nanocomposites. Hence, the epoxy containing 8 vol.-% zirconia + 3 vol.-% SR reach fracture toughness up to 3.17 $MPam^{1/2}$ that means four times higher than EP.

The fracture energy of the studied epoxies varies with same tendency but a higher proportion than the fracture toughness (Figure 4.43). The fracture energy of the neat epoxy (G_{ICo}=0.15 kJ/m^2) is enhanced up to 0.22 kJ/m^2 due to the addition of 1 vol.-% ZrO_2, that means an increment around 46 % in relation to EP. When the epoxy is modified with 8 vol.-% ZrO_2 its fracture energy triples up to 0.45 kJ/m^2. Hybrid compounds containing 3 vol.-% SR may register fracture energies more than 6 fold higher than the fracture energies of the nanocomposites.

4.2.9 Fracture Mechanisms

The increase in the toughness, as a result of the nanoparticle addition, can be explained analyzing the SEM pictures of the fracture surfaces of the modified epoxy resins ,Figure 4.44 and Figure 4.45.

Nanoparticle Toughening

The nanomodified epoxy having 5.5 vol.-% ZrO_2, shows fracture lines parallel to the load axis but also a variety of small paths, which reveal the existence of alternative fracture mechanisms induced by the filler. As stated, the toughening effect of the rigid particles has been explained in terms of specific fracture mechanisms, being the most recognized the crack pinning, crack deflection and plastic deformation.

COD values were determined for the neat epoxy and the nanocomposite containing 8 vol.-% ZrO_2, following Eq. (4.11). In those cases COD ranges between 2.1-5.2 μm,

respectively, values that are much greater than the particle size, also considering the agglomerate size. Hence, the existence of crack deflection and pinning seems doubt full.

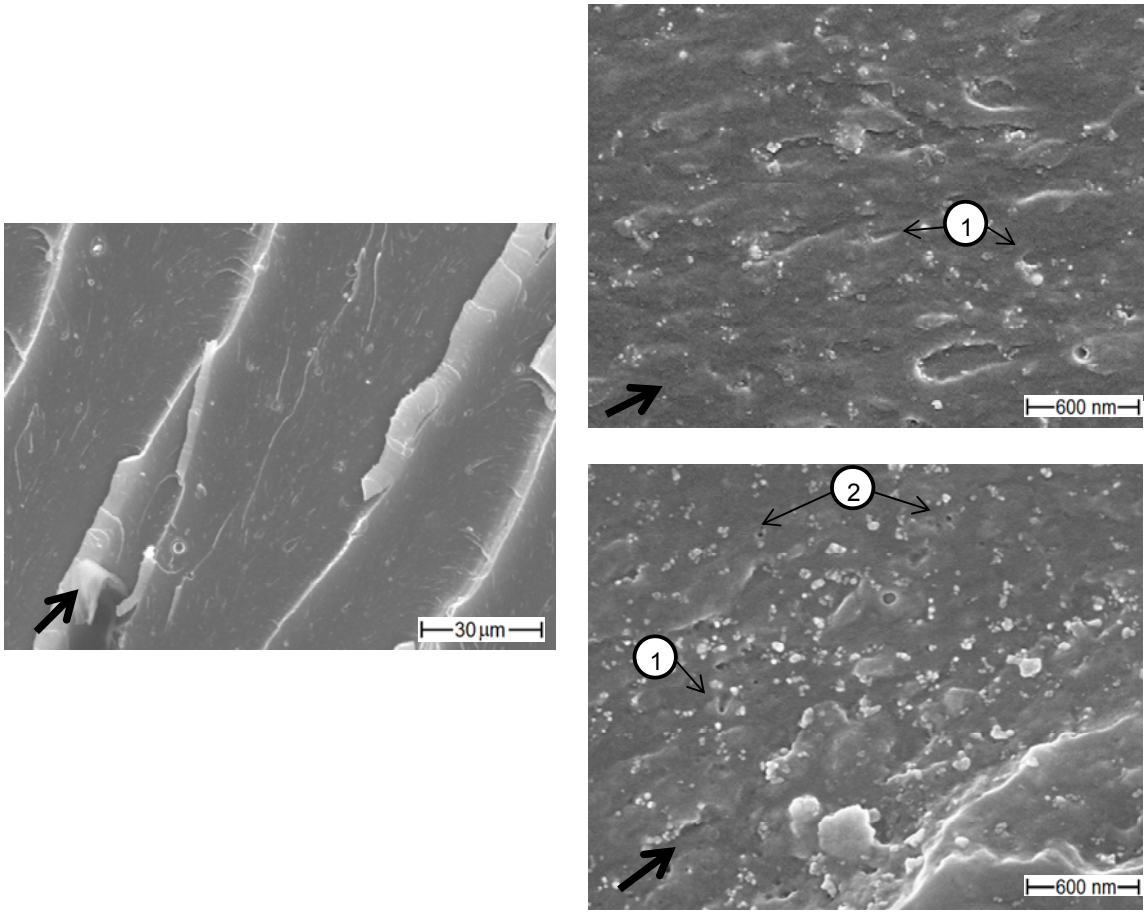

Figure 4.44: Fracture surfaces of 5.5 vol.-% ZrO_2 CT specimens.

Higher magnification micrographs of the nanocomposite fracture surface, show characteristic paths, (i.e. fracture bowing, tails and bifurcation) associated with crack pinning and deflection. Nevertheless, it is little probable that these mechanisms be responsible of the enhanced toughness of nanomodified epoxies.

The fracture surfaces of nanocomposites show the presence of circular voids with average size between 20-100 nm, which may be originated by debonding of particles or clusters. Some shear yielding paths are also appreciated. However, the incidence of these processes is so low, that they cannot be considered responsible of the

toughness increment [108]. This evidence supports the hypothesis that the obtained nanocomposites have a good particle-matrix bonding.

The particular behavior of the nanocomposites has been constantly described from the existence of an interfacial layer particle-matrix, formed by immobilized polymer chains adsorbed by the particle surfaces; which has physicochemical properties quite distinct from those of the bulk polymer matrix.

The existence of the interfacial layer can be confirmed using techniques as viscometry and thermal analysis. In this last it is expected, that the immobilization of the polymer chains increases the $T_{g.}$ Hence, in the present work, the results reported in Sections 4.2.7, together with the deviation between theoretical and experimental results reported in section 4.2.6, suggest the presence of a strong interfacial layer filler-matrix, which may constitutes also the main toughening mechanism induced by nanozirconia in the epoxy matrix [109].

Rubber Toughening

The rubber modified matrix presents also a textured fracture surface characterized for the presence of spherical cavities, attributed to the dilatation of the rubber particles in presence of triaxial stresses.

The presence of voids due to the cavitation of rubbery domains is the most important energy dissipating mechanism in the rubber modified epoxy [95,96]. Shear bands connecting the cavitated particles are also observed. Other important toughening mechanisms observed in the rubber modified epoxy resin include also crack deflection and pinning as well as particle debonding.

The dominant fracture paths in hybrid compounds are they derived from the rubber toughening effect. However, at higher magnification numerous small cracks are also observed. The amount of these small fracture paths increases at higher nanoparticle content. The superposition of fracture mechanisms, derived from the interaction of hard and elastic particles inside the epoxy matrix, explain the synergetic effect on the toughness, reported for the hybrid compounds with higher nanozirconia proportion.

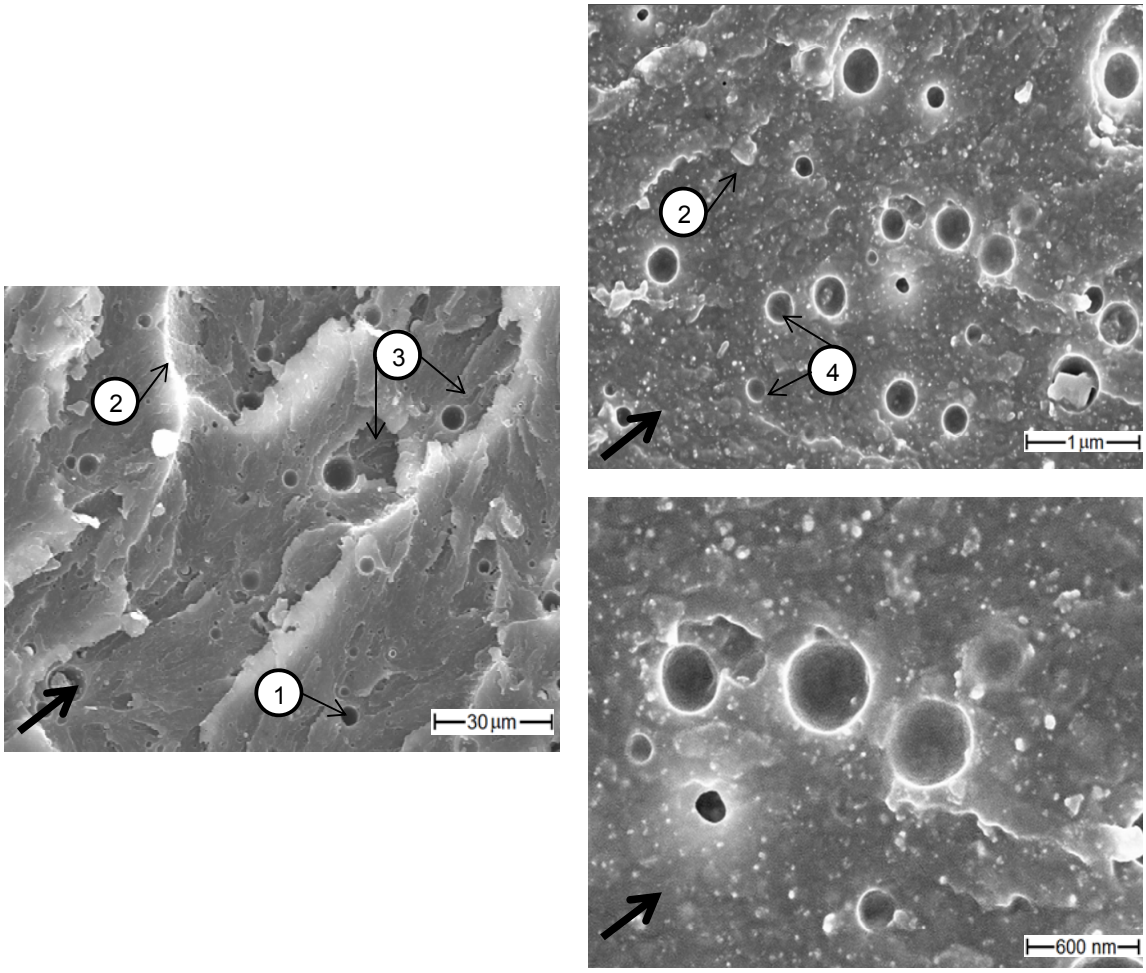

Figure 4.45: Fracture surfaces of 8 vol.-% ZrO_2 + 3 vol.-% SR, CT specimens.

4.2.10 Hardness

The results of the hardness test of the zirconia-rubber modified matrices are presented in Figure 4.46. It is observed that nanocomposites hardness increases as consequence of the ceramic addition. It is expected that zirconia confers better hardness to the polymer matrix, because of it is greatly harder than the epoxy resin. However, nanocomposite containing 1 and 3 vol.-% ZrO_2 records no hardness enhancement in comparison to EP; only appreciated at higher ceramic content. On the other hand, the addition of SR has a major impact on the matrix hardness. The addition of 3 vol.-% SR reduces EP as well as nanocomposite hardness up to 10% in average.

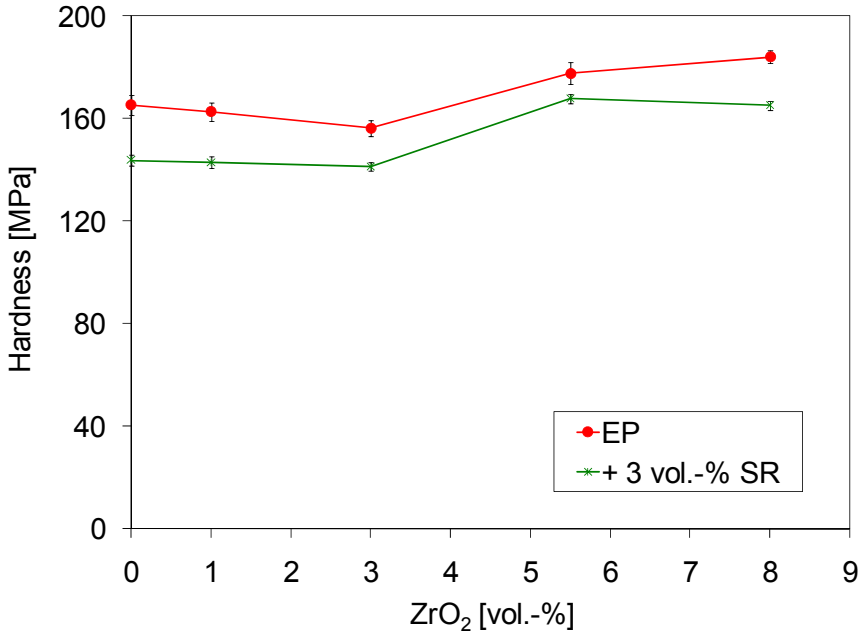

Figure 4.46: Micro-hardness of zirconia-rubber modified epoxies

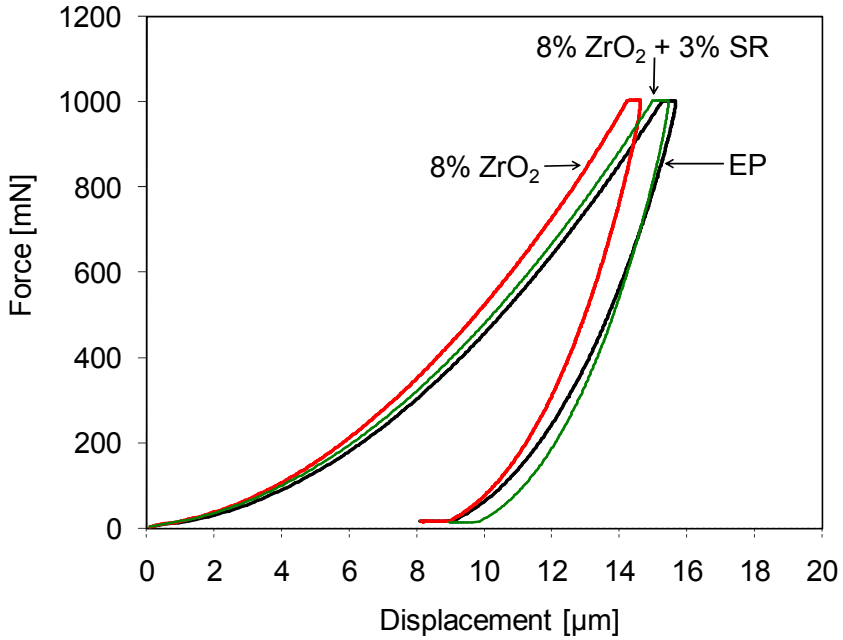

Figure 4.47: Micro-indentation force-displacement curve of zirconia-rubber modified epoxies

The hybrid modified epoxies with lower ceramic content are softer than EP, but epoxy compounds containing higher proportion zirconia record hardness at same level than EP. Higher ceramic concentration compensates the softening effect of rubber and no negative effect in hardness is longer observed.

Figure 4.47 shows the microidentation force-displacement curve, that makes evident the stiffening effect of zirconia on the epoxy resin, not only by the increment in elastic modulus (slope at first part of the curve) but also by the enhanced elastic recovery of the nanomodified matrix when the indenter force is removed. Zirconia stiffening effect prevails also in the hybrid compound.

4.2.11 Interparticle Distance

The interparticle distance of zirconia-rubber modified matrices was also calculated basis on the Basal-Ardnell equation, Figure 4.48. It is well known that zirconia particles are not spheres. However, the values obtained considering 100 nm particle size, agreed with the microscopy observations.

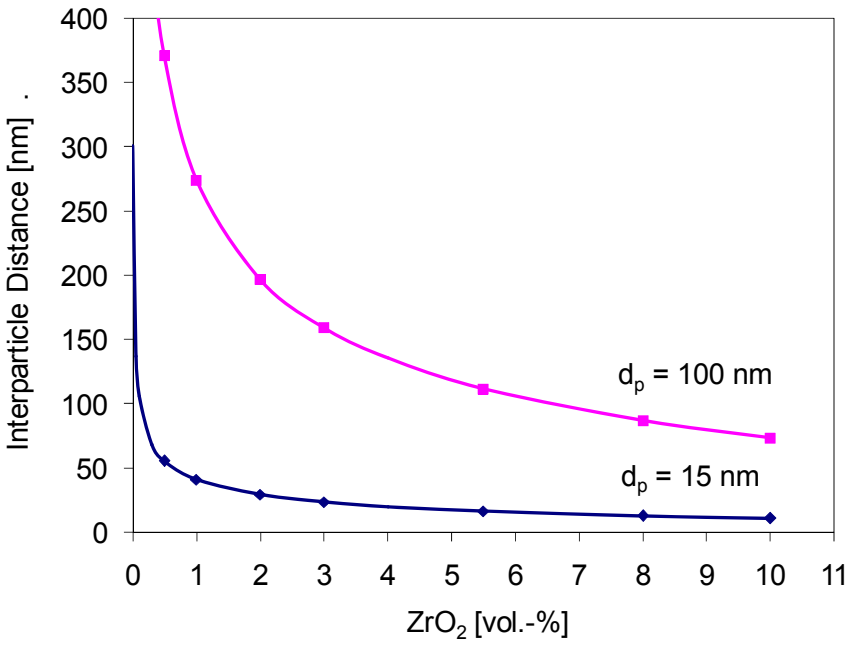

Figure 4.48: Interparticle distance in zirconia nanocomposites.

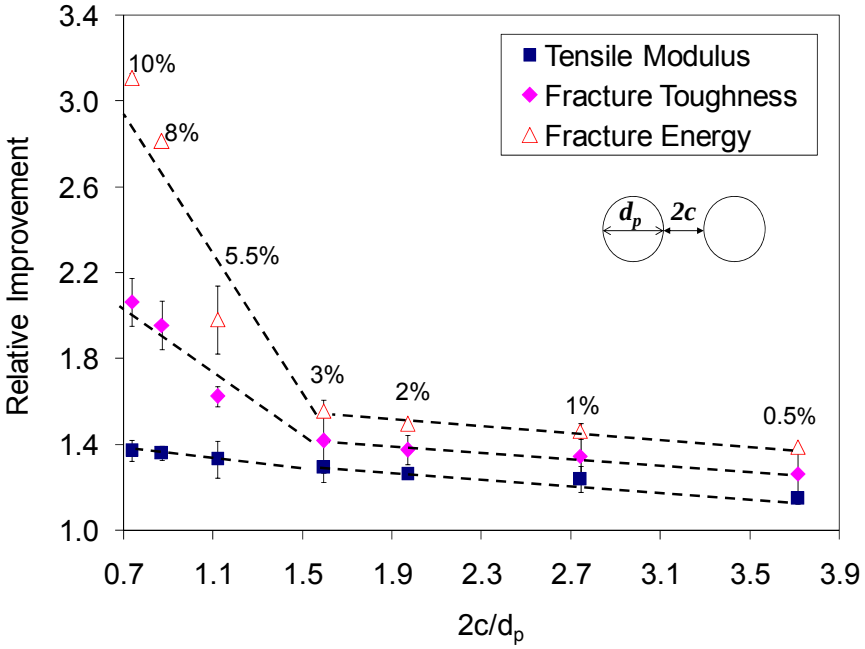

Figure 4.49: Relative improvement of mechanical properties as function of the inter-particle distance to zirconia nanocomposites

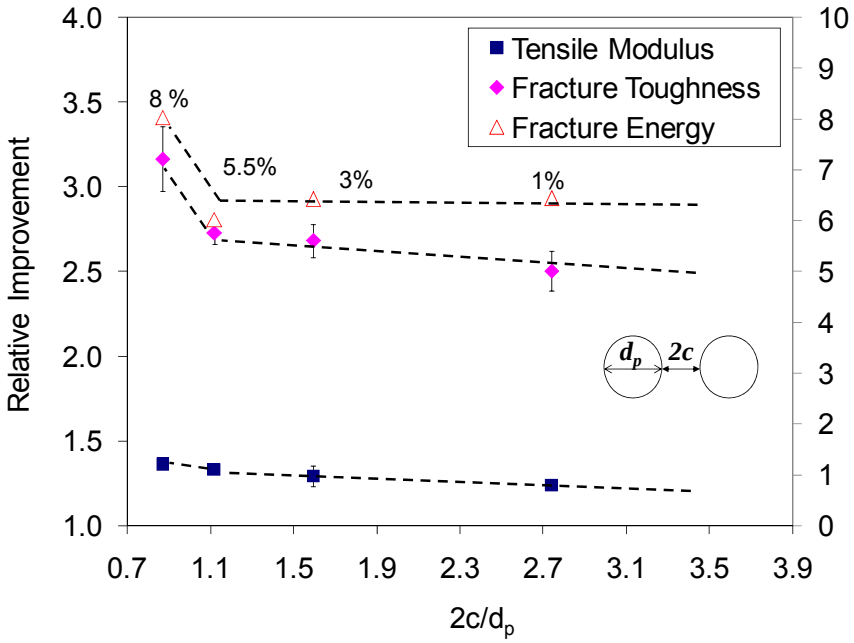

Figure 4.50: Relative improvement of mechanical properties as function of the inter-particle distance to zirconia-rubber hybrid compounds containing 3 vol.-%SR

As was stated previously, the interparticle distance is reduced with increasing filler content and once that this reach a critical value, filler-filler interactions may also occur. The interfaces of different particles overlap each other forming a tridimensional network throughout the composite and having a great impact on its final properties.

Figure 4.49 presents the relative improvement of the mechanical properties as function of the interparticle distance of the zirconia-nanocomposites. By the zirconia nanocomposites the turning point of the curves is located somewhere between 3 and 5.5 vol.-% ZrO_2, at interparticle distance lower than 1.6 times the particle diameter, at this position the graphic tangent changes its slope to higher values, which indicates that the improvement on properties is more noticeable from this point on. This is particularly true for the fracture energy and toughness. In the case of the tensile modulus the change in the curve at the defined critical particle distance seems quite modest.

The especial reinforcement effect of the nanoparticle interfaces is also evident by hybrid compounds, Figure 4.50; although, the presence of rubber displaces the critical interparticle distance to interfaces network formation to lower values. The graph turning point of the hybrid compound properties is appreciable only at particle distances lower that 1.1 the particle diameter.

4.3 Glass Fiber Reinforced Composites

4.3.1 Morphology

At starting point to determine the fiber reinforced composite quality, their internal structure was microscopically analyzed in order to determine the impregnation feature. Figure 4.51 shows the composite profiles, where fiber bundle are clearly observed as well as the resin domains between fibers. Fibers have circular structures (cross section) and the distances between fibers are in the range of several micrometers which provide free space for the polymer to enter.

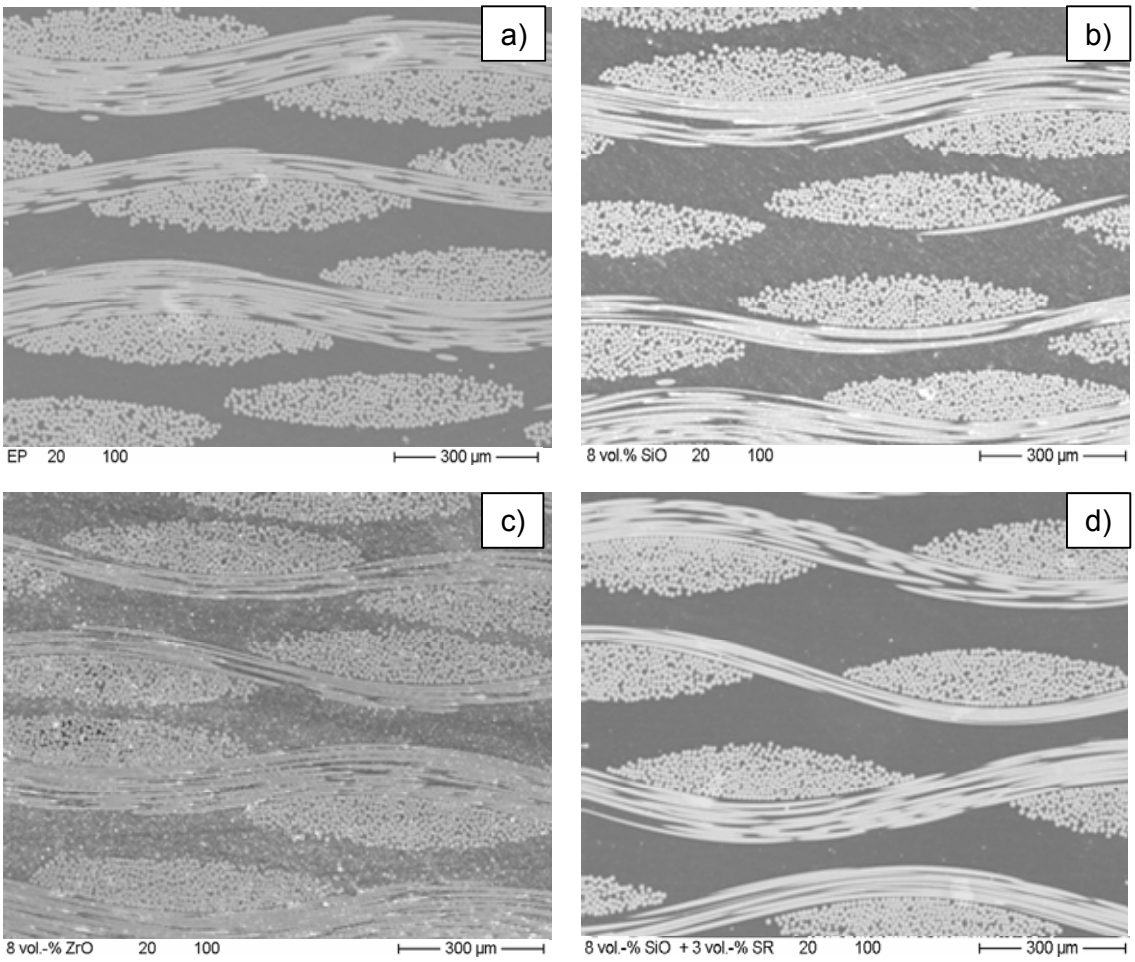

Figure 4.51: Profiles of GFRC from a)EP, b)8 vol.-% SiO_2, c) 8 vol.-% ZrO_2 and d) 8 vol.-% SiO_2 + 3 vol.-% SR.

On these images is possible to state that polymer matrices were well distributed into the mold cavity and a right fibers wetting was achieved. No delamination or voids are observed, neither fiber displacement.

Other important aspect to be considering during the FRCs production from filled matrices is the filler filtering effect that may be generated by compact fiber structures. This is important when microfillers are involved, in the case of nanosized fillers, this effect can be neglected.

In order to determine if filtering effect occur in the designed GFRCs, the particle distribution of representative RTM plates was monitored. Specimens were cut from the section immediately beside the injection site and also at one of the most remote positions from this point, and they were microscopically analyzed, using high magnifications. The sites at which the analyzed specimens where taken are illustrated in Figure 4.52. The corresponding particle distribution into GFRCs from hybrid modified matrices is presented in Figure 4.53 and Figure 4.54.

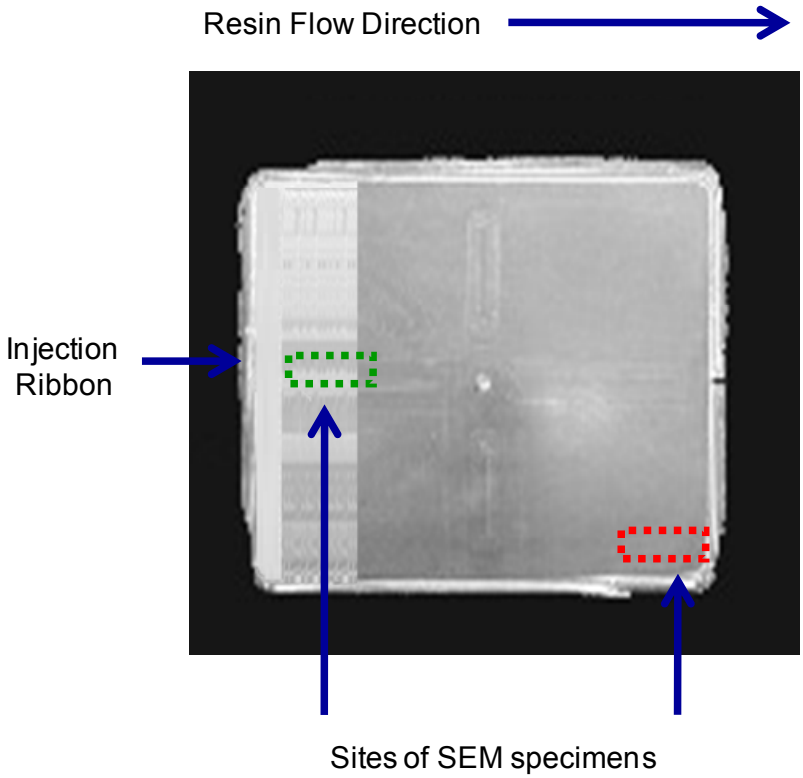

Figure 4.52: Sites of SEM specimens to analyze the particle distribution.

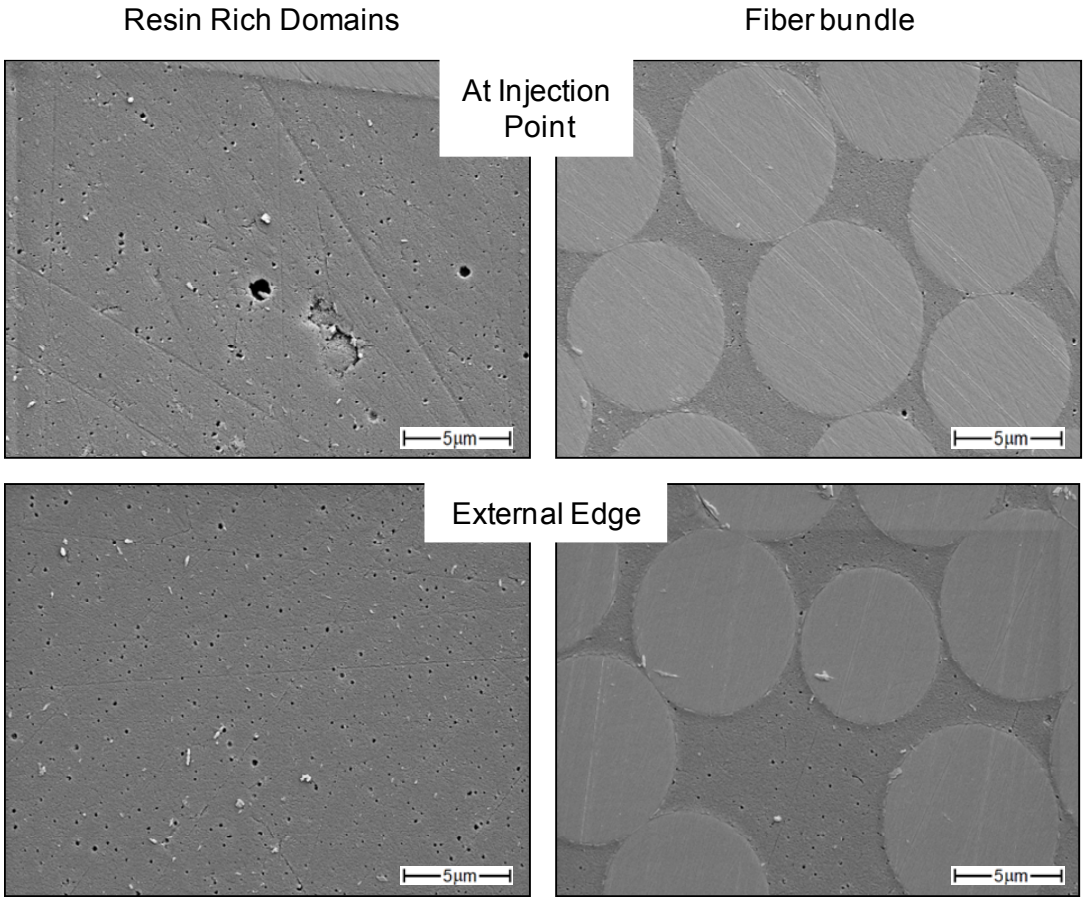

Figure 4.53: Particle distribution of the GFRC containing 8 vol.-% SiO_2 + 3 vol.-% SR

Once again rubber particles were detached from the composite surface due to the specimen treatment (grinding), but their distribution could be estimated from the de-bonding holes present in the samples.

Figure 4.53 and Figure 4.54 show no considerable difference in rubber particle distribution between the specimens located at the injection point and at the external edge of the same plate. Silicone rubber is uniformly distributed in the resin rich domains as also into the fiber bundle, although in these last sites rubber particles proportion is quite lower. This confirms that only rubber particles with smaller dimensions are able to move freely together with the resin between the fiber gaps. However, in the present case this fact does not represent relevant risks of mechanical failure.

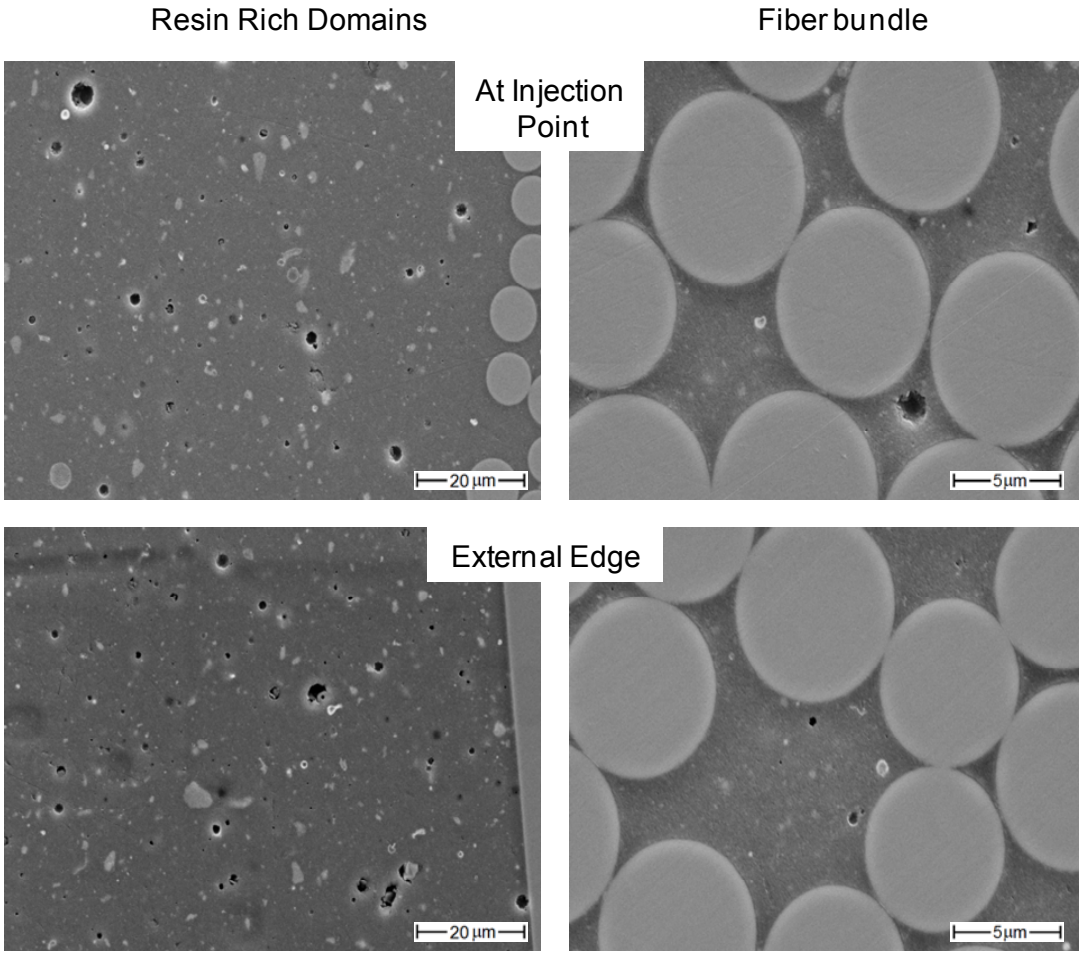

Figure 4.54: Particle distribution of the GFRC containing 8 vol.-% ZrO_2 + 3 vol.-% SR

Similarly to the rubber particles, zirconia clusters (that can reach sizes up to 100nm) are well distributed in the resin rich domains, the same at the position beside the injection point as at the external edge, but into the fiber bundle only very small agglomerates as well as isolated nanoparticles are present.

An important remark have to be done about the considerable difference in the rubber particle size observed between the hybrid matrices containing silica and the ones containing zirconia. Rubber particles in hybrid composites containing zirconia are in average 5-10 fold bigger than the ones in silica-rubber composites.

Detailed nanofiller distribution of nanofiller into the GFRCs is presented in Figure 4.55, which shows the matrix morphology between fibers of a bundle. It is observed

that nanoparticles maintain their homogeneous distribution, as reported in bulk matrix.

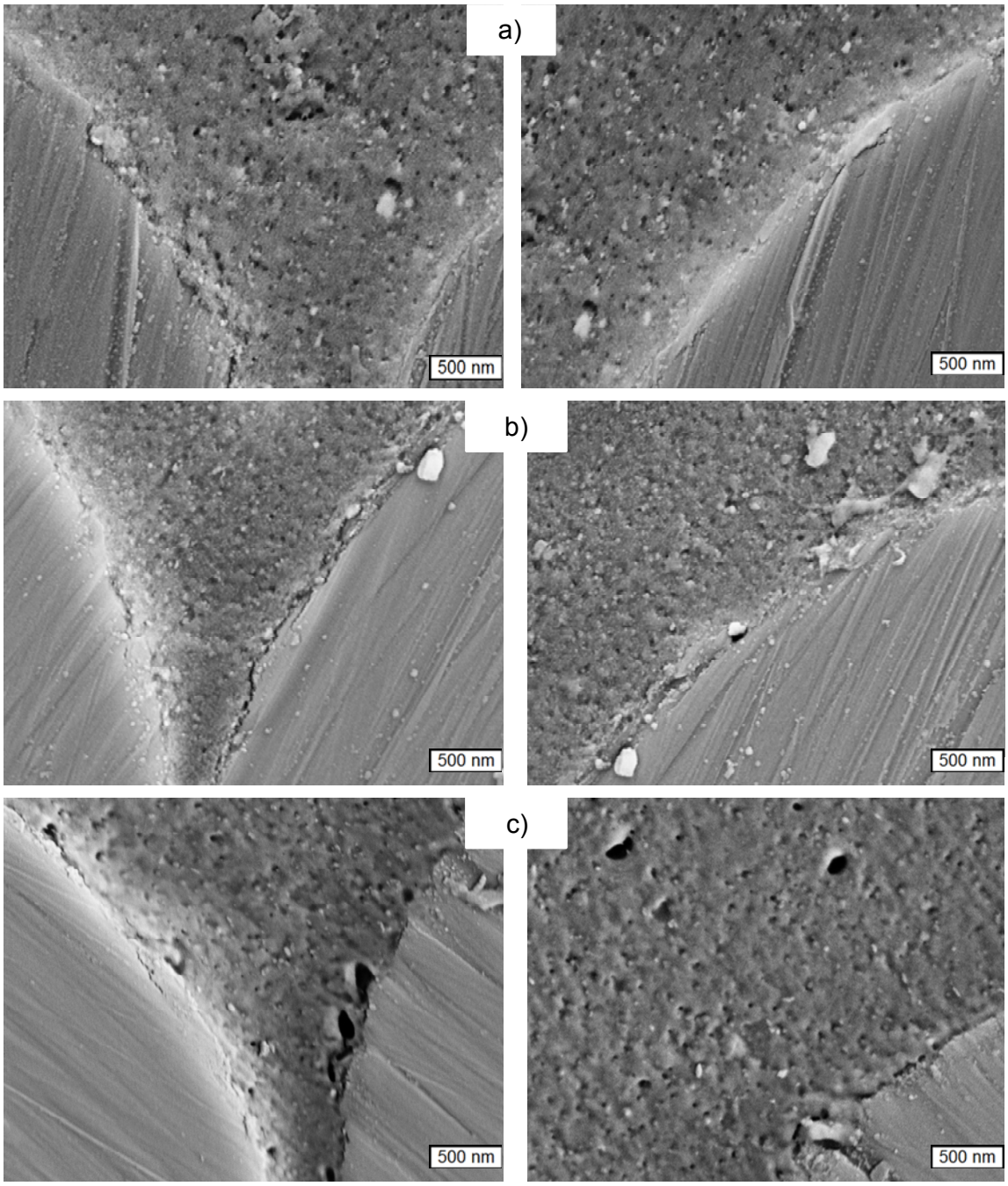

Figure 4.55: Particle distribution in GFRCs a) 8 vol.-% SiO_2, b)8 vol.-% ZrO_2, and c) 8 vol.-% SiO_2+3 vol.-% SR

These images give also a general idea about the matrix-filler bonding. In silica nanocomposite is possible to the see the uniformly distributed particles but also holes generated by particle debonding, that together with the results presented in section 4.1.8, confirm a relative weak silica nanoparticles-matrix bonding. However, the fiber-matrix bonding seems to be very strong.

Contrary, zirconia modified composite shows that particle/clusters are strongly attached to the matrix, the particles are evident and only low proportion of holes are observed, although the fiber-matrix bond appears to be slightly weaker than the previous case. In hybrid compounds also rubber particles affect the matrix-fiber bond producing localized micro detachment between both phases.

4.3.2 Tensile Properties

The tensile properties of the composites from the modified and non-modified epoxy matrices are summarized in Figure 4.56 and Figure 4.57.

The tensile modulus of the composites from nanomodified matrices follows the same tendency reported in bulk materials. Modulus increases almost linearly at rising ceramic content but the improvement is given in lower proportion than in bulk. The composite containing 8 vol.-% SiO_2 records an enhanced modulus up to 15% and the composite with same amount of zirconia display a modulus 25% higher than the composite from EP matrix.

Tensile strength in composites is not changed by nanomodification of the matrix; only marginal variations (< 5 %) in both studied systems are registered.

Other important aspect to remark is that composite tensile properties are not negatively affected by SR.

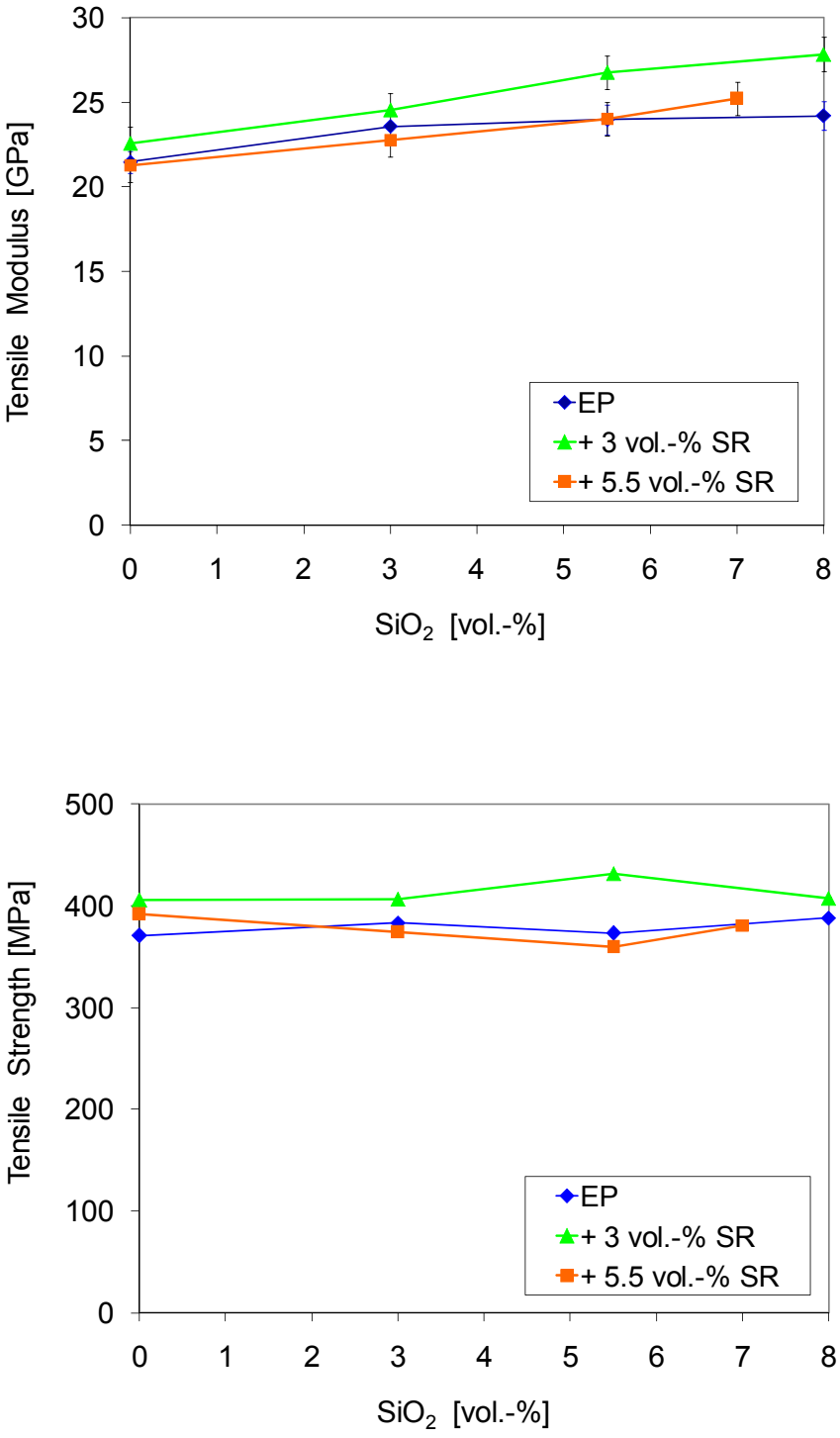

Figure 4.56: Tensile properties of GFRC from silica-rubber modified matrices

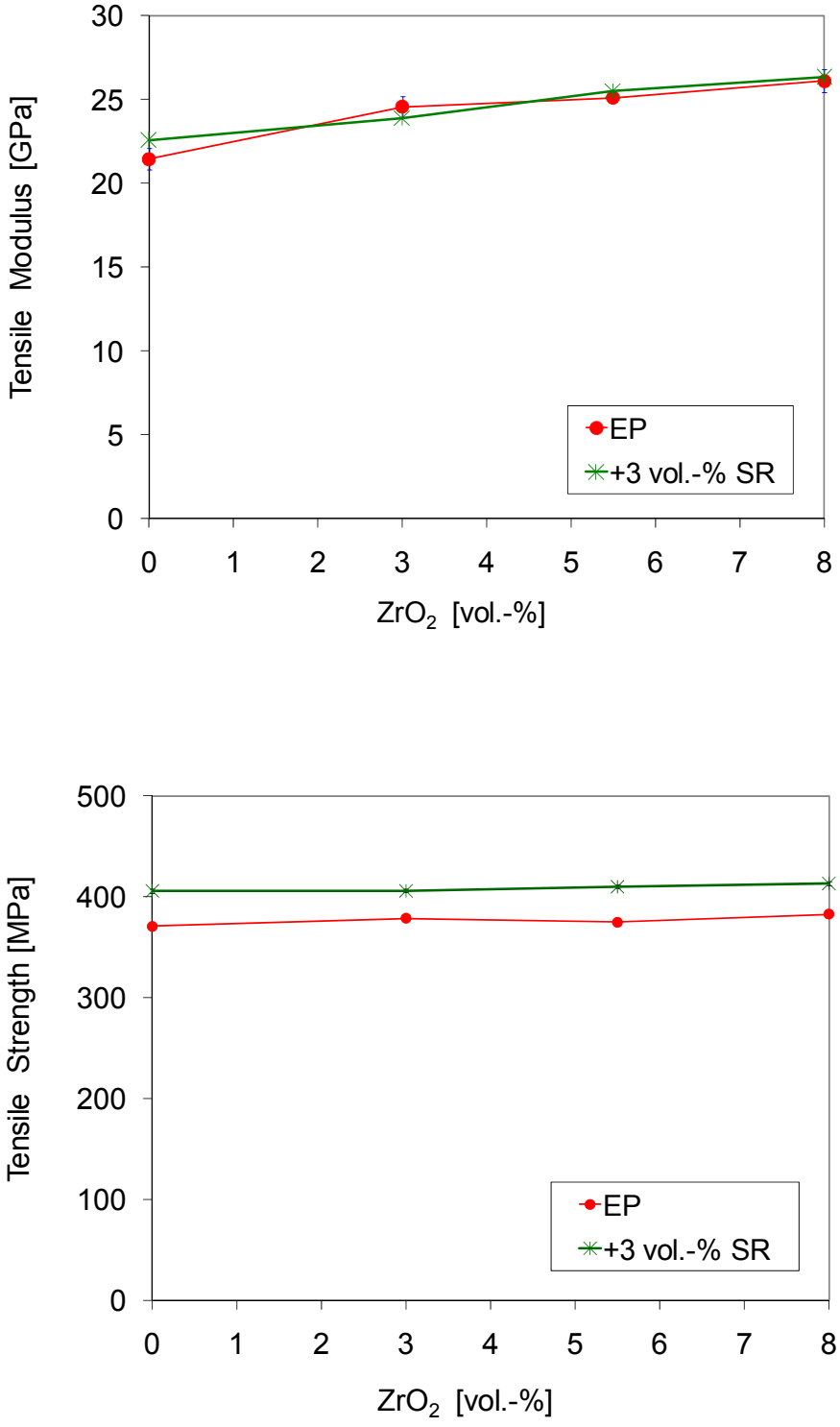

Figure 4.57: Tensile properties of GFRC from zirconia-rubber modified matrices

The response of composites to tensile loads is strongly determined by the stiffness and strength of the reinforcement fibers, since they are far higher than the resin system. When load is applied in fiber direction most of it is borne by fibers, the role of the interface and the matrix is limited to transfer the stress from highly stressed fibers to the neighboring ones that carry relatively low stresses. However, changes in failure mode may be strong influenced by the nature of the matrix and matrix-fiber bond.

Changes in failure modes resulting from the matrix modification are illustrated in Figure 4.58.

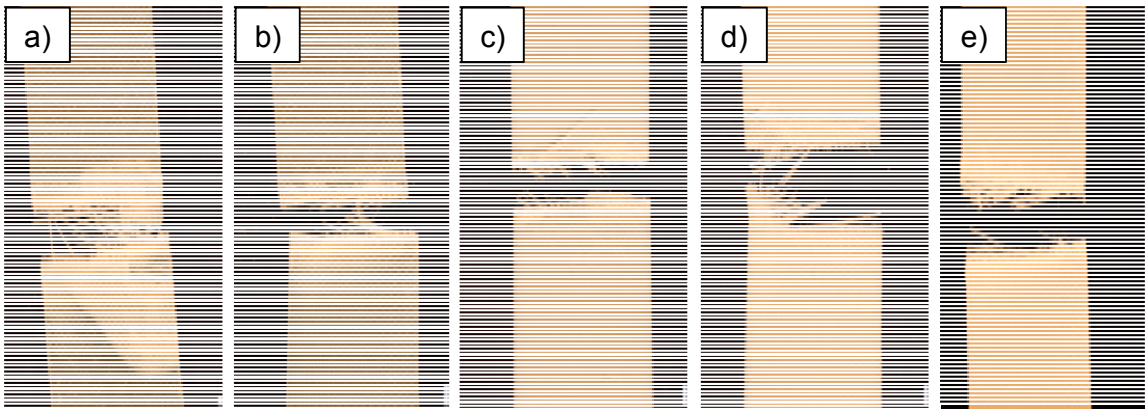

Figure 4.58: Tensile test specimens a) EP, b) 8 vol.-%SiO_2, c)8 vol.-ZrO_2, d) 8 vol.-% SiO_2 + 3 vol.-% SR and e) 8 vol.-ZrO_2 + 3 vol.-SR.

It is observed that the EP composite presents high debonding previous failure, the matrix fail first and the failure propagates between the weak matrix-fiber interface causing the stress concentration in fiber up to fiber failure. In nanomodified epoxies delamination is avoided because of an improvement in the matrix-fiber bonding; stresses are better distributed and the failure take place at higher loads and mainly in perpendicular direction to the load axis. The hybrid compounds show also no remarkably delamination but in this case the failure propagates not only perpendicular to the loading axis, but also by shearing through adjacent fiber plies, process that occur due to the enhanced toughness of the matrix [110].

Rule of Mixtures

Rules of Mixtures are mathematical expressions which give some property of the composite in terms of the properties, quantity and arrangement of its constituents.

Unidirectional fibers are the simplest arrangement of fibers to analyze. They provide maximum properties in the fiber direction, but minimum properties in the transverse direction [111,112].

A load applied in the fiber direction is shared between fiber and matrix, the stresses depend on the cross-sectional areas of fiber and matrix, but for compatibility, the strain, ε must be the same in both fiber and matrix; otherwise holes would appear in the composite ends. This is known as Isostrain rule; Poisson contraction has been ignored [78].

$$E = E_m(1-V_f) + E_f V_f \tag{4.14}$$

If a force is applied perpendicular to the fibers then the fibers and matrix will stretch in same direction. The total deflection is just the sum of the deflections in fiber and the matrix but the stress is the same in each phase this is known as Isostress rule of mixtures and can be written also as

$$E = \left(\frac{E_f E_m}{(1-V_f)E_f + V_f E_m} \right) \tag{4.15}$$

The majority of structures made from composites, are made from woven cloth rather than the simple uniaxial fibers described above. The analysis of the stiffness of a composite made from woven cloth is very complex. However, a simple approximation of the tensile modulus of a plain woven is safe to assume that half of the fibers are in wrap 0° orientation and the other half are in weft 90° directions

In such cases the rule of mixture can be applied to predict the tensile modulus

$$2E = E_m(1-V_f) + E_f V_f + \left(\frac{E_f E_m}{(1-V_f)E_f + V_f E_m} \right) \tag{4.16}$$

The theoretical approximations obtained from Equation (4.16) are compared with the experimental results in Figure 4.59 and Figure 4.60.

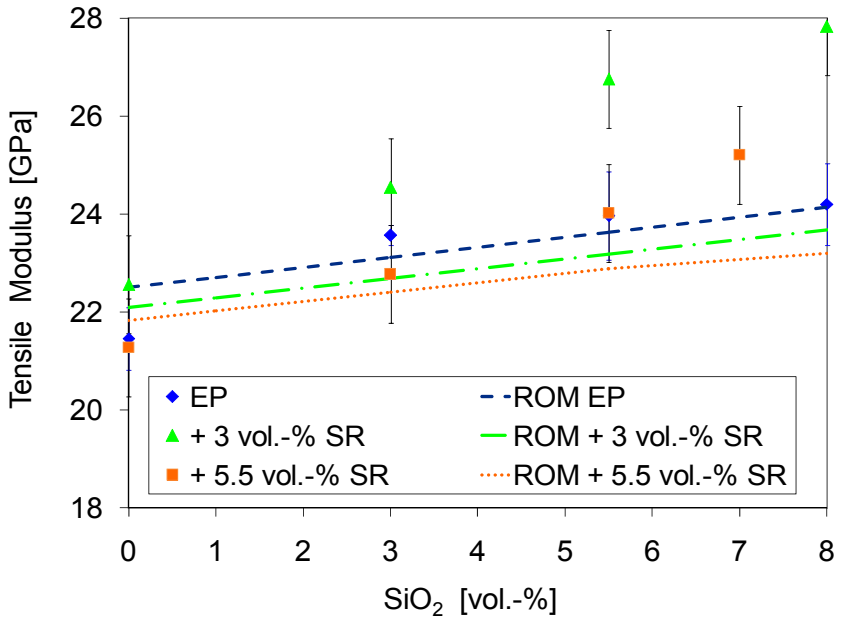

Figure 4.59: Experimental tensile modulus vs. ROM approximation to silica-rubber modified composites.

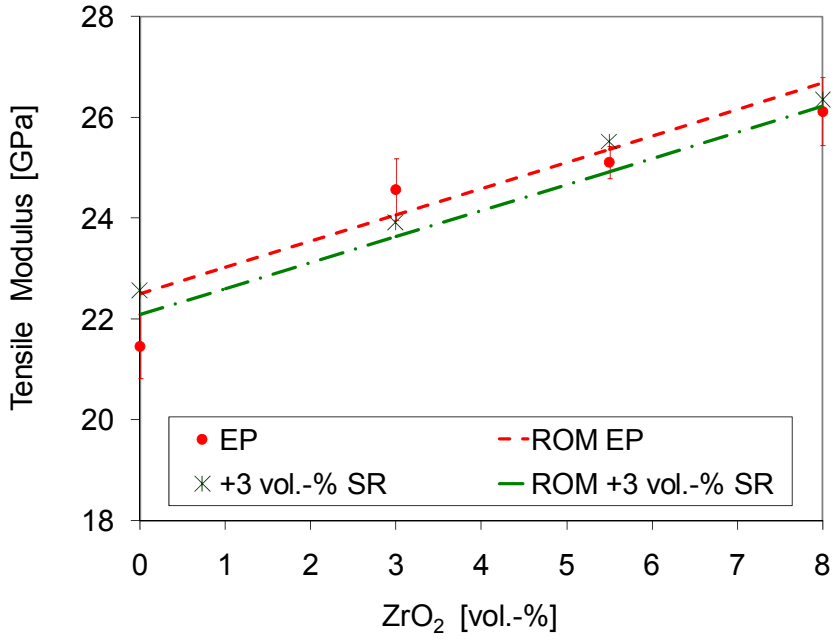

Figure 4.60: Experimental tensile modulus vs. ROM approximation to zirconia-rubber modified composites.

The rule of mixtures assumes perfect fiber-matrix bonding and ignores the variations resulting from imperfect fiber alignment, non-uniform fiber distribution, local non-homogeneities, void content, etc. In addition, the transverse deformations resulting from Poisson's effect are not considered.

ROM proportions accurate values in the studied cases. The highest deviation between experimental and theoretical results is of approximately +15%, recorded by silica-rubber modified matrices all cases. This suggests, according with the stated in previous paragraph, that in all cases the quality of the obtained laminates is very good.

4.3.3 Compressive Strength

Fiber-reinforced composites are very sensitive to compression loads. The compressive behavior is much more critical than the tensile one for most of the service applications of this class of advanced materials. [113]

The presence of nanoparticles into the epoxy matrix produces an increment in the composites compressive strength. This increment is higher when ZrO_2 is used as filler than when the epoxy is modified with SiO_2. The composite containing 8 vol.% ZrO_2 has a compressive strength 20% higher, than the neat epoxy (EP). While the GFRC containing 8 vol.% SiO_2 records a compressive strength approximately 15% higher than EP. The presence of micro silicone rubber into the epoxy matrix has no relevant effect on the compressive strength; the strength of the composites obtained from hybrid modified matrix is in average 2-6 % lower than the composites containing only nanoceramics.

As the tensile strength, the compressive strength was also determined by distributed defects or irregularities within the specimen. Failure initiates at weak points. They may consist of already existing debondings (microcracks), defects in the laminate structure (resin pockets or terminated plies), fractured fibers at the surface in consequence of specimen preparation, etc. But under compressive load, the composite response is ruled by the adhesive and stiffness properties of the matrix, as it is role of the resin to maintain the fibers as straight as possible in order to prevent them to buckling.

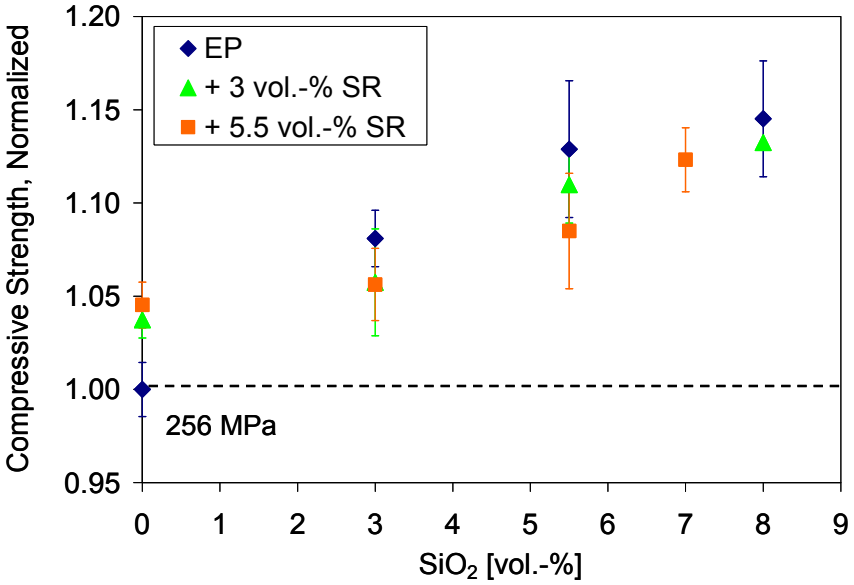

Figure 4.61: Compressive strength of silica-rubber modified composites.

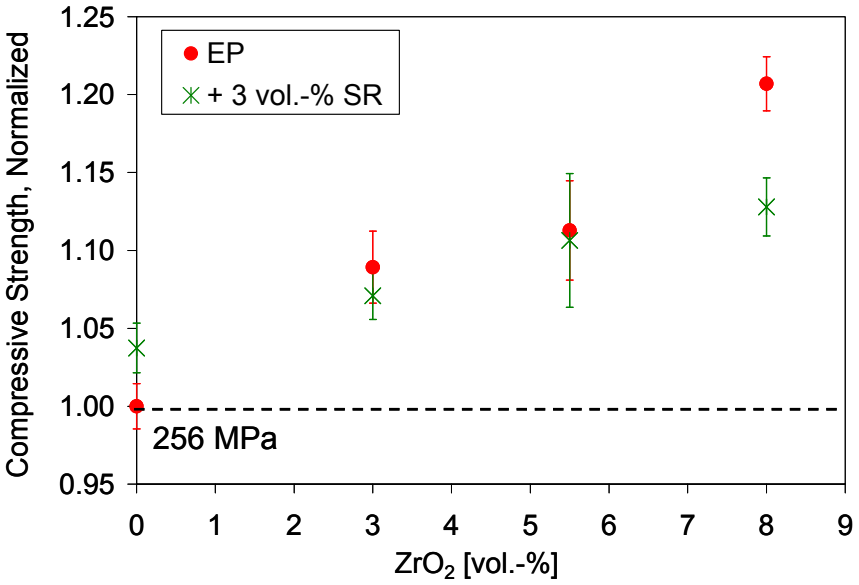

Figure 4.62: Compressive strength of zirconia-rubber modified composites.

The fracture occurred near the end-tab. However, the specimens did not separate into two pieces. The failure mode observed in the composites, from neat and modified epoxy matrices, was the shearing or double shearing of reinforcing fibers at 45° with respect to the loading axis.

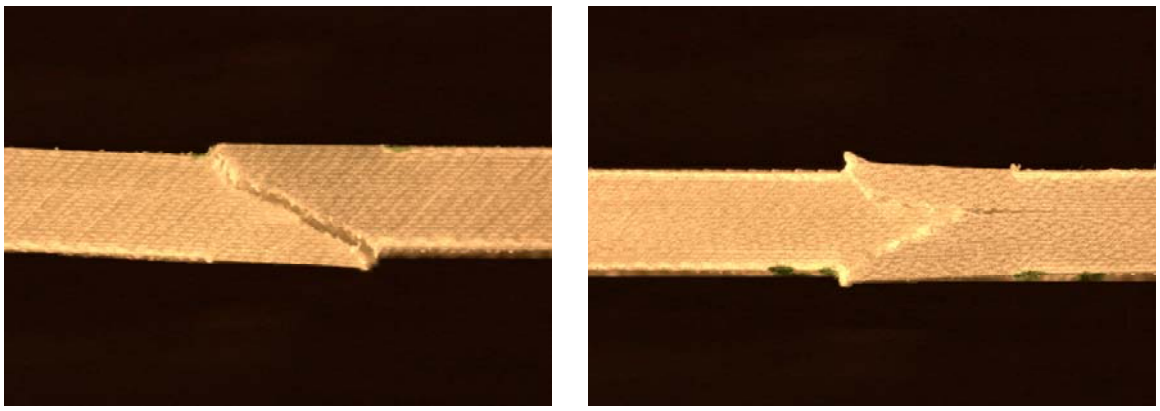

Figure 4.63: Characteristic fracture profile of obtained GFRC.

To better understanding of the improvement in compression strength in composites, the failure surfaces of tested specimens were investigated, Figure 4.64 and Figure 4.65.

Neat epoxy composite shows clearly clean fiber surfaces indicating extensive fiber-matrix interfacial failure. It is probably that delamination occurred first, and with increasing applied compressive load, this delamination buckled [114,115].

Nanomodified composites show better fiber-matrix bonding that provides additional flexural rigidity to the composite, improving the compressive strength. Fiber buckling that propagates along a line of maximum shear stress is observed together with debonded fibers and matrix cracking as well. Therefore, the compressive failure modes nanocomposites are fiber microbuckling, interfacial failure, and matrix failure [114].

In Hybrid compounds, fracture surfaces are much more rugged and they show fiber debris and fiber pull-out. The failure seems to occur in different planes, giving as result a stepped fracture surface. The fibers are closely held by the matrix and the fiber surfaces are coated with the matrix material indicating strong adhesion between fiber

and matrix. The major failure modes in hybrid compounds are characterized as compressive failure of fibers and matrix failure.

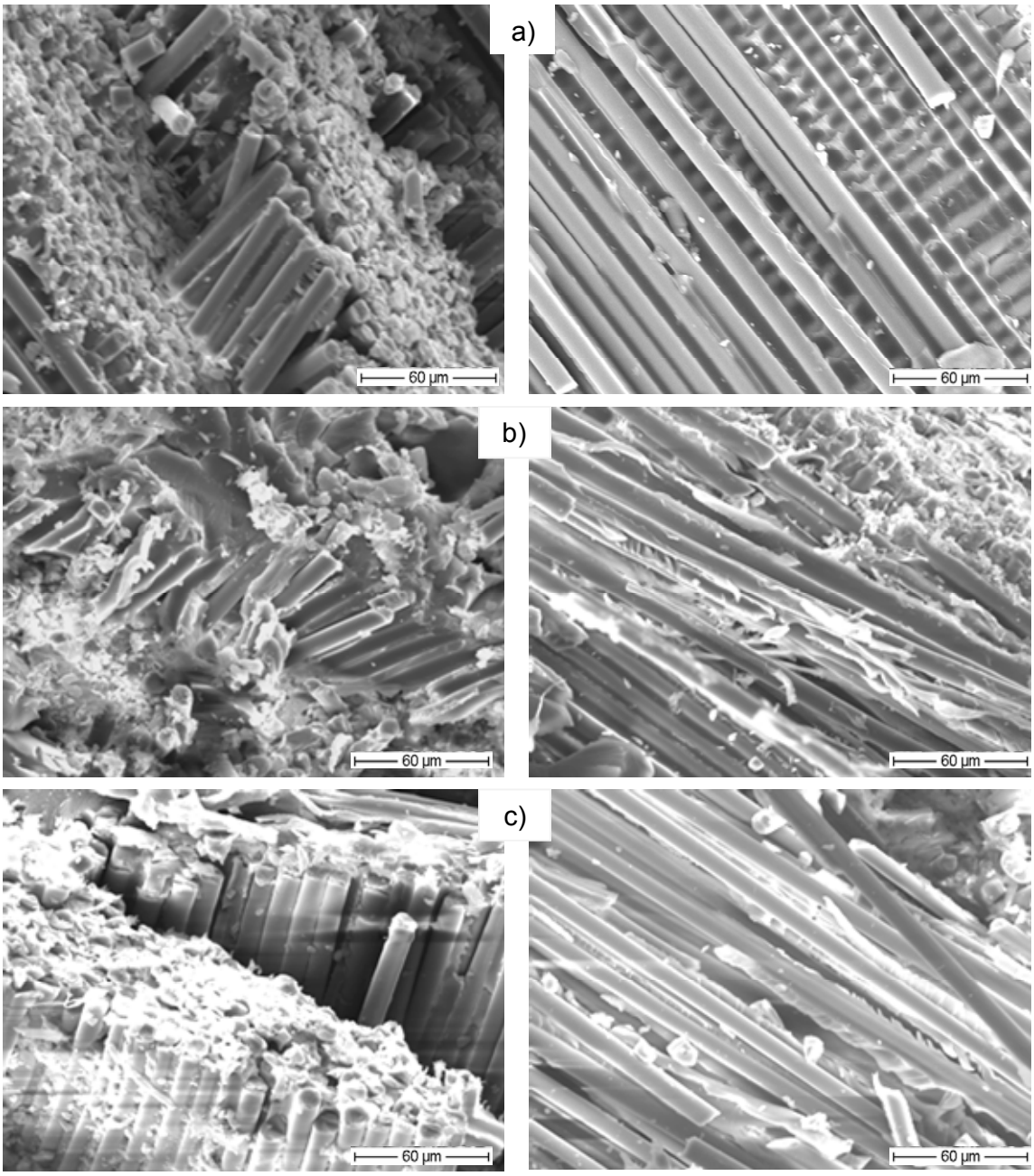

Figure 4.64: Fracture surfaces of compression test specimen a) EP, b) 8 vol.-% SiO_2 and c) 8 vol.-% ZrO_2.

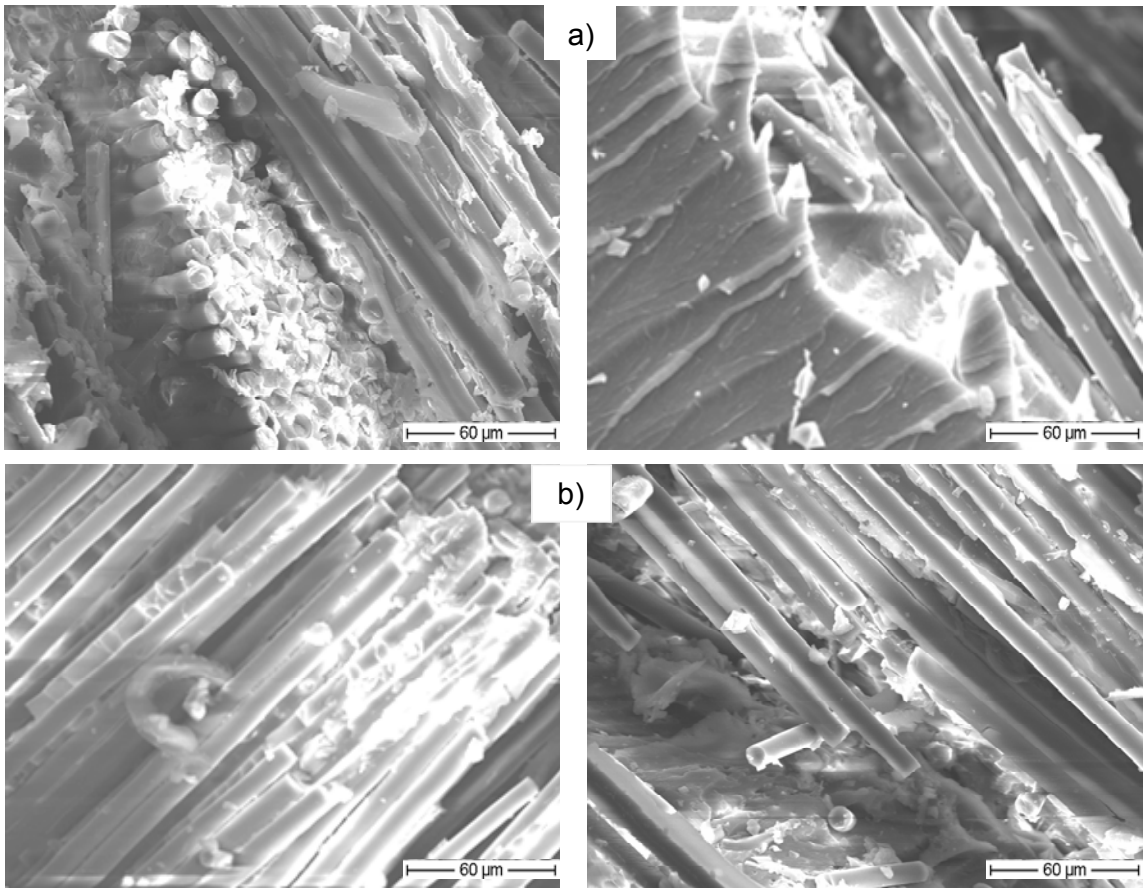

Figure 4.65: Fracture surfaces of compression test specimen a) 8 vol.-% SiO_2 + 3 vol.-% SR and b) 8 vol.-% ZrO_2 + 3 vol.-% SR.

4.3.4 Interlaminar Fracture Toughness

Delamination is one of the predominant modes of damage in composite structures. The resistance to delamination is known as the interlaminar fracture toughness, it is an important composite property and widely acknowledged by designers. Interlaminare fracture toughness normally associated with the matrix toughness.

The changes in interlaminate fracture toughness (G_{IC}) of the composites as function of the fracture energy of their matrix are represented in Figure 4.66 and Figure 4.67.

In general, is evident that the matrix modification plays an important role on the composite toughness improvement. However, it is observed that the large increase in polymer toughness no necessarily produce an enhancement in composite tough-

ness, which is according with Scott and Phillips founds. They determine that a tenfold increase in resin toughness increases the composite toughness just by a factor of 2 [116].

In the studied epoxy compositions the transfer factor, from matrix toughness to interlaminar fracture toughness of composites, depends on matrix toughness [116,117]. In brittle nanomodified matrices, containing either SiO_2 or ZrO_2, the transfer factor falls in average in the range 2 to 1.2. Meanwhile, the hybrid compounds, whit better toughness, only reach transfer factors in range 12 to 1.6.

However, as expected, the best absolute results, in order to enhance the composite toughness were reached by the hybrid compounding matrices. The hybrid compound containing 8 vol.-% SiO_2 + 3 vol.-% SR produces composites with more than 70% enhanced delamination resistance; and the use of the epoxy matrix modified with 8 vol.-% ZrO_2 + 3 vol.-% SR results in composites with up to 40% improved toughness.

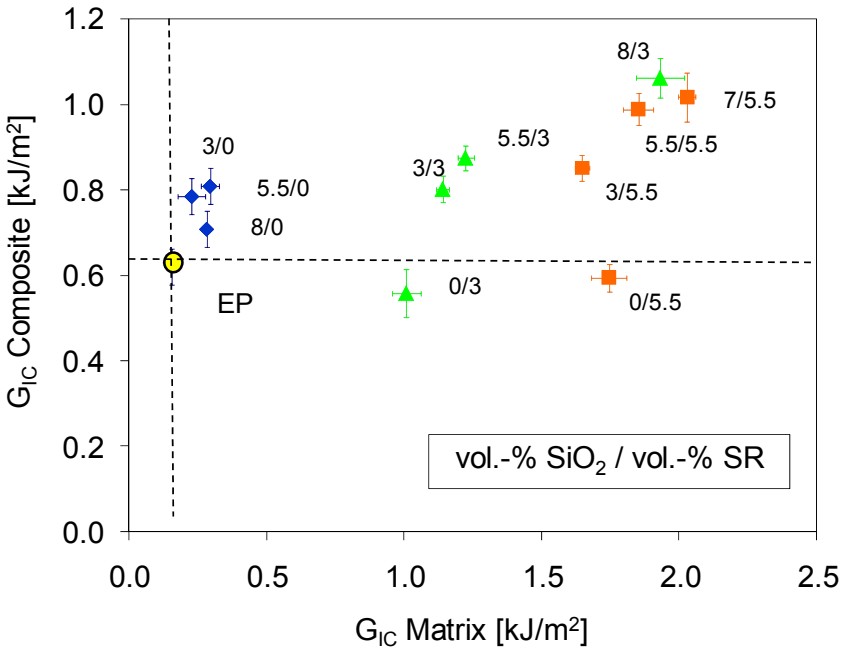

Figure 4.66: Interlaminar fracture toughness of silica-rubber composites

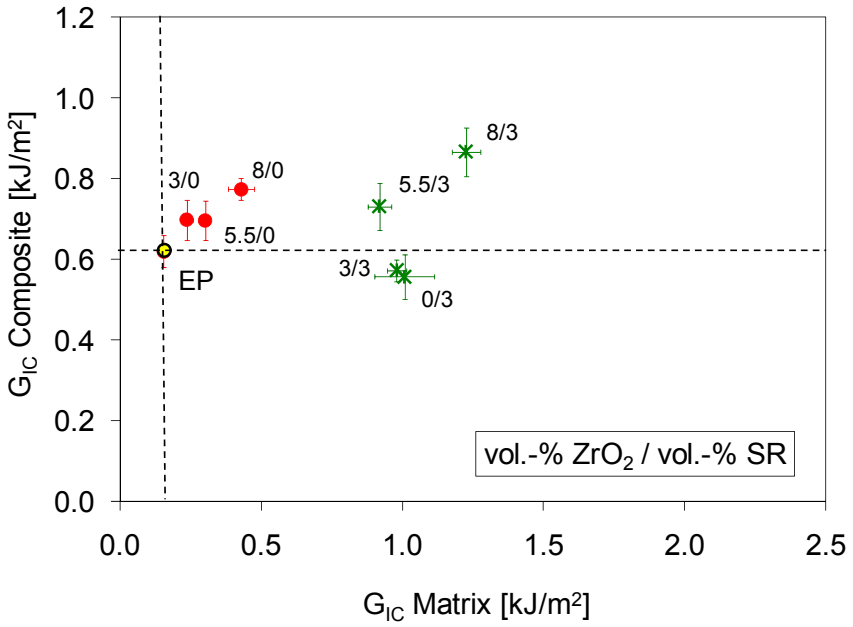

Figure 4.67: Interlaminar fracture toughness of zirconia-rubber composites

When silica and silicone rubber are used simultaneously as epoxy modifiers a synergetic effect between them results evident. It is particularly manifest by the hybrid compounds containing high proportion of ceramics.

The fracture surface morphologies of the representative specimens from the three groups of composites were examined by the SEM. The results show substantial differences in the morphology of the fracture surfaces as a function of fiber-matrix adhesion, Figure 4.68 and Figure 4.69. In the neat epoxy, fibers are completely devoid of matrix indicating extensive fiber-matrix interfacial failure, and there is no well-defined crack plane.

The matrix failure is characterized by clean matrix fracture (without hackle marks) and clean narrow channels as result of the fiber pull-out suggesting that the crack propagation occurred primarily in the mid-plane.

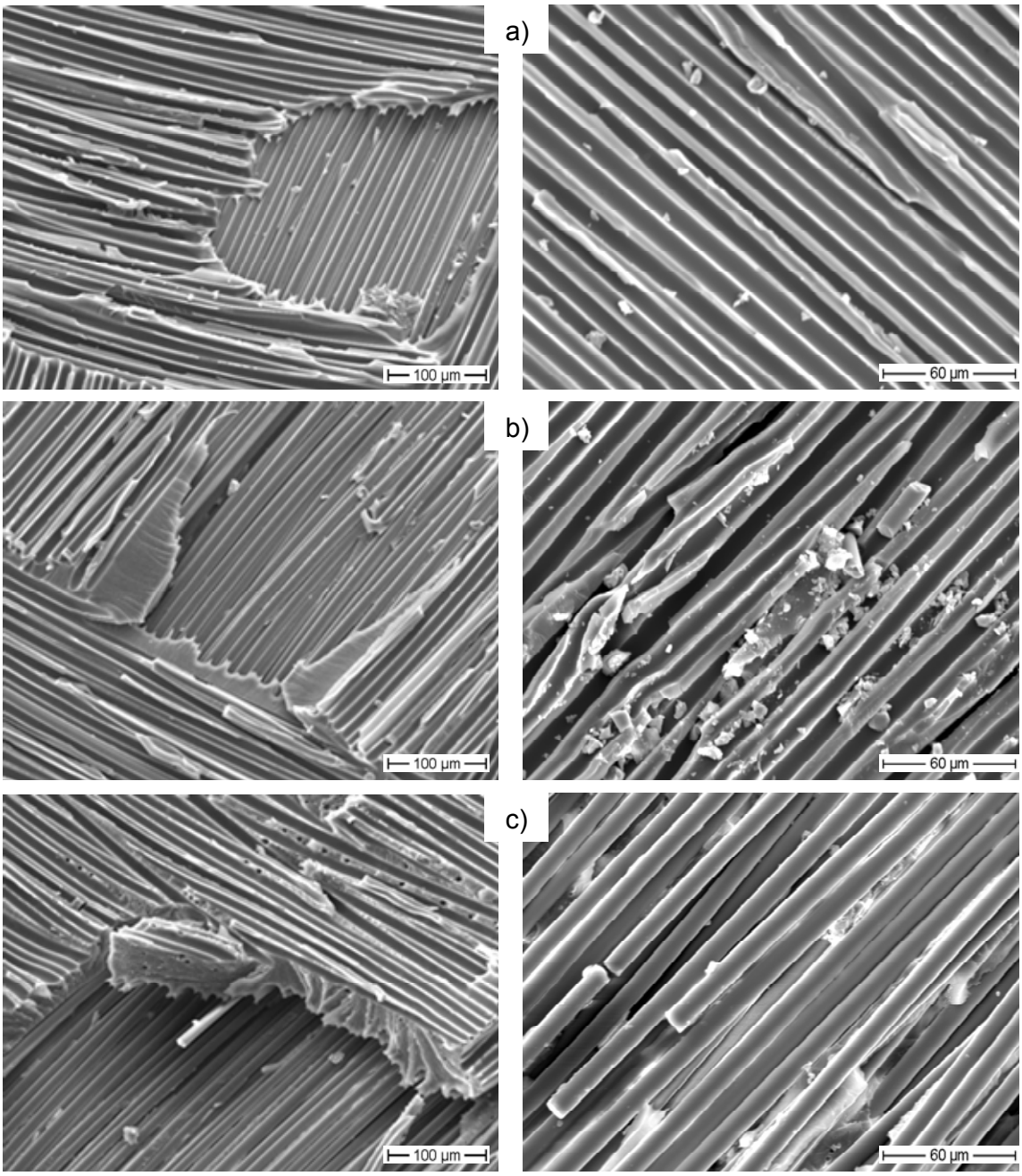

Figure 4.68: Fracture surface of DCB specimens a) EP, b) 8 vol.-% SiO_2, c) 5.5 vol.-% SiO_2 + 5.5 vol.-% SR

In nanocomposites, the micrograph also shows channels about four to five fiber diameters wide and about two to three fiber diameters deep that may have been left by fiber pull-out. The presence of these two to three fiber diameter deep channels sug-

gests that the crack did not always remain in the mid-plane, but in some instances at certain places the adjacent plies were also involved [118].

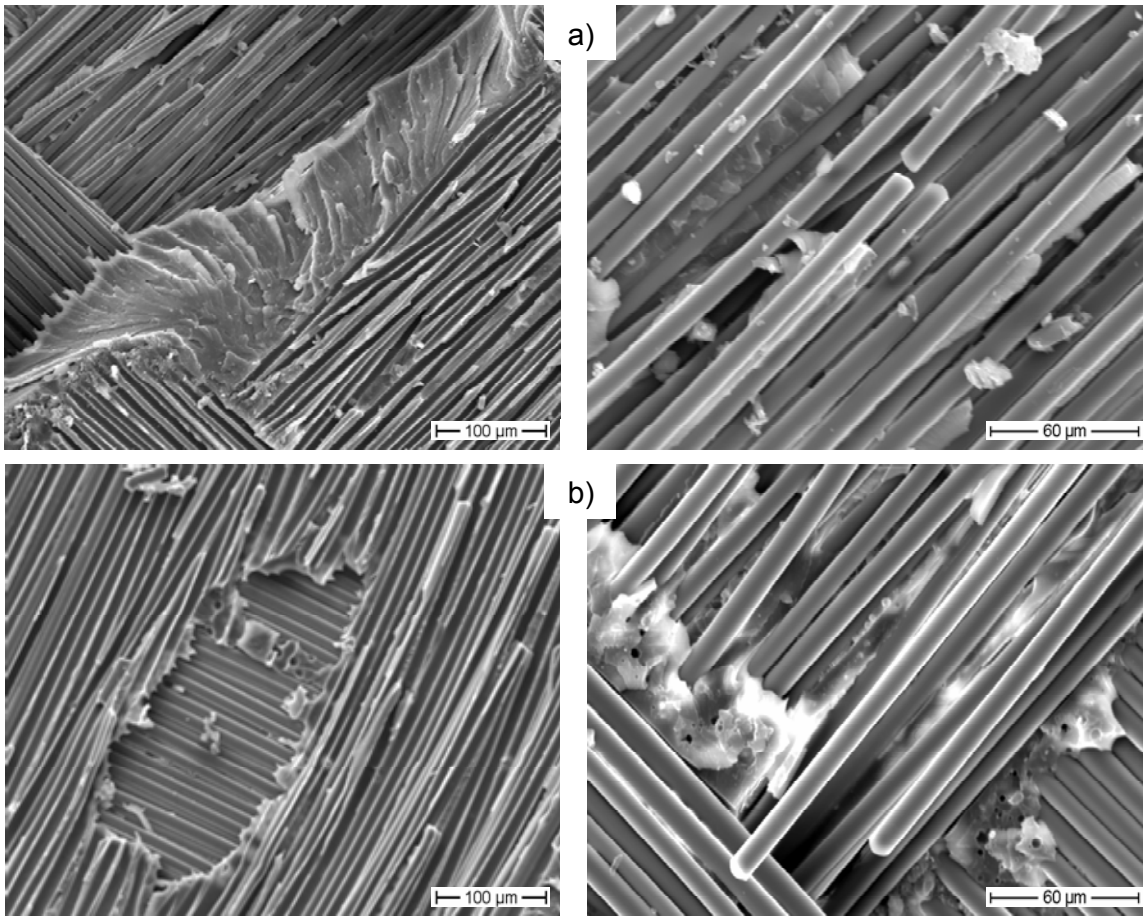

Figure 4.69: Fracture surface of DCB specimens a) 8 vol.-% ZrO_2, b) 5.5 vol.-% ZrO_2 + 3 vol.-% SR

The hackle marks in the matrix material seem to appear on the periphery of individual fibers. The origin of these hackle marks is attributed to yielding at the periphery of individual fibers or fiber bundles during fiber pull-out.

Hybrid compounds fracture surface is characterized by hackle markings at some places, limited interfacial failure, few fiber breaks, and fiber pull-out.

4.3.5 Interlaminar Shear Strength

The shear strength values of the obtained composites are presented in Table 4.5 and Table 4.6.

Table 4.5: Shear strength of silica-rubber modified laminates

	EP		3 vol.-% SR		5.5 vol.-% SR	
Content SiO_2 [vol.-%]	ILSS [MPa]	Std. Dev.	ILSS [MPa]	Std. Dev.	ILSS [MPa]	Std. Dev.
0	30.77	0.99	31.26	1.64	28.67	1.83
3	31.79	0.20	32.92	1.78	30.86	1.01
5.5	32.76	1.70	33.48	2.28	32.35	0.72
7	-------	-------	-------	-------	33.68	1.12
8	33.45	1.00	34.34	5.92	-------	-------

Table 4.6: Shear strength of zirconia-rubber modified laminates

	EP		3 vol.-% SR	
Content ZrO_2 [vol.-%]	ILSS [MPa]	Std. Dev.	ILSS [MPa]	Std. Dev.
0	30.77	0.99	31.26	1.64
3	33.85	0.45	33.86	1.07
5.5	32.42	1.25	37.09	2.58
8	33.98	0.75	38.30	0.23

In general shear strength in composites is concentrated in the matrix and is determined basically by the interfacial adhesion fibers-matrix and the matrix toughness.

From the results listed above, it is observed that the shear strength in significant influenced by the matrix modification. Nanocomposites show higher shear stress because nanoceramics enhance the matrix toughness but also improve the bonding fibers-matrix. Hybrid compounds show also further improvement in shear strength, derived from the superior toughness induced by SR in the epoxy matrices.

5 Conclusions

The proposal to formulate hybrid compounds basis nanoceramics and silicone rubber represents a novel alternative to toughen epoxy matrices not only without detriment but also with a simultaneous improvement of other important properties as modulus, strength and thermal stability.

The analysis of the achieved results makes it clear that the properties of the nano- and hybrid-modified matrices are mainly determined by three factors: the inherent properties of the matrix and fillers, the right distribution of fillers into the matrix bulk, and the compatibility filler-matrix; and in the case of hybrid compounds also the compatibility filler-filler.

About the particle distribution, it was proved that the in-situ sol-gel technique is an effective method to produce agglomerate-free compounds with rather high filler content. Silica nanocomposites and hybrid modified matrices obtained from this method registered a homogeneous particle distribution, fact that was immediately reflected in their rheological behavior. They recorded a gradual viscosity increment directly related with both filler content.

On the other hand, the in-situ modification of epoxy resins by direct incorporation of nanoparticles into the prepolymer only by using mechanical shear forces, showed a limited ability to produce a uniform distribution of particles. Zirconia nanocomposites and hybrid compounds, obtained by this procedure, present high proportion of agglomerates with irregular form and wide size distribution. Their viscosities are considerably higher than the neat epoxy and vary exponentially as function of the nanoparticle volume fraction.

In spite of the important increment on the epoxy viscosity due to its modification with particles, both series of ceramic-rubber modified matrices demonstrated their suitability to be processed by RTM. It was also clear that the particles modify slightly the curing kinetic of the matrix but this situation does not determine the modification of the curing program.

A comparative of the properties of the most representative modified matrices is shown in Figure 5.1.

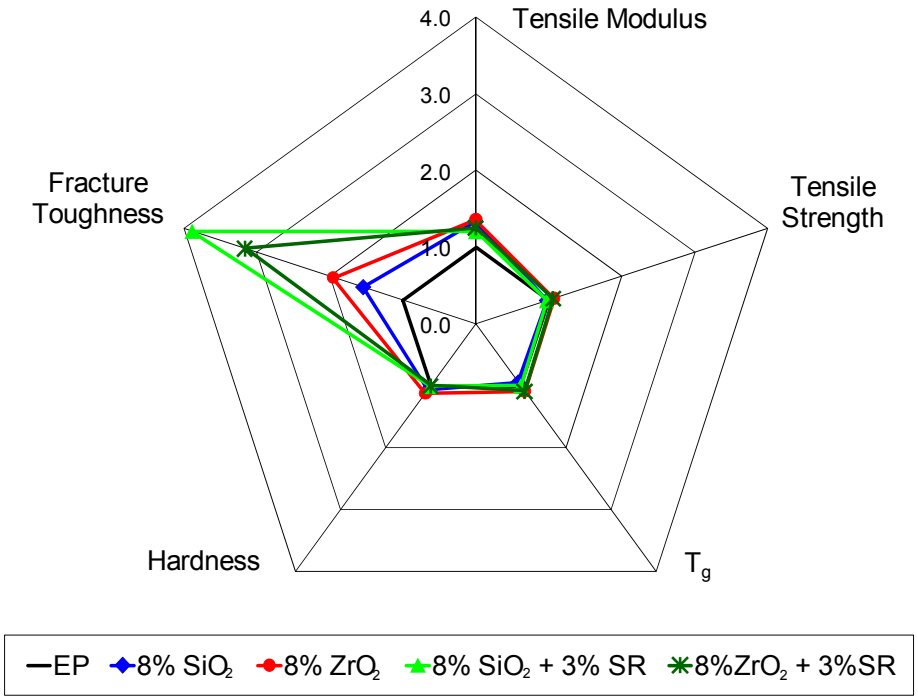

Figure 5.1 Relative improvement of modified epoxy matrices

Silica increases the tensile modulus but has no effect in the strength, has a negative impact on T_g, increases slightly the hardness and confers the resin up to 50% improvement in toughness. The reduction in T_g, the noticeable hysteresis during the hardness test and the microscopical analysis of fracture surfaces, which show particle debonding and plastic deformation as permanent energy dissipation mechanisms; are facts normally related with a weak bonding particles-matrix.

On the other hand, zirconia generates an improvement in all the properties in range from 10% in T_g and strength, up to 100% in toughness. These results suggest the existence of a strong interface bonding that permit the right load distribution in the matrix bulk. This statement may be also supported by the microscopical analysis of the fracture surfaces, which show particles well attached to the polymer matrix.

The addition of silicone rubber to the nanocomposites confers them a superior toughness and improves their thermal stability, without important detriment in mod-

ulus and hardness. Therefore, although nanocomposites present a simultaneous improvement in some mechanical properties, the best properties balance was reached combining rigid ceramic nanoparticles and rubber.

Here is important to remark that the best properties were reached by a hybrid modified matrix containing silica, despite of the fact that the nanocomposites containing zirconia have better performance. This result may be attributed to the compatibility rubber-nanoparticles. Considering the nature of silica and silicone rubber, it is clear that they are highly compatible to each other.

According to percolation theory at the critical filler content, the interface around the particles may interconnect creating a three-dimensional network throughout the matrix which would dominate the performance of the nanocomposites. This phenomenon was demonstrated in both studies systems. But surprisingly both silica and zirconia modified epoxies registered almost same critical filler content, in spite of their important differences in interface. Therefore, it is doubt that percolation theory be only a phenomenon of surfaces.

It is generally accepted that the improvement of a matrix properties is not necessarily reflected in its GFRCs. Figure 5.2 shows how is the transfer of toughness from the modified epoxy matrices to their respective composites, compared with the theoretical prediction.

It is observed that the transfer factor, from matrix toughness to composites, depends on the matrix toughness. To the brittle matrices, containing either SiO_2 or ZrO_2, the transfer factors (≈2 to 1.2) fall over the theoretical proposed but to hybrid modified matrices, whit higher toughness; the transfer factors (≈ 12 to 1.6) fall around 40% below the theoretical predicted. The transfer factor is better to brittle than to highly toughened matrices. However, despite of the poor transfer factor, the best absolute results to enhance the composite toughness were given be by hybrid compounds, containing a high proportion of nanoparticles and with a ratio nanoparticles content / rubber content higher than one.

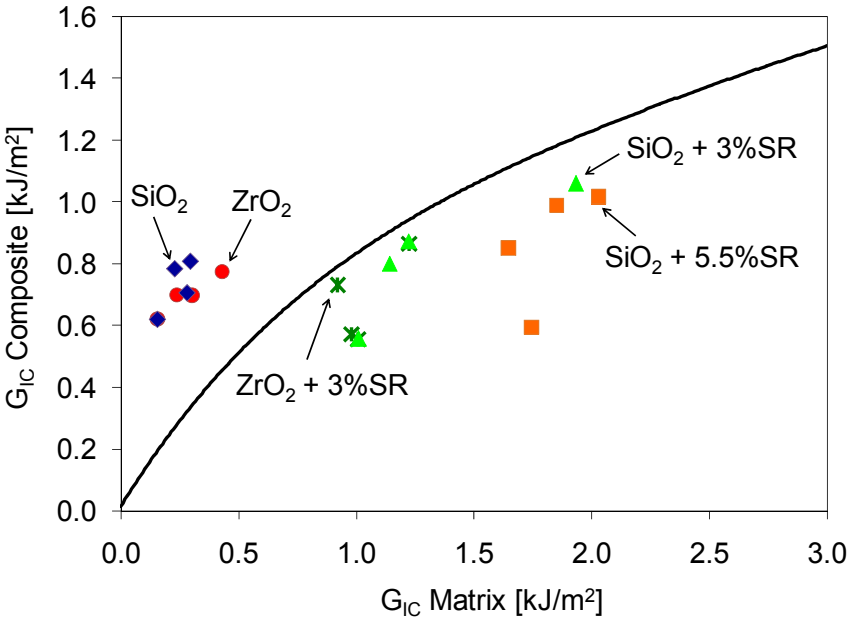

Figure 5.2: Experimental vs. theoretical toughening transfer ratio from matrix to composites.

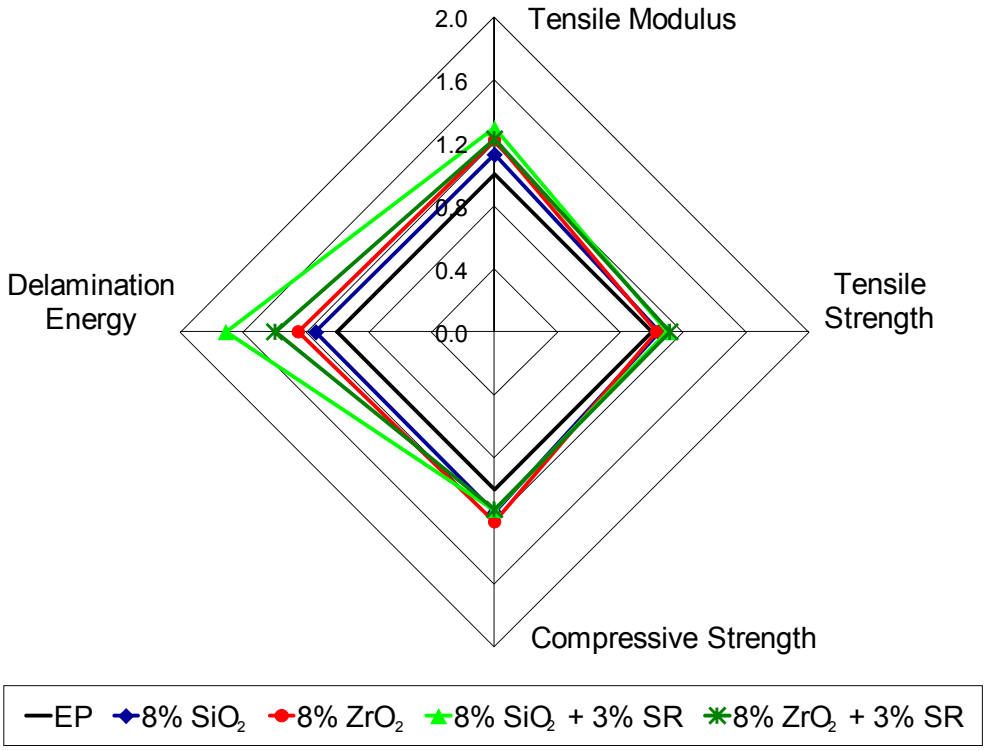

Figure 5.3: Relative improvement of GFRCs

Figure 5.3 summarizes the improvement recorded by the most representative GFRCs. It is clear that the enhancement in matrix properties leads to better performance in composites. Nanomodified matrices produce composites with a simultaneous improvement up to 20% in modulus, compressive strength and delamination energy. The only aspect that seems almost unaffected by the nanoparticles presence is the tensile strength.

Once again, the hybrid modified matrices generate the best properties ensemble in fiber reinforced composites. It is possible to improve the strength in 20% and the toughness up to 60%, using a ratio 8/3 vol.% of nanoparticles/silicon rubber.

6 Summary and Outlook

The present work focused in the obtaining of toughened epoxy resins to be used as matrices in manufacturing fiber reinforced composites by RTM. A DGEBA epoxy matrix was modified by addition of SiO_2 and ZrO_2 nanoparticles and micro-sized silicone rubber.

Series of nanocomposites and hybrid compounds were obtained, by systematical mixing and dilution of in-situ modified master batches. The rheology and curing process of the different modified resins were analyzed in order to determine their suitability to be processed by RTM. It was found that, although the viscosity of the modified resins is considerable superior due to the filler presence, this fact was non restrictive for their processing by Resin Transfer Molding.

The obtained matrices were intensively mechanical and thermal characterized, and their behavior was compared with theoretical models, in order to explain the contribution of each type of filler in the final properties of the matrix. Especial attention was paid to describe the fracture mechanisms induced by the fillers in the resin bulk, as well as to define the filler-matrix compatibility to each kind mixture.

It was demonstrated that nanoparticles improve considerably the performance of the epoxy matrix. However, the improved toughness of the nanocomposites seems to be not enough to fulfill the requirements of very demanding application. On the other hand, silicone rubber addition to the epoxy resins confers then a superior toughness. Thus, the best properties balance was reached by the hybrid compounds, which not only record superior toughness but also enhanced modulus and thermal stability.

The modified matrices were used to produce GFRCs by RTM. High quality composite plates, with uniform structure and very good superficial appearance were obtained. The composites were also characterized looking to establish a relationship between matrix improvement and composite performance.

Although the improvement in matrices was not directly reflected by the composite structures, the successful matrix modification results in GFRCs with enhanced modulus, strength and toughness.

During the present research, appeared some results and special situations that require more intensive analysis to be completely understood or solved:

The homogeneous dispersion of nanozirconia into the epoxy resin, using conventional milling/mixing procedures is still an unsolved issue. Aggregates of micron size were found especially in composites with higher particle content. Large agglomerates may have adverse effect on the mechanical properties. Thus, this process would be optimized.

Inorganic particle toughening is a very complex process. Usually several mechanisms occur simultaneously and each of them makes a certain contribution to the total fracture toughness of the material. The existent models were designed having micro sized fillers as reference. Further investigation is needed to develop suitable models to quantify the contribution of each mechanism into the toughening effect of the rigid nanofillers and to predict the fracture toughness of nanocomposites.

It is stated that the nanocomposites performance depends directly on the interfacial surface formed between filler-matrix. Interfacial physicochemical behavior requires detailed analysis to define its real contribution to the final material performance.

Combination of rigid and elastic particles as fillers can dramatically enhance the fracture toughness of a polymer matrix. This effect is attributed to synergetic effect of the components, phenomenon that require extensive research in order to determine its origin.

In the composites obtained from hybrid modified matrices it was observed a considerable difference, 5-10 folds in average, in the rubber particle size between the matrices containing silica and the ones containing zirconia. It is important to define the cause of this situation and of course to determine the effect of these rubber rich domains on the mechanical performance of the composites.

7 Literature

[1] Han, J. T.; Cho, K.: Nanoparticle-induced enhancement in fracture toughness of highly loaded epoxy composites over a wide temperature range. J. Appl. Polym. Sci., (2006), pp.

[2] Toughened, fiber-reinforced thermosetting resin matrix prepregs and composites made there from US Patent Issued on May 6, 1997

[3] Nigam, V.; Setua, D.K.; Mathur, G.N.: Failure analysis of rubber toughened epoxy resin. J. Appl. Poly. Sci., 87 (2003), pp. 861-868.

[4] Di Pasquale, G.; Motta, O.; Recca ,A.: New high-performance thermoplastic toughened epoxy thermosets. Polymer, 38 (1997), pp. 4345-4348.

[5] Weiping, L.; Soung, V. H.; Martin, P.: Organoclay modified high performance epoxy nanocomposites. Comp. Sci. and Tech., 65 (2005), pp. 307-316.

[6] Verchere, D.; Sautereau, H.; Pascault, J.P.: Rubber modified epoxy. Influence of CTBN . J. Appl. Polym. Sci., 41 (1990), pp. 467-76.

[7] Lovell, P.A.: Rubber toughened plastics strategies for their preparation and evaluation. Internal report. Manchester Materials Science Center (1997).

[8] Kinloch, A.J.; Yuen, M.L.; Jenkins, S.D.: Thermoplastic toughened epoxy polymers. J. Mat. Sci. 29 (1994), pp. 3781-90

[9] Hodgkin, J.H.; Simon, G.P.; Varley, R.J.:Thermoplastic toughening of epoxy resins: a critical review. Polyms. for Adv. Tech., 9 (1998), pp. 3-10

[10] Wetzel, B.; Rosso, P.; Haupert, F.; Friedrich, K.: Epoxy nanocomposites – fracture and toughening mechanisms. Eng. Frac. Mech., 76 (2006), pp. 2375-98.

[11] Wetzel, B.; Haupert, F.; Zhang, M.Q.: Epoxy nanocomposites with high mechanical and tribological performance. Comp. Sci. and Tech., 63 (2003), pp. 2055.

[12] Zhang, K.; Wang, L.; Wang, F.; Wang, G.; Li, Zuobang: Preparation and characterization of modified clay reinforced and toughened epoxy resin nanocomposites. J. of Appl. Polym. Sci., 91 (2004), pp. 2649-2652.

[13] Gam, K.T.; Miyamoto, M.; Nishimura, R.; Sue, H.J.: Fracture of core shell rubber-modified clay epoxy nanocomposites. Polym. 43 (2003), pp. 1635-1645.

[14] Weiping, L.; Soung, V. H.; Martin P.: Morphology and Performance of epoxy nanocomposites modified with organoclay and rubber. Polym. Eng. and Sci., 44 (2004), pp. 1178-1186.

[15] Bickerton, S.; Stadtfeld C. H.; Steiner, V. K.; Advani S.C.: Active control of resin injection for the resin transfer molding process. ASC, 13th Technical Conference of Polymer Materials, Baltimore, 1998

[16] Peters, S.T. (Editor). Handbook of composites.Chapman & Hall. London 1998.

[17] Pascault J.P. et all in Thermosetting Polymers. Marcel Dekker Inc. New York (2002) pp 389-419.

[18] Sun, L.: Thermal rheological Analysis of cure Process of Epoxy Prepeg. Dissertation. Lousiana State University. May, 2002.

[19] Lelli, G.; Terenzi, A.; Vedova, C.; Torre, L.; Kenny, J. M.: Modelling of the Chemo–Rheological Behaviour of Thermosetting Polymer Nanocomposites. Excerpt from the Proceedings of the COMSOL Users Conference 2006 Milano.

[20] Zhang, Y,; Pickles, C.A.; Cameron, J.: The production and mechanical properties of silicone carbide and alumina whisker-reinforced epoxy composites. J. of Reinf. Plas. and Comp., 11 (1992), pp. 1176-86

[21] US Patent 7311972. Filled epoxy resin compositios. 2007

[22] Walter, R.; Friedrich, K.; Privalko, V.; Savadori, A.: On modulus and fracture toughness of rigid particulate filled high density polyethylene. J. Adhesion 64 (1997), pp. 87-109.

[23] Wetzel, B.; Haupert, F.; Friedrich, K.; Zhang, M. Q.; Rong, M. Z.; Proceedings of the 13th ICCM Beijing, 2001

[24] Zhang, M. Q.; Rong, M. Z.; Zheng, H.M.; Friedrich, K.: Improvement of tensile properties of nano-SiO_2/PP composites in relation to he percolation mechanism. Polymer 42 (2001) pp. 3301-04

[25] Karger-Kocsis, J.; Zhang, Z.: Structure property relationship in nanoparticle semicristalline thermoplastic composites. In mechanical properties of polymers based on nanostructure and morphology. Edited by Balta Calleja. CRC Press, NY 2005.

[26] Wetzel, B.: Mechanische Eigenschaften von Nanoverbundwerkstoffe. Dissertation. Institute für Verbundwerkstoffe (2006)

[27] Kinloch, A. J.; Taylor, A. C.: The mechanical properties and fracture behavior of epoxy-inorganic micro- and nano-composites. J. Mater. Sci., 41 (2006), pp. 3271-97.

[28] Yang, F.; Ou, Y.; Yu, Z.: Polyamide 6/silica nanocomposites prepared by in situ polymerization. J.of Applied Polymer Science, 69 (1998), pp. 355-61

[29] Adebahr, T.; Roscher, C.; Adam, J.; Reinforcing nanoparticles in reactive resins, European Coatings Journal 4 (2001), pp.144-49

[30] Dewimille, L.; Bresson, B.; Bokobza, L.: Synthesis, structure and morphology of poly(dimethylsiloxane) networks filled with in-situ generated silica particles. Polymer 46 (2005) pp. 4135-43

[31] Musto, P.; Ragosta, G.;Scarini, G.; Mascia, L.: Toughness enhancement of polyimides by in-situ generation of silica particles. Polymer 45 (2004) pp. 4265-74

[32] Person, R.A.; Yee, A.F.: Toughening mechanisms in elastomer-modified epoxies. Part 3 The effect of cross-link density. J.Mater. Sci., 24 (1989), pp. 2571-80.

[33] Riew, C.K.; Gillham, J.K.: Rubber modified thermoset resins. Advances in Chemistry Series, 208, American Chemical Society, Washington DC 1984.

[34] Scherzer, T.: Characterization of diol modified epoxy resins by near- and mid-infrared spectroscopy. J. Appl. Polym. Sci., 51 (1994), pp. 491-502

[35] Sankarprasad, B.; Basudam, A.: Toughening of epoxy resins by hydroxy-terminated, silicon-modified polyurethane oligomers. J. of Appl. Polym. Sci., 90 (2003), pp. 1497-1506

[36] Ohtsuka, K.; Hasegawa, K.; Fukuda, A.: Synthesis and curing behaviour of urethane modified epoxy resin. Polym. Int. 31(1993) , pp. 25

[37] Urbaczewski, E.; Pascault, J.P.; Sautereau, H.: Macromol. Chem. 191 (1990), pp. 943.

[38] Huang, Y.; Hunston, D.L.; Kinloch, A.J.; Riew, C.K.: Toughened Plastics I. Edited by Riew. Advances in chemistry series 233, American Chemical Society, Washington DC 1993.

[39] Zhang, Z.; Rong, M. Z.; Friedrich, K.: in From- nano- to- macro-scale. Edited by, K. Friedrich, S. Fakirov and Z. Zhang. Springer, New York, 2005

[40] Hartwig, A; Sebald, M.; Pütz D.; Aberle, L.: Preparation, characterization and properties of nanocomposites based on epoxy resins - an overview. Macromol. Symp., 221 (2005), pp. 127-35.

[41] US Patent 5434226. Epoxy resin toughened with a polyether sulfone and polyarylsulfidesulfone. 1994

[42] Seunghan, S.; Jyongsik, J.: Toughness improvement of high performance epoxy resin using aminated PEI. J. Appl. Polym. Sci. 65 (1998) 2237-2246.

[43] Wang, Q.; Shen, W.; Xue, Q.: The friction and wear properties of nanometer SiO2 filler polyetherketone. Tribol. In., 30 (1997), pp. 193-197.

[44] Raghava, R.S., Role of matrix-particle interface adhesion on fracture toughness of dual phase epoxypolyethersulfone blend. J. Polym. Sci. Part B: Polym- Phys. 25 (1987) pp 1017-31.

[45] Di Liello, V.; Martuscelli, E.; Musto, P.; Ragosta, G.; Scarinzi, G.: Toughening of highly crosslinked epoxy resins by reactive blending with bisphenol A poly-

carbonate. II. Yield and fracture behaviour. J. of Polym. Sci. B: Polym. Physics, 32 (1994), pp. 409-419.

[46] Zhang, L.; Berglund, A.: Deformation and fracture of glass bead/CTBN-rubber/epoxy composites. Polym. Eng. and Sci., 33 (1993), pp. 100-107.

[47] Chikhi, N.; Fellahi, S.; Bakar, M.: Modification of epoxy resin using reactive liquid ATBN rubber. European Polymer Journal, 38 (2002), pp. 251-264.

[48] Hwang, J.F., Manson, J.A., Hertzberg, R.W., Miller, G.A., and Sperling, J.H., Polym. Eng. Sci., 29, 1466 (1989).

[49] Ki Tak Gam. Structure-property relationship in core-shell rubber toughened epoxy nanocomposites. Dissertation Texas A&M University. 2003

[50] Garg, A.C.; Mai, Y.W.: Failure mechanisms in Toughened Epoxy Resin – A review. Comp. Sci. and Tech., 31 (1988), pp.I179-223.

[51] Ji, Q.; Todd, M.; Edwards, M: Evaluation of various elastomers as modifiers to reduce stress in liquid epoxy encapsulants and flip chip underfills. Loctite corporation,Technical Paper, 2002.

[52] Jörg Fröhlich. Nanostructured thermoset resins and nanocomposites containing hyperbranched blockcopolyether liquid rubbers and organophilic layered silicates. Dissertation. Institut für Makromolekulare Chemie der Albert-Ludwigs-Universität 2003.

[53] Collyer, A.: Rubber toughening engineering plastics. Chapman and Hall. Great Britain 1994.

[54] Zweben, C.; Hahn, H.T.; Chou T.V.: Mechanical Behavior and Properties of Composites Materials; Delaware Composite Design Encyclopedia, Volume 1; 1989.

[55] Hyer, W. M.: Stress Analysis of Fiber-Reinforced Composite Materials. USA: WCB McGraw-Hill 1998.

[56] SP Guide to Composites. Gurit 2008.

[57] Tang, B.: Fiber reinforced polymer composites applications in USA. First Korea/USA Road workshop proceedings. January 1997.

[58] Mahrholz, T.; Mosch, J.; Röstermundt, D.; Riedel, U.; Herbeck, L.: New high-performance fiber reinforced materials with nanocomposites. 20th AAAF Colloquium – Materials for Aerospace Applications, Paris Nov. 24-26, 2003.

[59] Stark, E.B.; Breitigam W.V.; Farris R.D.: Resin Transfer Molding (RTM) of high performance resins. Technical paper. Resolution Performance Products, USA 2001

[60] Technical Data Sheet VP 823-30 R. Chemicals and Technologies for the Polymers GmbH. Germany, 2005.

[61] European patent. EP 1 236 765 A1. Silicium Dioxide disperssion. 2002.

[62] Technical Data Sheet VP 823-33 R. Chemicals and Technologies for the Polymers GmbH. Germany, 2005.

[63] Technical data sheet. Albidur 2240 A Nanoresins GmbH. Germany 2004.

[64] Wacker silicones. Genioperle. Nanoscalige silicone particles.Mayo 2007.

[65] Technical Data Sheet VP Zirconium Dioxide PH. Degussa AG.Germany, 2004.

[66] Technical Data Sheet VP 823-2H. Chemicals and Technologies for the Polymers GmbH. Germany, 2005.

[67] Interglass fabric catalog. Germany 2000.

[68] Xiao, K.; Ye, L.; Kwok, Y.S.: Effects of pre-cracking methods on fracture behavior of an Araldite-F epoxy and its rubber-modified systems. J. of Mat. Sci., 33 (1998), pp. 2831.

[69] Instrumented Indentation. National Physical Laboratory. United Kingdom 2008.

[70] Hancox, N.L.: The compression strength of unidirectional carbon fibre reinforced plastic. J. Mat. Sci., 10 (1975) pp. 234-42

[71] Einstein, A.: Einstein's Annalen Papers: The complete collection 1901-1922. Wiley VCH, 2005

[72] Roscoe, R.: The viscosity os suspensions of rigid spheres. Brit. J. Appl. Phys. 3 (1952), pp.267

[73] Nielsen, E. L.; Landel, R.F.: "Mechanical properties of polymers and composites" (Marcel Dekker, New York, 1994).

[74] Lelli, G.; Terenzi, A.; Vedova, C.; Torre, L.; Kenny, J.M.: Modelling of the Chemo–Rheological Behaviour of Thermosetting Polymer Nanocomposites. Excerpt from the Proceedings of the COMSOL Users Conference 2006 Milano.

[75] Gonis, J.; Simon, G. P.; Cook, W. D.; Cure Properties of Epoxies With Varying Chain Length as Studied by DSC. J. Appl. Polym. Sci., 72(1999), 1479.

[76] Halpin, J.C.; Kardos, J.L.: The Halpin-Tsai equations: A review. Polym. Eng. Sci., 16 (2004), pp. 344-52.

[77] Lewis, T.B.: Nielsen, L.E.: Dynamic mechanical properties of particulate filled composites. J. Appl. Polym. Sci., 14 (1970), pp. 1449-71.

[78] Hull, D.: An Introduction to composite materials. Cambridge solid state science series. Cambridge University Press. 1981

[79] Cox, H.L.: The elasticity and strength of paper and other fibrous materials. Brit. J. Appl. Phys. 3 (1952), pp.72

[80] Brook, R.; Cahn, R.. Concise Encyclopedia of advanced ceramic materials. Pergamon, Oxford, 1991.

[81] Tomanek A.: Silicone & Technik. Hanser. München 1990.

[82] Sun, Y.; Zhang, Z.; Moon, K.S.; Wong, C.P.: Glass transition and relaxation behaviour of epoxy nanocomposites. J. Polym. Sci.- Polym. Phys., 42 (2004), pp. 3849-58.

[83] Liu, Y.L.; Hsu, C.Y.; Wei, W.L.; Jeng, R.J.: Preparation and thermal properties of epoxy silica nanocomposites from nanoscale colloidal silica. Polym., 44 (2003), pp. 2159-2167.

[84] Roulin-Moloney, (Editor) “Fractography and failure mechanisms of polymers and composites” (Elsevier Appl. Sci., London, 1989) p. 233.

[85] Tadaharu, A.; Wakako, A.; Takuya, N.; Akihiko, Y; Masahiro, G.: Fracture toughness of silica particulate-filled epoxy composite. J. of Appl. Polym. Sci., 86 (2002), pp. 2261-2265.

[86] Zhao, Q.; Hoa, S.V.: Toughening mechanisms of epoxy resins with micro/nano particles. J. Comp. Mats. 41 (2007), 201-19

[87] Lange, F.F.: The interaction of a crack front with a second phase dispersions. Phil. Mag., 22 (1970), pp. 983.

[88] Evans, A.G.: The strength of a brittle material containing second phase dispersions. Phil. Mag., 26 (1972), pp. 1327.

[89] Green, J.D.; Nicholson, S.P.; Embury, J.D.: Fracture of brittle particulate composite. J. Mat. Sci., 14 (1979), pp.1657.

[90] Faber, K.T.; Evans, A.G.: Crack deflection process. Acta Metall. 31 (1983), pp. 565-76.

[91] Faber, K.T.; Evans, A.G.: Crack deflection process II. Experiment. Acta Metall. 31 (1983), pp. 577-84

[92] Kinloch, A. J.; Young, R.J.: Fracture behaviour of polymers. London. Applied Science Publishers 1983.

[93] Kim, J.K.; Robertson, R.E.: Toughening of thermoset polymers by rigid crystalline particles. J. Mater. Sci., 27 (1992), pp.161-74.

[94] Adachi, T.; Araki, W.; Nakahara, T.; Yamaji, A.; Gamou, M.: Fracture toughness of silica particulate-filled epoxy composite. J. Appl. Polym. Sci., 86 (2002), pp. 2261-65.

[95] Zhang H.: Fracture of nanoparticle filled polymer composites. Dissertation Institute of Composite Materials, Kaiserslautern, 2007.

[96] Argon, A.S.; Cohen R.E.: Toughenability of polymers. Polymer 44 (2003), pp. 6013-32

[97] Bagheri, R.; Pearson, R. A.: Role of plastic cavitation in rubber toughened epoxies. Polymer 37 (1996), pp. 5597-600

[98] Kinloch, A. J.; Maxwell, D.L.; Young, R.J.: The fracture of hybrid-particulate composites. J. Mat. Sci., 20 (1985), pp. 4169-84

[99] Verchere, D.; Sautereau, H.; Pascault, J.P.: Rubber modified epoxy. Influence of CTBN . J. Appl. Polym. Sci., 41 (1990), pp. 467-76.

[100] Yee, A.F.; Pearson, R.A.: Toughening mechanisms in elastomer modified epoxies. J. Mater. Sci. 21 (1986) 2462

[101] Huang, Y.; Kinloch, A. J.: Modelling of the toughening mechanisms in rubber-modified epoxy polymers. J. Mat. Sci., 27 (1992), pp. 2763-69.

[102] Kunz-Douglas, S.; Beaumont, P.W.R.; Ashby, M.F.: A model for the toughness of epoxy rubber particulate composites. J. Mat. Sci., 15 (1980), pp. 1109.

[103] Kovacs, J.Z.; Velagala, B.S.; Schulte, K.; Bauhofer, W.: Two percolation threshols in carbon nanotube epoxy composites. Comp. Sci. And Tech., 67 (2007) pp 922-28

[104] Sok W.K., Byeongmin, C.; Sang, H.L.; Kweon H. K.: Measurement of thermophysical properties of particulate filled polymer composites, High Temperatures-High Pressures, 37 (2008) pp. 21-30

[105] Bansal, P.P.; Ardell, A.J.: Average nearest neighbor distances between uniformly distributed particles. Metallography, 5 (1972), pp. 97-111.

[106] LB-550 Dynamic light scattering nano-particle size analyzer. Horiba Jobin Yvon. France 2008

[107] Richerson D.W. “Modern Ceramics Engineering” . Marcel Dekker, New York, 1992 p.166,756.

[108] Johnsen, B.B.; Kinloch, A.J.; Mohamed, R.D.; Taylor, A.C.; Sprenger, S.: Toughening mechanims of nanoparticle-modified epoxy polymers. Polymer, 48 (2007), pp. 530-41.

[109] Medina, R.; Haupert, F.; Schlarb, A. K.; Improvement of tensile properties and toughness of an epoxy resin by nanozirconium-dioxide reinforcement. J. Mat. Sci. (2007), pp.

[110] Faulstich de Paiva, J. M.; Mayer, S.; Cerqueira R. M.: Comparison of tensile strength of different carbon fabric reinforced epoxy composites. Mats. Research, 9 (2006), pp. 83-89.

[111] Kim, J.; Baillie, C.; Poh, J.; Mai, Y.W.; Fracture toughness of CFRP with modified epoxy resin matrices. Comp. Sci. Tech., 43 (1992) 283-97.

[112] Xiao, K.; Ye, L.: Fracture mechanisms of rubber modified epoxies and their fibre composites. Structural Integrity and Fracture, (2000) pp. 71-77.

[113] Schneider, K.; Lauke, B.: Determination of Compressive Properties of Fibre-Reinforced Polymers in the In-Plane Direction According to ISO 14126. Part 2: A Critical Investigation of Failure Behaviour. Appl Compos Mater 14 (2007), pp. 177–191

[114] Drzal, L. T.; Madhukar M.: Fibre-matrix adhesion and its relationship to composite mechanical properties. J. Mater. Sci., 28 (1993), pp. 569-610.

[115] Sudarisman; Davis, I. J.; Hamada, H.: Compressive failure of unidirectional hybrid fibre-reinforced epoxy composites containing carbon and silicon carbide fibres. Compos. Part A, 38 (2007), pp. 1070-1074.

[116] Scott, J.M.; Phillips, D.C.: Carbon fiber compositeswith rubber toughened matrices. J. Mat. Sci. 10 (1975), pp.551-62

[117] Zheng, Y.; Ning, R.; Zheng, Yi.: Study of SiO2 nanoparticles on the improved performance of epoxy and fiber composites. J. of Rein. Plas. And Comp., 24 (2005), pp. 223-33

List of Publications

1. Medina R., Haupert F., Schlarb A.K.: Improvement of tensile properties and toughness of an epoxy resin by nanozirconium dioxide reinforcement. J. Mat. Sci. 2008: 43, 9, 3245-3252.
2. Medina R.: Glass Fiber Reinforced Composites (GFRCs) from toughened and nanomodified epoxy matrices. Internes Kolloquium. Institute für Verbundwerkstoffe, Technische Universität Kaiserslautern. 7. April 2008.
3. Walter R., Medina R., Haupert F., Schlarb A.K.: Improved toughness and stiffness of epoxy resins modified by preformed rubber microparticles and SiO_2 nanoparticles for Resin Transfer Molding Applications. 2nd International Conference „Micro and Nano-Technology“ March 14-16, 2007, Vienna, Austria.
4. Medina R., Walter, R., Haupert, F., Schlarb, A. K.: Influence of hard and elastic particles on the mechanical properties of epoxy resins. Polymerwerkstoffe 2006. Martin Luther Universität, Halle/Saale, 27.-29. September 2006.
5. Medina R., Walter R., Mang P., Haupert F.: Influence of the hard and elastic particles on the interlaminar fracture toughness of epoxy RTM-plates. Internes Kolloquium. Institute für Verbundwerkstoffe, Technische Universität Kaiserslautern. 6. Februar 2006.
6. Walter R., Medina R.,Mang P., Haupert F., Einfluss von harten und elastischen Partikeln in epoxidharz auf die interlaminare Bruchzähigkeit vom RTM Platten. „Werkstoffprüfung 2005“ Deutscher Verband für Materialforschung und -prüfung e.V. Berlin. 01. und 02. December 2005.

Directed Thesis

Study of the curing process of rubber toughened and nanoparticle modified epoxy resins. Bachelor Thesis, Javier Matas Corral, 2007.